PETROVIETNAM JOURNAL

An Official Publication of the Vietnam National Oil and Gas Group Vol. 10 - 2022

ISSN 2615-9902

PETROVIETNAM JOURNAL IS PUBLISHED MONTHLY BY VIETNAM NATIONAL OIL AND GAS GROUP

CONTACT ADDRESS
16th Floor, VPI Tower, Trung Kinh street, Yen Hoa ward, Cau Giay district, Ha Noi
*Tel: (+84-24) 37727108 * Fax: (+84-24) 37727107 * Email: tcdk@pvn.vn/pvj@pvn.vn*
Mobile: (+84)982288671

Cover photo: Ha Long Bay, Vietnam. Photo: Freepik

Publishing Licence No. 100/GP-BTTTT dated 15 April 2013 issued by Ministry of Information and Communications

PETROVIETNAM JOURNAL
Volume 10/2022, pp. 19 - 27
ISSN 2615-9902

A SUCCESSFUL PILOT APPLICATION OF THE COMPLEX MIXTURE SURFACTANT POLYMER VPI SP TO ENHANCE OIL RECOVERY FACTOR FOR THE LOWER MIOCENE, BACH HO FIELD

Dinh Duc Huy[1], Nguyen Minh Quy[1], Pham Truong Giang[1], Hoang Long[1], Le Thi Thu Huong[1], Cu Thi Viet Nga[1], Pham Xuan Son[2], Nguyen Lam Anh[2], Ho Nam Chung[2], Pham Trung Son[2], Nguyen Quynh Huy[2], Tran Thanh Nam[2]
[1]Vietnam Petroleum Institute
[2]Vietsovpetro
Email: huydd@vpi.pvn.vn
https://doi.org/10.47800/PVJ.2022.10-03

Summary

Enhanced oil recovery (EOR) implementation at field scale is complex. Therefore, pilot applications are usually conducted before field execution. This paper introduces a pilot project successfully applied for the Lower Miocene, Bach Ho field. Topics covered include: (i) pilot area selection, (ii) chemical preparation, (iii) specification and pilot design for execution, (iv) implementation, (v) pilot observation and interpretation, (vi) efficiency evaluation. The implementation of pilot projects is achieved on 23 January 2022. The evaluation shows that 2,700.2 tons of oil gained thanks to the application of the surfactant-polymer complex mixture (VPI SP).

Key words: Enhanced oil recovery, VPI SP, Lower Miocene, Bach Ho field.

1. Introduction

Bach Ho oil field started producing oil from the Miocene in 1986 while the south dome in 2011 on BH-441. The initial oil in place of the Miocene was approximately 80.05 million tons, of which 27.17 million tons came from the Lower Miocene, south dome (BK14/16). The reservoir in BK14/16 consists of 5 main sand bodies from layer 22 to layer 27 with an average depth of 2,300 mTVDss. The target layer in the pilot plan is layer 23, sandstone formation; the remaining oil volume in place is ~5 million tons. Layer 23 formation distribution is wide and thick, with medium to high permeability and support energy from the flank water (Figure 1).

2. Pilot area selection

The implementation of enhanced oil recovery plans at field scale is complex and difficult. Thus, before applying at field scale, the size of the solution should be first scaled down then increased step by step [1]. In addition, defining clear pilot objectives and execution will lead to a successful pilot. On the other hand, pilots carrying out need to weigh against the time and expense [2]. To minimise the uncertainty of chemical injections for increasing oil recovery of the Lower Miocene, Bach Ho field, a few key points need to be specified to prioritise the objects to consider.

- The preliminary screening evaluation in the pilot area is convincing technically and economically;
- Well pattern/well configuration is typical in the field with the extent of the communication between injector and producer, and effective water injection is preferable in this case;
- The volume of oil remains after the secondary stage;
- Available facilities in the pilot area are adaptable to the technology of EOR implementation.

The objective of the pilot plan is carefully selected. The results indicate that the location of injector 1609/BK16 is the likely area for EOR execution as follows:

- The results of dynamic model simulation and feasible study show the highest value [3];
- Distribution of the main reservoir (layer 23 sand body) is wide and fairly thick (23-0: 3.3 m, 23-1: 4.3 m, 23-2: 16.5 m) (Figures 1 & 3);

Date of receipt: 9/9/2022. Date of review and editing: 9/9 - 20/9/2022.
Date of approval: 5/10/2022.

19

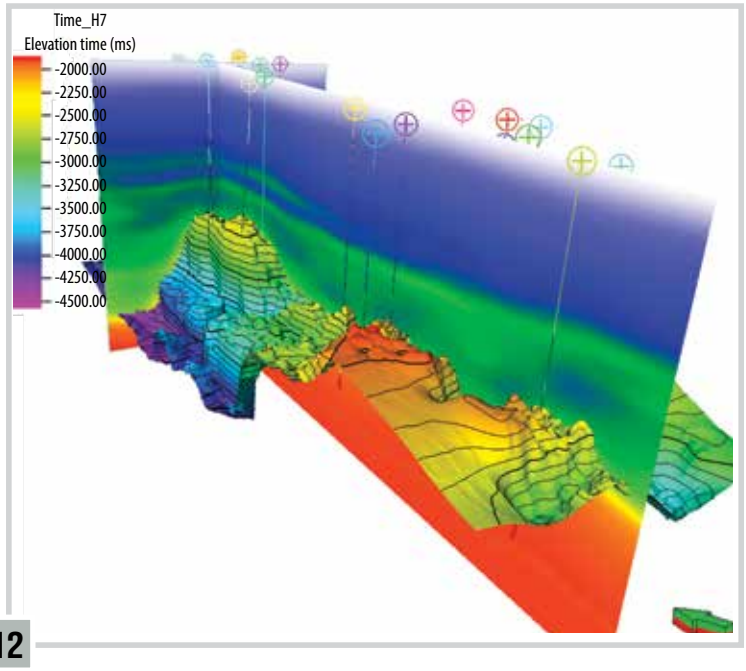

12

SCIENTIFIC RESEARCH

PETROLEUM EXPLORATION & PRODUCTION

PETROLEUM TECHNOLOGIES

RESEARCH & DISCUSSION

PETROVIETNAM JOURNAL
Volume 10/2022, pp. 3 - 11
ISSN 2615-9902

A QUICK COMPARISON OF PLIOCENE AND UPPER MIOCENE SHALE RESOURCES IN NORTHERN, CENTRAL AND SOUTHERN PARTS OF SONG HONG BASIN WITH REFERENCE TO THEIR GAS POTENTIAL

Vo Thi Hai Quan[1], Pham Huy Giao[1,2]
[1]Vietnam Petroleum Institute
[2]Petrovietnam University
Email: giaoph@vpi.pvn.vn
https://doi.org/10.47800/PVJ.2022.10-01

Summary

This research is a follow-up of a more comprehensive PhD study on assessment of shale gas resources in the northern Song Hong basin that was conducted at the Asian Institute of Technology (AIT). The Song Hong basin, a typical pull-apart Cenozoic basin, had experienced a post-extensional stage accompanied by seafloor spreading from Upper Oligocene to Lower Miocene with its stratigraphy characterised by a fault-controlled syn-rift continental sequence followed by a post-rift marine sequence. In recent years, a number of gas fields have been discovered in the Song Hong basin with the Oligocene-Eocene and the Lower-Middle Miocene shales as the major and minor source rocks, respectively. On the other hand, the Pliocene and Upper Miocene shales, present in the stratigraphy from the north to the south of the Song Hong basin, have generally been considered as the seals, but not the source rocks in some previous studies. In July 2020, an exploration well (Ken Bau-2X) was drilled in Block 114 by ENI, reaching a total depth of 3,658 m and encountering a pay of about 110 m in several intervals of Upper Miocene sandstones interbedded with shales, confirming a considerable gas accumulations discovered in Vietnam so far. The interesting thing is that this well only encounter the Pliocene and Upper Miocene shales, the Oligocene-Eocene or Middle-Lower Miocene sediments underlying is absent or very thin. Therefore, potential source rock of these shales should be considered in the area, in particular with reference to petroleum system of the central Song Hong basin.

In this study, a preliminary comparison of the Pliocene and Upper Miocene shale resources in the northern, central and southern blocks in the Song Hong basin was conducted based on the analysis results of XRD, Rock-Eval pyrolysis, vitrinite reflectance, respectively. While the Pliocene and Upper Miocene shales in many areas of Song Hong basin, show a very low or no hydrocarbon generation potential, the very deep and thick Pliocene and Upper Miocene shales in the center and adjacent areas, deposited in a marine environment under the special conditions of abnormal pressure and high geothermal gradient, can be potential source rocks that have possibly generated and released a large amount of hydrocarbons. Further geochemical analyses and petroleum system modelling of the Pliocene and Upper Miocene shales in particular and for the whole central Song Hong basin are recommended.

Key words: Song Hong basin, shale gas, Ken Bau discovery, Rock-Eval pyrolysis, vitrinite reflectance, XRD.

1. Introduction

In July 2019, ENI has confirmed a considerable hydrocarbon accumulation in the Ken Bau discovery, further expanding its potential in the Song Hong basin, offshore Vietnam [1] with the announcement that the first exploration KB-1X well, drilled in Block 114 in the Song Hong basin to a total depth of 3,606 m, discovered gas and condensate in several intervals of Miocene sandstones interbedded with shales. The water depth is 95 m deep at the well site. The well, however, was subsequently plugged and abandoned before reaching deeper levels as planned due to some technical problems. One year later, in July 2020 according to ENI [1] the second exploration well, KB-2X, drilled 2 km apart from the first discovery well of KB-1X to a total depth of 3,658 m, encountered a pay of about 110 m in several intervals of Miocene sandstones

Date of receipt: 6/4/2021. Date of review and editing: 6/4/2021 - 14/7/2022.
Date of approval: 5/10/2022.

interbedded with shales. The second well was considered a success, confirming a considerable hydrocarbon accumulation. The news on Ken Bau discovery has been covered extensively in all Vietnamese mass media, e.g. [2]. It is hoped that this big gas discovery would have an impact on the national energy development strategy to 2030 and outlook to 2045.

2. Overview of geology and petroleum systems in the northern, central and southern parts of Song Hong basin

A number of studies were conducted to understand to a certain extent the geology in general and the petroleum system in the Song Hong basin [3 - 11]. During the Upper Cretaceous to Upper Oligocene, the crust of the East Sea's continental margin had been stretched and thinned, forming a series of rift basins in Southeast Asia, including the Song Hong basin, a typical Cenozoic pull-apart basin that is stratigraphically characterised by a fault-controlled syn-rift continental sequence and a post-rift marine sequence. From the Upper Oligocene to Lower Miocene, the basin was in a post-extensional stage accompanied by seafloor spreading. Thus, a number of gas fields from the north to the south of the Song Hong basin have been discovered, proving the prospects and opportunities for offshore gas exploration and production in this basin.

The central part of the Song Hong basin consists of very thick sediments, deeply deposited up to approximately 15 km deep with a significant amount of organic matters that is the reason why the drilled wells in the central part are deeper in comparison with those wells in the northern and southern parts. Practically, the central wells only penetrated to Pliocene to Upper Miocene, having not reached Middle Miocene yet. It is commonly accepted that the Oligocene-Eocene shales are the main source rocks in the Song Hong basin, while the Lower Miocene and Middle Miocene shales are the minor ones. On the other hand, the Pliocene and Upper Miocene shales are generally considered as seals, not source rocks, in most previous studies. This study presents a new outlook for shale gas potential of

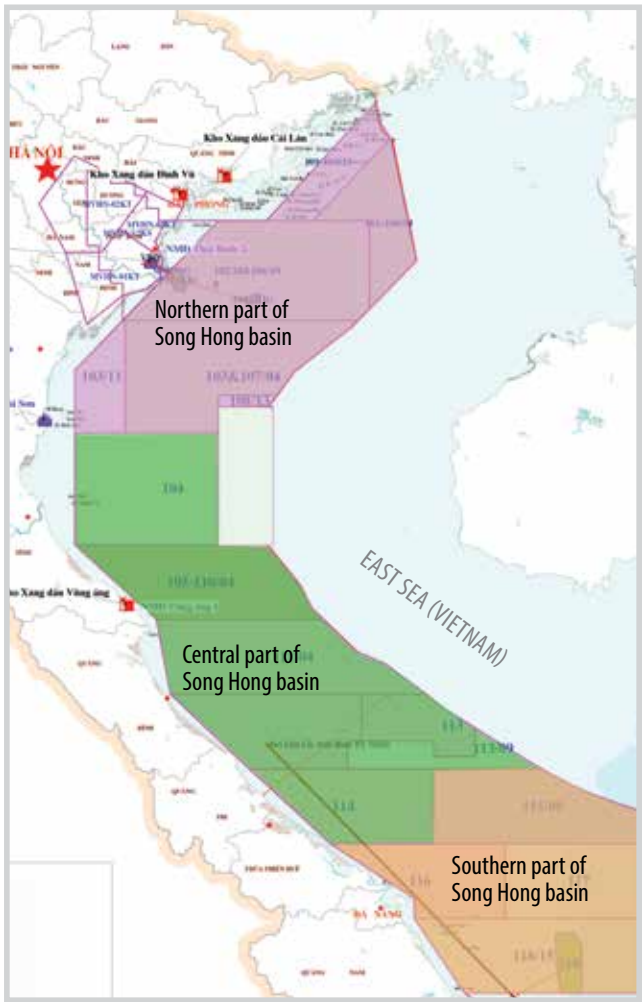

Figure 1. *Schematic distribution of the northern, central and southern parts of Song Hong basin based on [4].*

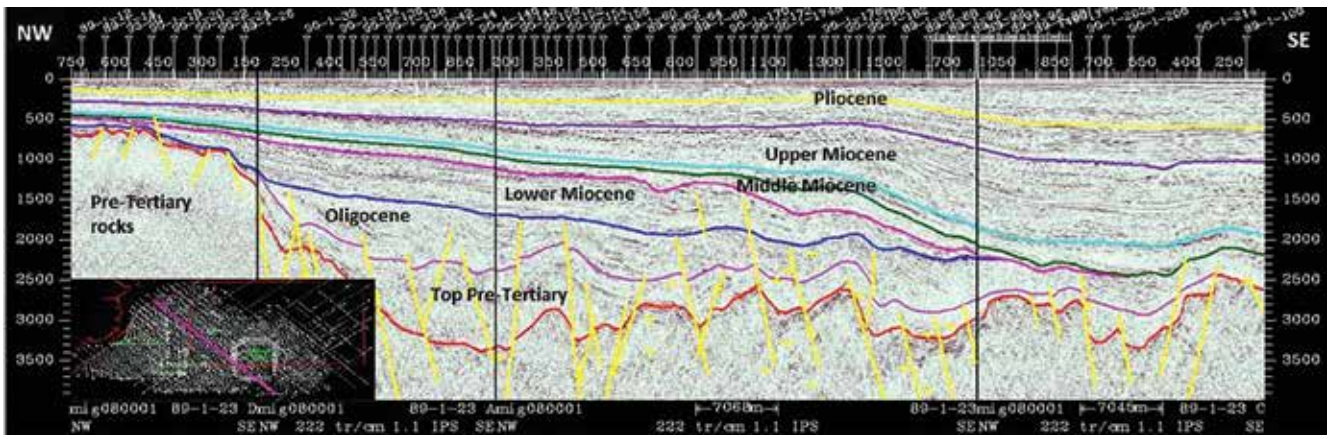

Figure 2. *Pliocene formation deposited above the base Pliocene unconformity, northern Song Hong basin after [11].*

the Pliocene and Upper Miocene shales in these parts of Song Hong basin. Three wells from the northern, central and southern Song Hong parts were selected for a preliminary geochemical assessment of their gas generation potential (Figures 1 and 2).

3. Samples and analytical methods

Three representative wells in the northern, central and southern parts of the Song Hong basin were selected for assessment and comparison between Pliocene and Upper Miocene shales based on the analytical results of Rock-Eval pyrolysis, vitrinite reflectance measurements and XRD tests. They are named as northern, central and southern wells in this research article.

The Rock-Eval (RE) pyrolysis is applied for source rock characterisation. The instrument is a completely automated device consisting of two micro-ovens which can be heated up to 850°C controlled by a thermocouple located in contact with the rock sample. Basically, the steps to operate the RE analysis are as follows: measuring the weight of a rock sample, typically about 50 - 100 mg, placed it into a crucible, which will be put into the pyrolytic oven. The rock samples are heated in inert gas helium (He) atmosphere at 300°C and the isothermal condition is kept

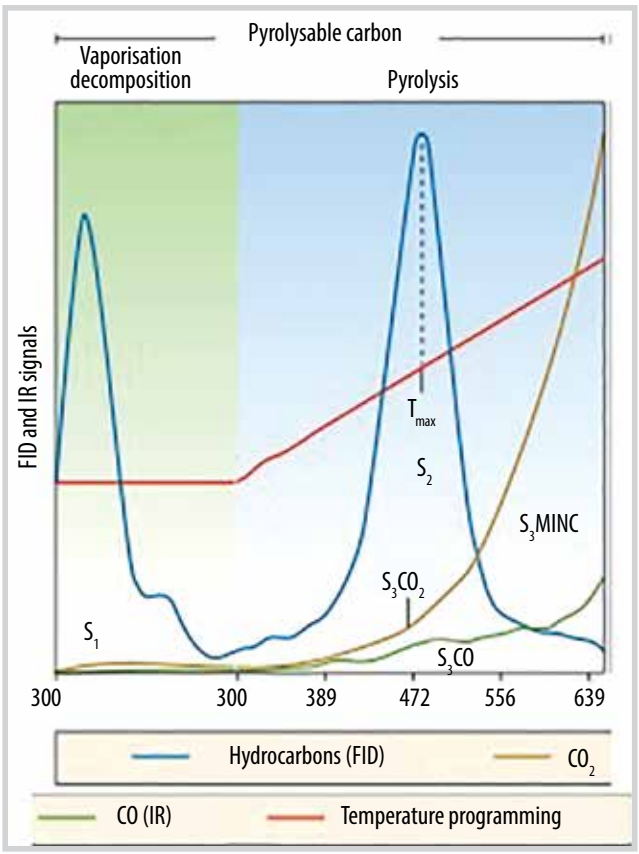

Figure 3. *Programmed pyrolysis results by Rock-Eval 6 [12].*

for up to 5 minutes, during which the evaporative organic materials are recorded by a flame ionisation detector (FID) and named as S_1 peak. Continuing the step of isothermal heating, rock samples are still kept in the linear thermal condition from 300°C to 650°C with step of 25°C/1 min, and the S_2 peak is recorded. The temperature T_{max} (°C) is defined at the maximum peak of S_2 and is also used as a thermal maturity parameter. An infrared cell (IR) detects amount of CO_2 (mg CO_2/g original rock) named as S_3 peak. This CO_2 content is generated during the progress of isothermal heating steps and setting up to 400°C. CO_2 released between 400°C and 650°C is measured by the decomposition of carbonate minerals through heating [12] as shown in Figure 3.

4. Results and discussion

The lab test results of Pliocene and Upper Miocene shales of three study wells are presented in Tables 1 and 2, respectively, that display the main data for the interpretation together with Figures 4 - 9. The details are presented as follows:

4.1. Pliocene shales of some wells in the northern and central blocks

For the Pliocene shales, there are no geochemical and XRD data for the southern well, and no XRD data for the central well either. Therefore, comparison of this formation is done based on Rock-Eval pyrolysis and vitrinite reflectance data of the northern and central wells only. Sediments in the northern well mainly comprise thick sands/silts interbedded with thin layers of shale (100 - 250 m), while those in the central well are very thick shales (~1,000 m) interbedded with thin sands/silts. The organic-richness and pyrolysis yields of these shales are generally of poor potential source rocks (TOC < 0.5%, S_2 < 2 mg HC/g rock). The organic matter are predominantly type III kerogen (HI < 200 mg HC/g TOC) of thermogenic gas-prone and deposited in deltaic to shallow marine environments. The organic matters in the northern well are in the immature stage, while the organic matters in the central well are in low mature to mature stages with R_o ranging from 0.45% to 0.65%, T_{max} ranging from 407°C to 435°C, and falling into mesodiagenesis phase. Therefore, an amount of gas probably was generated and released from the mature organic matters, causing original TOC and S_2 parameters decrease in these shales. The XRD data of the samples in the northern well show a dominance of authigenic quartz of more than 40% together with carbonate and clay minerals (illite-type). High quartz

contents are thought to be a favorable condition for the brittleness of shales that can affect the performance of hydraulic fracturing operations and the production rate (Table 1 and Figures 4 - 5, 7 - 9).

4.2. Upper Miocene shales of some wells in the northern, central and southern blocks

The thickness of shales gradually increases from the northern and southern to the central basin. Sediments in the northern well comprise sands/silts interbedded with thin shales, while deposits in the southern and central wells comprise thick shales interbedded with thin sands/silts. These shales all reveal similar properties, i.e. containing poor to fair organic-richness (TOC<1 %) and poor pyrolysis yields (S_2 < 2.5 mg HC/g rock), mainly originating from type III and a minor type II kerogen, have been deposited in coastal plain to shallow marine environments. The Upper Miocene shales comprise authigenic quartz (>40%) and clay minerals (illite-type), which is a favorable condition for brittleness of shales. The available geochemical analysis results show that the organic matters of the northern and southern wells are in the immature to marginal mature of mesodiagenesis stage with R_o ranging from 0.32% to 0.55%, whereas the organic matters in the central well vary with depth and reached peak of hydrocarbon generation in late diagenesis to catagenesis stage with R_o up to 0.93%, i.e., TOC contents are low in the upper part (2,705 - 2,942 m), ranging from 0.19% to 0.24%, which are typically poor source rock potential for hydrocarbon generation; TOC contents vary from 0.56% to 0.79% in the lower part (3,007.5 - 3,599 m), indicating fair potential source rocks for hydrocarbon genration (Table 2 and Figures 6 - 7). All the evidences are thought to be the available Upper Miocene shale samples in the northern and southern wells are poor potential source rocks, giving very low or no hydrocarbon generation potential (Table 3), whereas a large amount of gas could possibly be generated and released from the Upper Miocene shales in the central block and the reservoirs could possibly be in Pliocene sands and/or it self-source and self-reservoir. Moreover, the central block shows favorable conditions for shale gas sections, i.e., shales are deposited more widely and thicker in a marine environment under the abnormal pressure and high geothermal gradient conditions that were possibly caused by: (i) a rapid sedimentation rate; (ii) a continuous loading and incomplete gravitational compaction of sediments; (iii) faulting; (iv) phase changes in minerals during compaction; (v) shale diapirism; and (vi) tectonic compression.

Table 1. *Comparison of Pliocene shales in the northern, central and southern wells*

Items	Northern well	Central well	Southern well
Number of samples	RE: 2 R_o: 2 XRD: 61	RE: 19 R_o: 19 XRD: 0	-
Depth (m)	945 - 1,365	1,520 - 2,645	700 - 1,000
Lithology	Sands, silts interbedded with very thin shales	Thick shales interbedded with thin sands and silts	Very thick shales interbedded with thin sands, silts
Minerals	Quartz + Feldspar, carbonate and clay minerals (Illite-type)	-	-
Shale diagenesis	Mesodiagenesis (60 - 70°C)	-	-
Depositional environment	Deltaic to shallow marine	Coastal plain, shallow marine	Shallow marine
Estimated thickness of shale (m)	100 - 200	~1000	~250
Organic richness (TOC, %)	0.14 - 0.24	0.15 - 0.21	-
Quality of OM, S_2 (mg HC/g rock)	0.09 - 0.24	0.17 - 0.32	-
HI (mgHC/g TOC)	60 - 100	103 - 196	
Type of kerogen	III	III	
Genetic OM	Higher plant	Higher plant	
R_o (%)	0.38	0.45 - 0.65	
T_{max} (°C)	419 - 421	407 - 435	
HC generation potential	No source potential	Poor to fair source potential	-
Origin of gas	-	Thermogenic gas	-
Remarks	No hydrocarbon generation potential	Poor to fair potential SRs, favorable conditions for generating gas	-

Note: RE = Rock-Eval pyrolysis, R_o = Vitrinite reflectance, XRD = X-Ray diffraction

Table 2. *Comparison of Upper Miocene shales in the northern, central and southern wells*

Items	Northern well	Central well	Southern well
Number of samples	RE: 6 R_o: 6 XRD: 12	RE: 16 R_o: 16 XRD: 20	RE: 32 R_o: 17 XRD: 0
Depth (m)	1,495 - 2,637	2,705 - 3,599	1,000 - 1,930
Lithology	Sands, silts. interbedded with thin shales, coal	Thick shales interbedded with thin sands, silts, limestones	Thick shales interbedded with thin sands, silts., limestone
Minerals	Quartz and clay minerals (Illite-type), some carbonate	Quartz and clay minerals (Illite-type), some carbonates	-
Shale diagenesis	High mesodiagenesis (70 - 80°C)	Intermediate to late diagenesis (70 - 90°C)	-
Depositional environment	Delta plain to shallow marine	Coastal plain, inner shelf	Coastal plain, shallow marine
Estimated thickness of shale (m)	100 - 200	800 - 900	600 - 700
Organic richness (TOC, %)	0.21 - 0.54	0.21 - 0.79	0.25 - 0.80
Quality of OM, S_2 (mg HC/g rock)	0.22 - 2.70	0.37 - 2.05	0.17 - 1.07
HI (mg HC/g TOC)	100 - 500	109 - 296	9 - 181
Type of kerogen	Type III/II	III and minor II	Mainly type III
Genetic of organic matter	Higher plant and little amount of marine algae	Higher plant and little amount of marine algae	Higher plant
R_o (%)	0.42 - 0.55	0.70 - 0.93	0.32 - 0.42
T_{max} (°C)	423 - 435	377 - 433	407 - 431
HC generation potential	Poor source rock potential	Poor to fair source rock potential, reached peak of HC generation	Poor to fair source rock potential
Origin of gas	Thermogeneic	Thermogenic	Thermogenic
Remarks	Poor potential SRs, possibly for gas/oil	Low to fair potential SRs, favourable conditions for gas generation	Low potential SRs, possibly for gas generation at higher maturity

Note: RE=Rock-Eval pyrolysis, R_o=Vitrinite reflectance, XRD=X-Ray diffraction

Table 3. *Hydrocarbon generation potential and thermal maturity of source rock [13]*

HC potential	TOC (%)	S_2 (mg HC/g rock)
Poor	< 0.5	< 2.5
Fair	0.5 - 1	2.5 - 5
Good	1 - 2	5 - 10
Very good	2 - 4	10 - 20
Excellent	> 4	> 20

Maturity	R_o (%)	Tmax (°C)	PI
Immature	< 0.55	< 435	< 0.10
Mature			
Early	0.55 - 0.65	435 - 445	0.10 - 0.15
Peak	0.65 - 0.90	445 - 450	0.25 - 0.40
Late	0.90 - 1.35	450 - 470	> 0.40
Post mature	> 1.35	> 470	

5. Conclusions and recommendations

Although sediments in the central Song Hong basin are younger than the others, the rapid sedimentation rate of the sediments deposited in this basin had caused them subjected to a quick increase of temperature with depth, which is the very reason why the organic matters

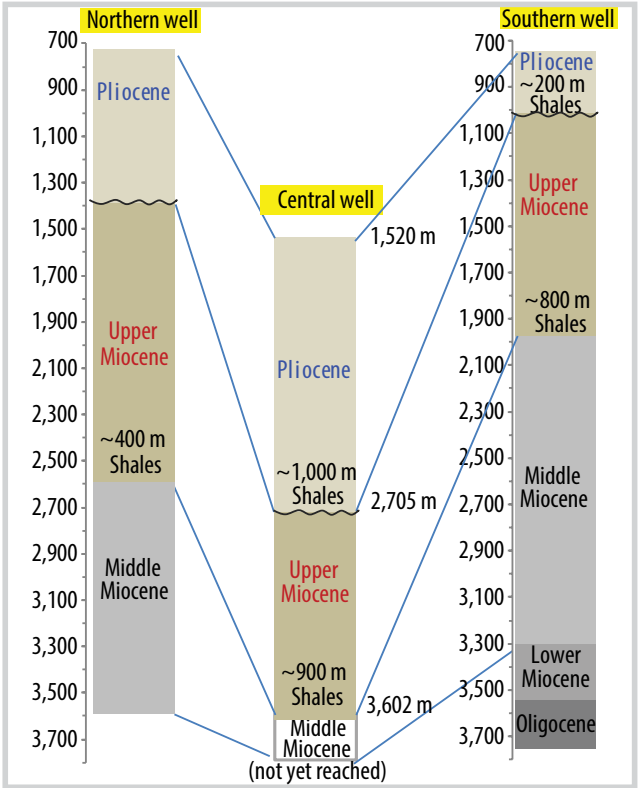

Figure 4. *A scheme of three studied wells in the northern, central and southern parts of the Song Hong basin.*

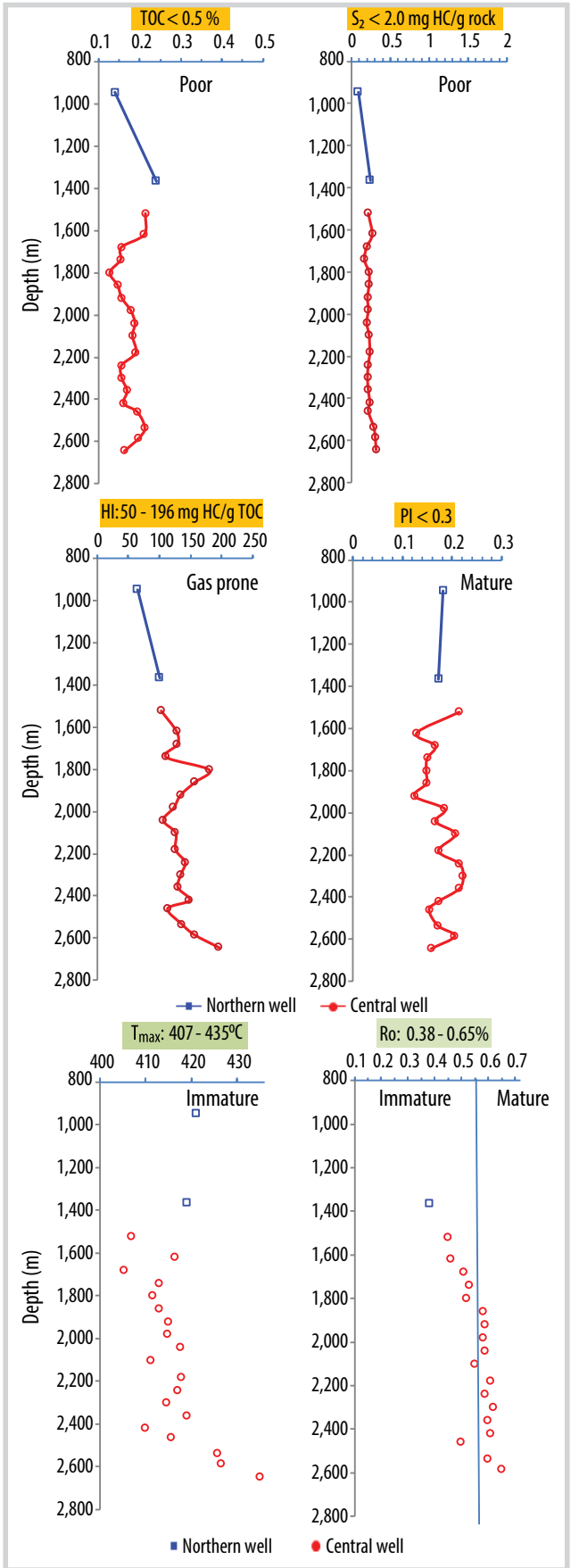

Figure 5. *Comparison of Rock-Eval parameters of Pliocene shales in the northern, central and southern wells.*

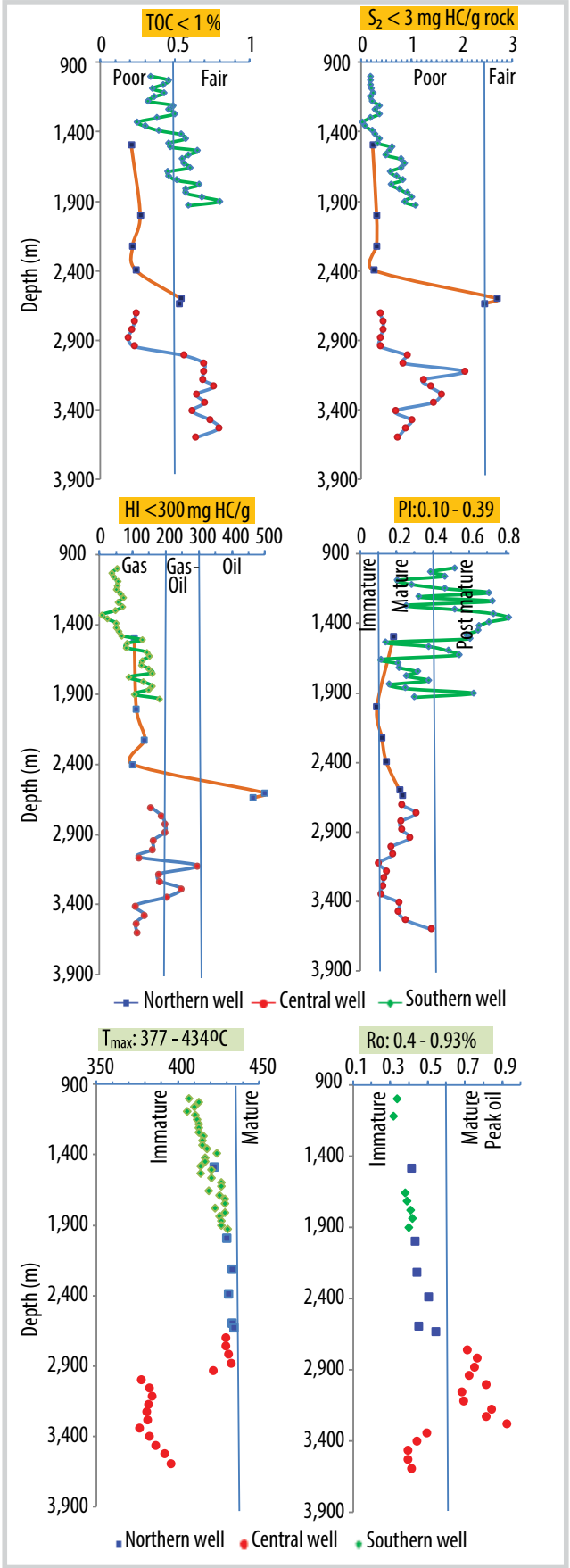

Figure 6. *Comparison of Rock-Eval parameters of the Upper Miocene shales in the northern, central and southern wells.*

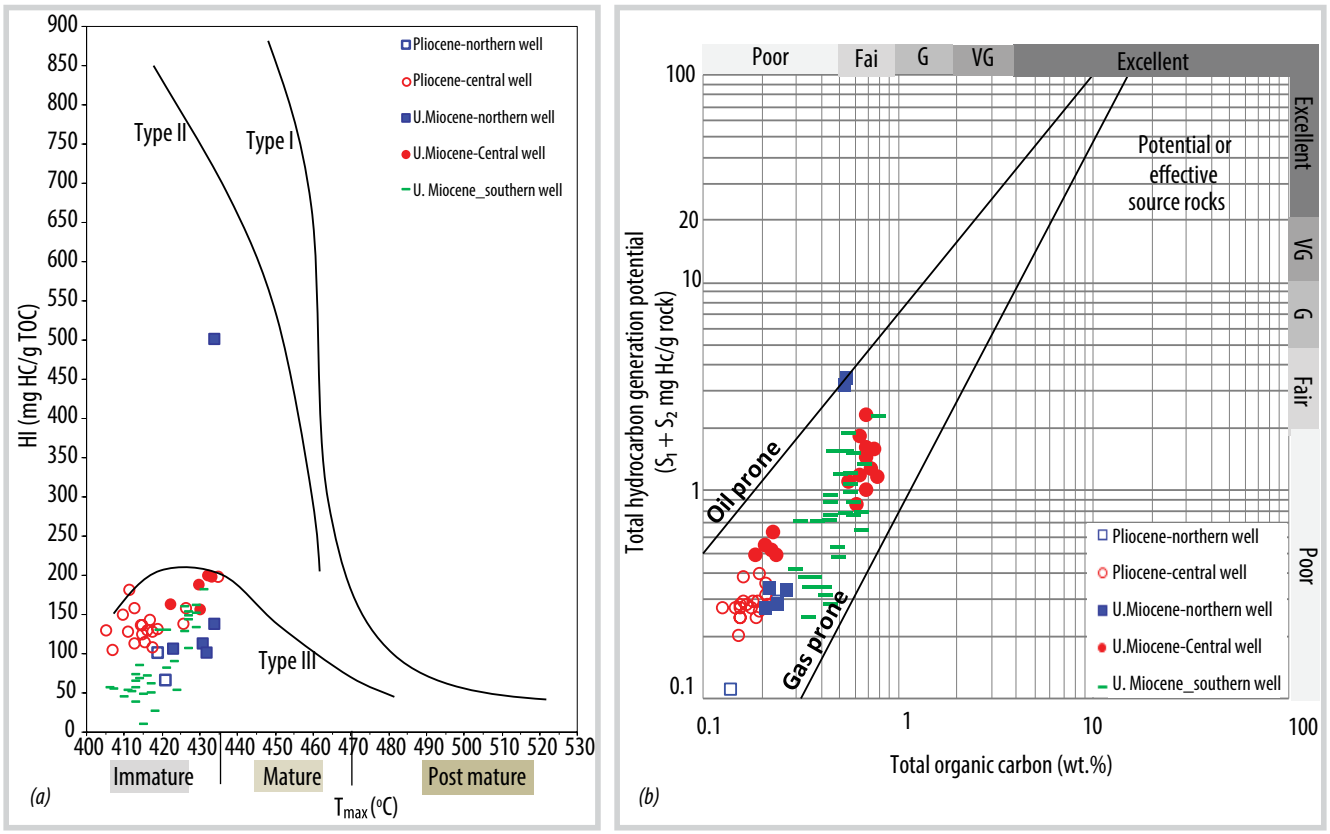

Figure 7. *Kerogen types of organic matter (a) and hydrocarbon generation potential of organic matter (b) in the northern, central and southern wells.*

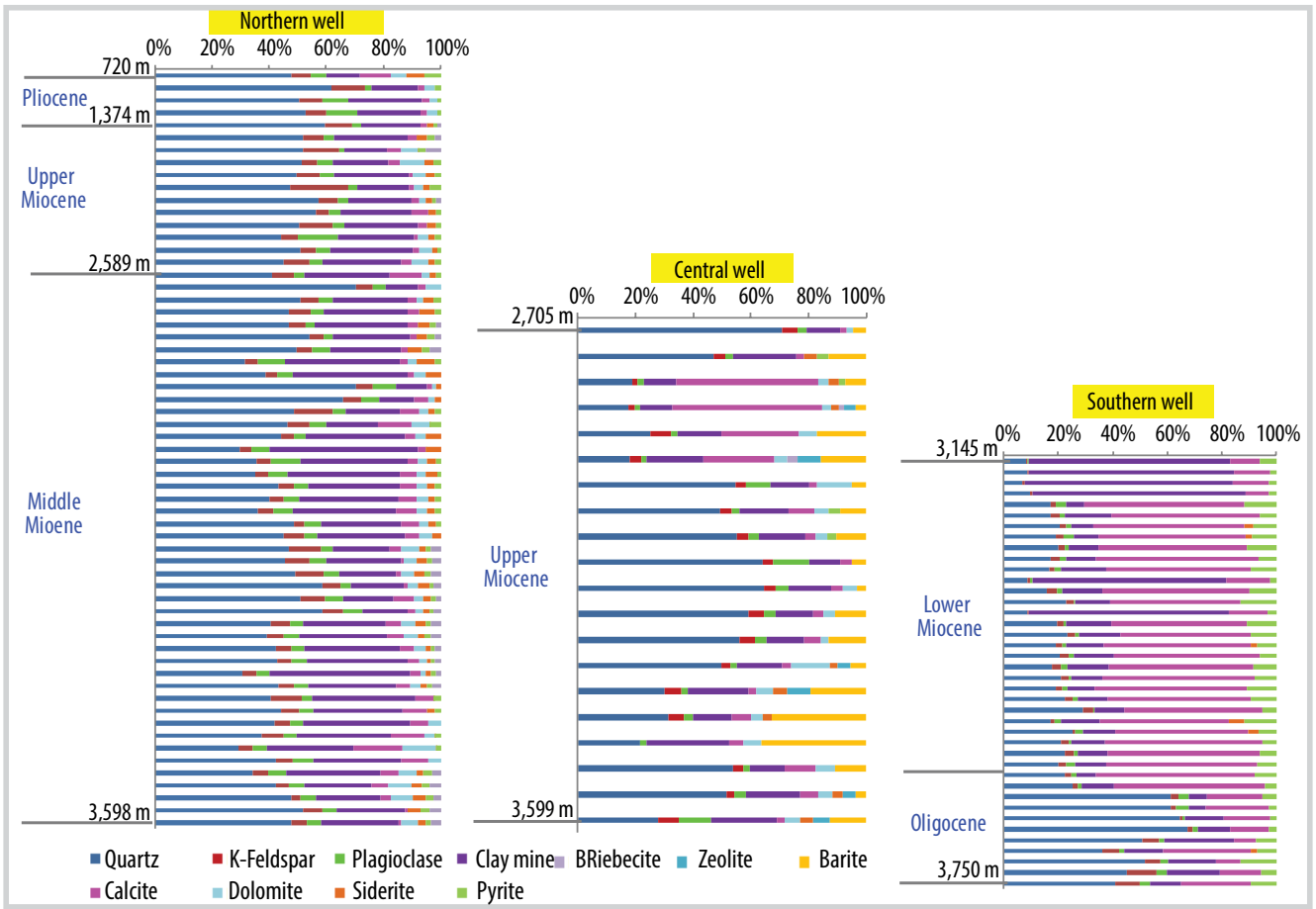

Figure 8. *Minerals of shales in the northern, central and southern wells.*

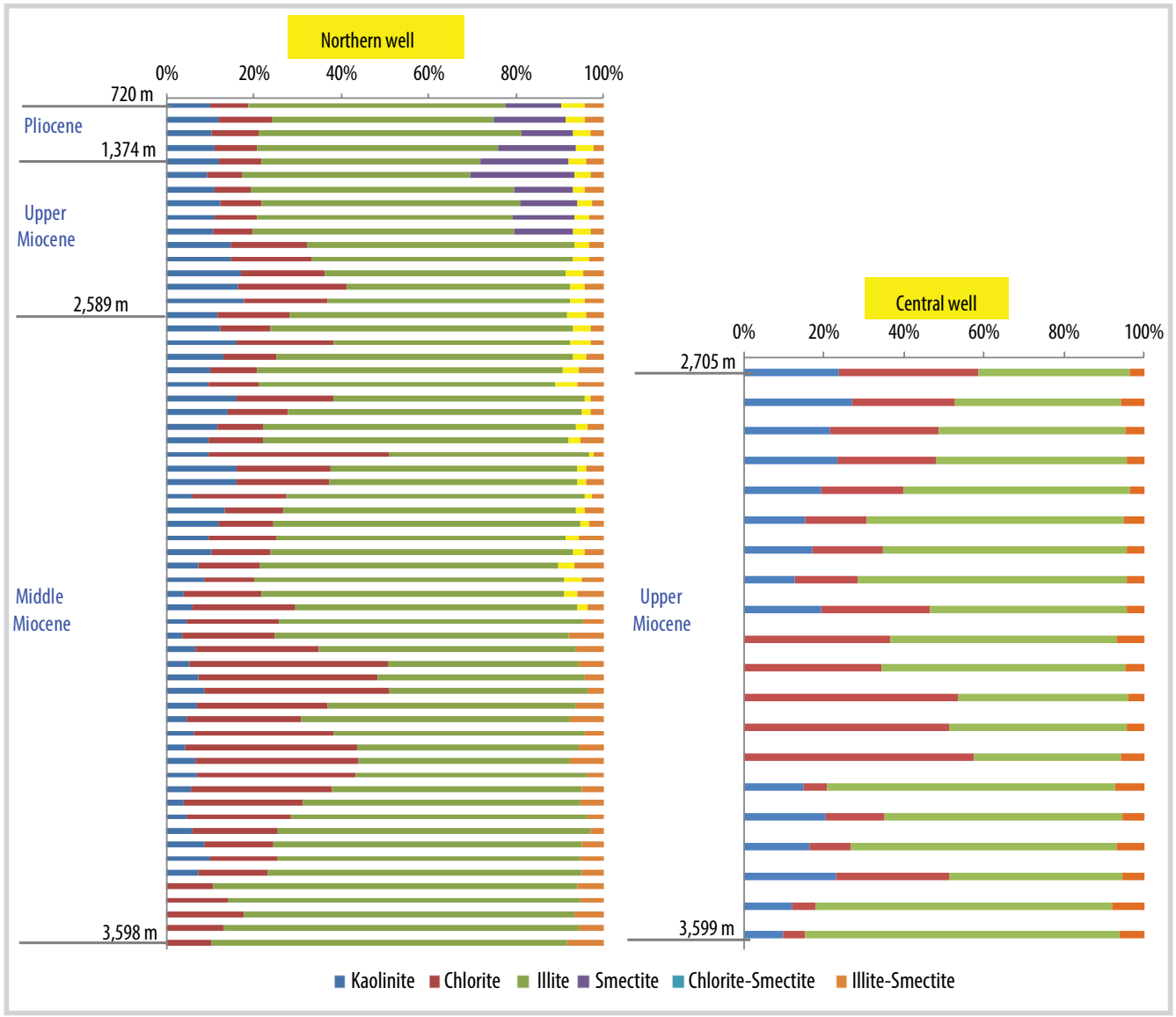

Figure 9. *Clay minerals of shales in the northern, central and southern wells.*

are in mature stage and could have been generating hydrocarbons in the Upper Miocene shales in this part. Some quick findings in this study can be outlined as follows:

- Pliocene and Upper Miocene shales in the northern and southern wells have their TOC, S_2, HI, T_{max} and R_o values of less than 0.5%, 2.5 mg HC/g rock, 200 mg HC/g rock, 435°C and 0.55%, respectively, which indicate poor potential source rocks for little gas generation possibly.

- The Upper Miocene shale samples in the central well comprise TOC varying in two parts of 2,705 - 2,942 m and 3,007 - 3,599 m, i.e., TOC contents are low in the upper part, ranging from 0.19% to 0.24% that indicate typical poor potential source rocks, whereas TOC values range from 0.56% to 0.79% in the lower part, which suggest fair potential source rocks. Moreover, shales in the central part of the Song Hong basin are possibly more favorable conditions for shale gas sections, i.e., these shales are deposited more widely and thicker in a marine environment under the abnormal pressure and high geothermal gradient conditions that are caused by rapid sedimentation rate, continuous loading and incomplete gravitational compaction of sediments, faulting, and phase changes in minerals during compaction, etc. Therefore a considerable amount of gas could possibly be generated from the Upper Miocene shales of the central part into the possible overlying reservoirs in Pliocene sands and/or the Upper Miocene sediments, which can play the double roles of self-source and self-reservoir.

- It is strongly recommended the Pliocene/ Upper Miocene shales and sands be investigated further as potential source rocks and reservoirs. More geological

and structural studies are recommended for a better characterisation of these three major blocks of the Song Hong basin, i.e., the northern, central and southern ones.

Acknowledgements

We would like to thank the reviewer and the editorial team of the Petrovietnam Journal for the constructive comments that help to improve our manuscript.

References

[1] ENI, "ENI confirms and expands gas and condensate potential in the Ken Bau discovery in Block 114, Song Hong basin, offshore Vietnam", 27/7/2020. [Online]. Available: https://www.eni.com/en-IT/media/press-release/2020/07/eni-confirms-and-expands-gas-and-condensate-potential-in-the-ken-bau-discovery-in-block-114.html.

[2] Tập đoàn Dầu khí Việt Nam, "Lô 114 - điểm sáng trong hoạt động tìm kiếm thăm dò ngoài khơi thềm lục địa Việt Nam", 29/7/2020. [Online]. Available: http://pvn.vn/Pages/detail.aspx?NewsID=c80187ba-02e6-4562-a5e5-a2b03ff3b207.

[3] Petrovietnam, *The petroleum geology and resources of Vietnam*, 2nd edition. Science and Technology Publication, 2019.

[4] Vietnam Petroleum Institute, *"Regional study of Song Hong and Phu Khanh basins, Blocks 105-110/4, 114 and 120"*, 2014.

[5] Connah Andersen, A. Mathiesen, Lars Henrik Nielsen, P.V. Tiem, Henrik I. Petersen, and P.T. Dien, "Distribution of source rocks and maturity modelling in the northern Cenozoic Song Hong basin (Gulf of Tonkin) Vietnam", *Journal of Petroleum Geology*, Vol. 28, No. 2, pp. 167 - 184, 2005. DOI:10.1111/j.1747-5457.2005.tb00078.x.

[6] Nguyen Thi Hong Lieu, *"Holocene evolution of the central Red River delta, Northern Vietnam, lithological and mineralogical investigation"*, PhD Thesis, Ernst-Moritz-Arndt-University, Greifswald, Germany, 2006.

[7] Michael B.W. Fyhn, Henrik I. Petersen, Lars Henrik Nielsen, Tran C. Giang, Le H. Nga, Nguyen T.M. Hong, Nguyen D. Nguyen, and Ioannis Abatzis, "The Cenozoic Red River and Beibuwan basins, Vietnam", *Geologic Survey of Denmark and Greenland Bulletin*, Vol. 26, No. 26, pp. 81 - 84, 2012. DOI: 10.34194/geusb.v26.4769.

[8] L.H. Nielsen, A. Mathiesen, T. Bidstrup, O.V. Vejbaek, P.T. Dien, and P.V. Tiem, "Modelling of hydrocarbon generation in the Cenozoic Red River basin, Vietnam: A highly prospective basin", *Journal of Asian Earth Sciences*, Vol. 17, pp. 269 - 294, 1999.

[9] Vo Thi Hai Quan and Pham Huy Giao, "Visual kerogen typing: A case study of the Northern Song Hong basin, Vietnam", in *Advances in Petroleum Engineering and Petroleum Geochemistry*. Springer, 2018, pp. 131 - 134. DOI: 10.1007/978-3-030-01578-7_31.

[10] Vo Thi Hai Quan and Pham Huy Giao, "Geochemical evaluation of shale formations in the northern Song Hong basin, Vietnam", *Journal of Petroleum Exploration and Production Technology (JPEPT)*, Springer Nature, Vol. 9, pp. 1839 - 1853, 2019. DOI: 10.1007/s13202-019-0667-0.

[11] Phạm Khoa Chiết, Nguyễn Thế Hùng, và Trần Đăng Hùng, "Đặc điểm tướng và môi trường trầm tích Miocen sớm - giữa khu vực Lô 102 - 106, Bắc bể Sông Hồng", *Tạp chí Khoa học Đại học Quốc gia Hà Nội: Các Khoa học Trái đất và Môi trường*, Số 32, Tập 2S, trang 153 - 163, 2016.

[12] Kevin McCarthy, Katherine Rojas, Martin Nienmann, Daniel Palmowski, Kenneth E. Peters, and Artur Stankiewicz, "Basic petroleum geochemistry for source rock evaluation", *Oilfield Review*, Vol. 23, No. 2, pp. 32 - 43, 2011.

[13] Kenneth E. Peters, "Guideline for evaluating petroleum source rocks using programmed pyrolysis", *The AAPG Bulletin*, Vol. 70, No. 3, pp. 318 - 329, 1986. DOI: 10.1306/94885688-1704-11D7-8645000102C1865D.

PETROVIETNAM JOURNAL
Volume 10/2022, pp. 12 - 18
ISSN 2615-9902

A MACHINE LEARNING APPROACH FOR CALIBRATING SEISMIC INTERVAL VELOCITY IN 3D VELOCITY MODEL

Le Hong Quan[1], Tran Dong[2], Nguyen Van Tien[1], Nguyen Dac The[2]
[1]Russia - Vietnam Joint Venture (Vietsovpetro)
[2]Schlumberger
Email: quanlh.hq@vietsov.com.vn
https://doi.org/10.47800/PVJ.2022.10-02

Summary

Velocity model technique is routinely used to convert data from the time-to-depth domain to support prospect evaluation, reservoir modelling, well engineering, and further drilling operation. In Vietnam, the conventional velocity model building workflow oversimplifies the interval velocities as only well interval velocities are populated into 2D grids for depth conversion or oversimplified calibration interval velocities by applying a single scaling factor function. This study explores the 3D velocity model workflow to obtain accurate and high-resolution interval velocities using a machine learning approach for both fields A and B in Cuu Long basin, offshore Vietnam.

To design an effective approach to depth conversion, the anisotropy factor analysis was performed to understand the differences between the seismic and well interval velocities in geological layer in the 3D structural model. The seismic interval velocity was multiplied by the anisotropy factor to achieve the scaling seismic interval velocity. The scaling seismic interval velocity, elastic attributes, geometric attributes, structural and stratigraphic attributes were used as training features (variables) for predicting interval velocity using the supervised learning algorithm in the machine learning model. Supervised learning offers an opportunity to develop an expert-knowledge-based automated system, which incorporates both domain knowledge and quantitative data mining [1]. The random forest regression algorithms were selected for predicting interval velocity after evaluating several machine learning algorithms. To provide insight into the uncertainty of final interval velocity, a depth uncertainty analysis was conducted using a blind well test for 24 wells and 7 horizons.

The comprehensive 3D velocity model using machine learning approach was built for the first time in Cuu Long basin, offshore Vietnam. The result showed the machine learning algorithm can address the disadvantages of conventional velocity calibration to create highly accurate depth representations of the subsurface including a measure of the uncertainty.

Key words: Velocity model, seismic attribute, depth uncertainty analysis, machine learning, Cuu Long basin.

1. Introduction

The velocity profile of the field can be simple or complex depending on the data quality and the complexity of geological data, the calibration interval velocity played a significant role in providing accurate time-depth conversion results. The conventional approach of calibrating internal velocity is a linear relationship between seismic interval velocity with well interval velocity. The high uncertainty associated with time-to-depth conversion can lead to unreliable reservoir depth models, ambiguous reservoir volumetric calculations and potential drilling hazards.

Machine learning is a branch of artificial intelligence (AI) and computer science which focuses on the use of data and algorithms to imitate the way that humans learn, gradually improving its accuracy. Encouraged by the rapid growth of machine learning techniques and by their huge success in other industries, the geoscience community has embarked upon initiatives to integrate machine learning capabilities into geophysical data analysis [2].

In this study, the supervised learning algorithms (multiple linear regression, multiple polynomial regression, gradient boosting regression, random forest

Date of receipt: 15/8/2022. Date of review and editing: 15/8 - 5/10/2022.
Date of approval: 5/10/2022.

regression) were used for predicting interval velocity. The machine learning model was trained on selected input data (the scaling seismic interval velocity, geometric attributes, structural and stratigraphic attributes) and supervised with well interval velocity. As a result, the best supervised learning algorithms were selected for being capable of predicting further outcomes (interval velocity) for a 3D velocity model.

This paper showed an innovative methodology for calibrating interval velocity by predicting interval velocity from the machine learning approach. The final calibrating interval velocity was evaluated numerically, visually, and for geological consistency, while the depth uncertainty could be estimated from a depth error analysis in a blind well test method.

2. Methodology

2.1. 3D Structural model

In this case study, the 3D structural model was created by using seven horizons in the time domain with reasonable horizontal and vertical velocity resolution (Figure 1). This is because seismic velocities in general can provide a reliable regional velocity trend and the velocity field varies smoothly with depth. Therefore, the small horizontal and vertical resolution is not necessary for the velocity model process. The vertical resolution can be measured via standard variogram analysis, and it is recommended not to be greater than half of the vertical range [3].

2.2. Velocity data preparation and analysis

There are several areas we need to focus on during the review of velocity data to ensure the good quality input data for velocity model building. Poorly positioned wells, miscorrelated horizons, and inconsistent formation tops can introduce distortions in the implied velocity field and result in false structuring.

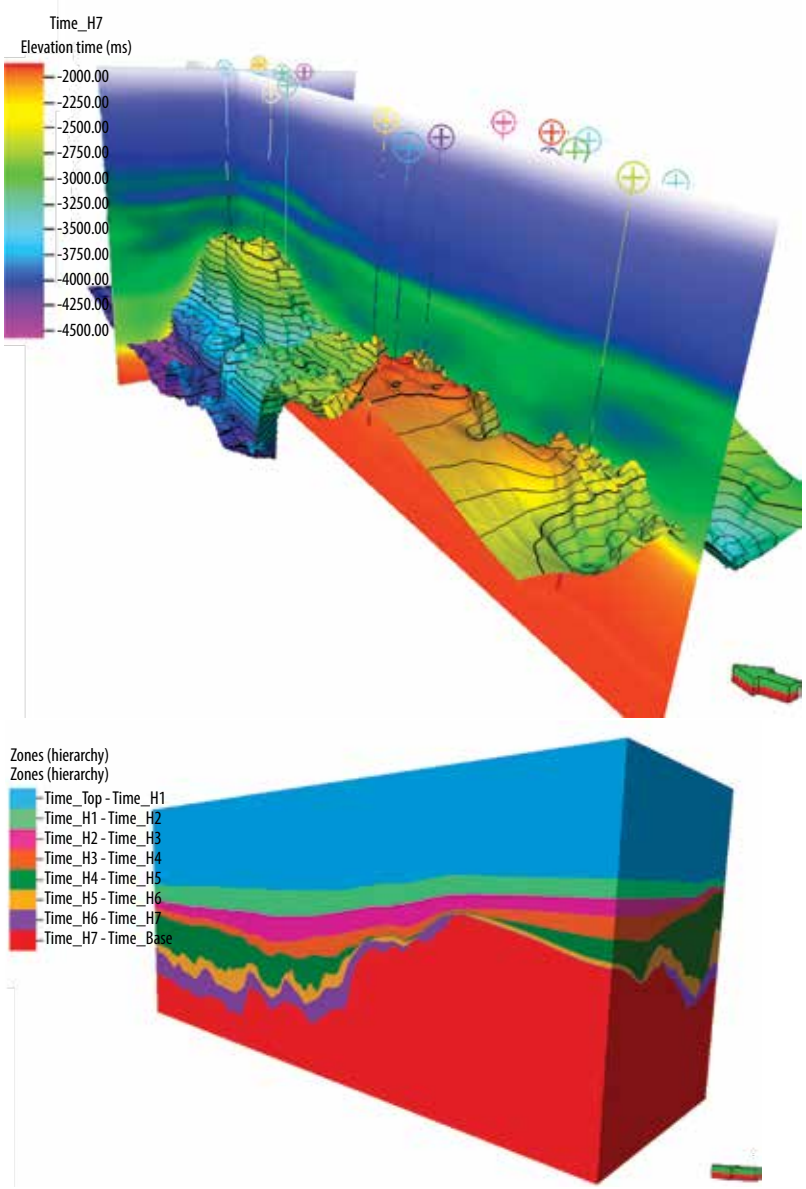

Figure 1. *3D structural model creation.*

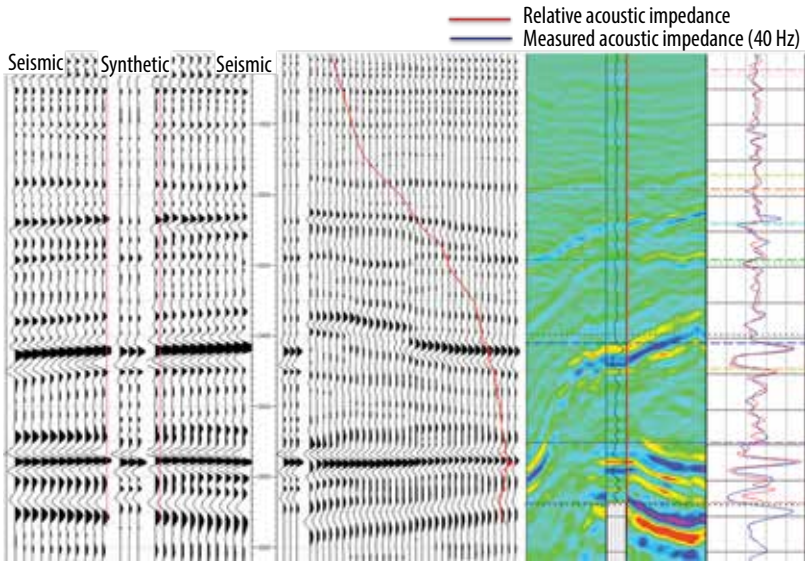

Figure 2. *The seismic well-tie QC step.*

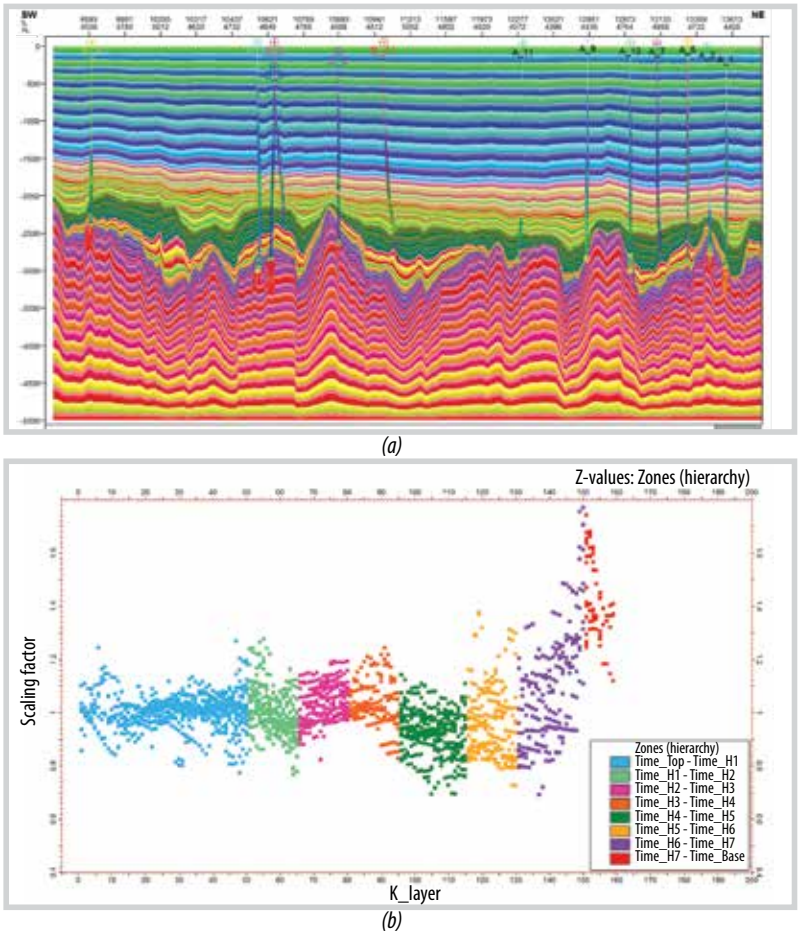

Figure 3. *The scaling factor varies with the geological layer in the 3D structural model.*

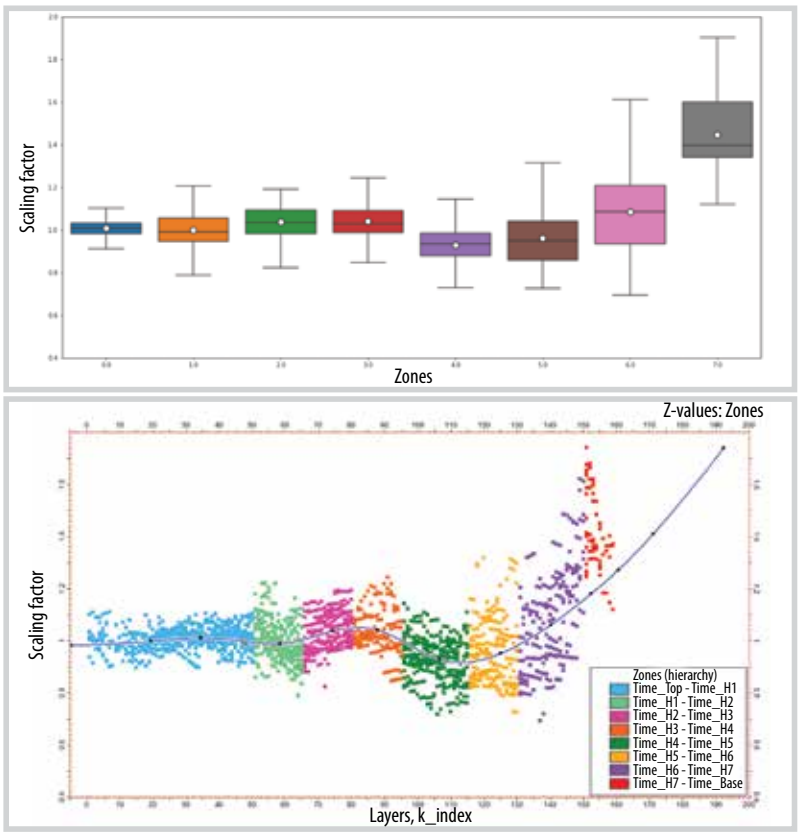

Figure 4. *The best-fit curve for scaling seismic interval velocity.*

The seismic well-tied is one of the key components of the velocity modelling workflow. It is the bridge between geological information (well data in depth) and geophysical information (seismic in time). The seismic well-tie was done for 24 wells in this study. The generated synthetic was compared with seismic data to determine the amount of time shift/ stretching required on the time-depth relationship (TDR) to improve the matching between well logs and seismic data. The relative acoustic impedance (generated using preliminary inversion parameters) was also compared with the measured acoustic impedance log at well location with the well-tied TDR.

The scaling factor is the quotient of well interval velocity and seismic interval velocity and is a function of geological layer in the 3D structural model. The objective of the scaling factor process was to scale the seismic interval velocity to the well interval velocity by understanding how the velocity varies vertically and horizontally.

The intersection in Figure 3a shows the geological layer in the study area and the cross-plot in Figure 3b shows how the scaling factor varies with the geological layer in the 3D structural model. The X-axis shows the geological layers (K_layer) while the Y-axis displays the scaling factor which is the quotient of well interval velocity and seismic interval velocity. The scaling factor value equals to 1 means the well interval velocity has the same value as the seismic interval velocity. The scaling factor value is greater than 1 means the well interval velocity is faster than the seismic interval velocity. The well interval velocity is slower than the seismic interval velocity when the scaling factor value is less than 1.

The scaling factor can be displayed as boxplot and removed interval velocity outlier of each zone before digitising a best-fit curve for scaling seismic interval velocity (Figure 4). The scaling factor points above the best-fit curve (blue curve) has positive

error while the scaling factor points below the best-fit curve has negative error.

The scaling interval velocity quality was examined by the residual scaling factor (the quotient of the wells interval velocity and the scaling seismic interval velocity) and the correlation between scaling seismic interval velocity with well interval velocity. The scaling factor value was reduced and improved the correlation between seismic interval velocity with well interval velocity after applying the scaling factor (Figures 5 and 6). However, the high variation of residual scaling factor was presented below the H4 zone since the complex structural geology of these zones. Often, the degree of geological complexity causes significant variation of the residual scaling factor when seismic interval velocity is calibrated with well interval velocity using the single scaling function.

2.3. Machine learning approach for interval velocity prediction

Machine learning can support interpretation through the identification and characterisation of underlying patterns in seismic and log data that are beyond human comprehension or obscured through traditional means of visualising and interacting with the data [1]. The elastic attributes (acoustic impedance, density and the compressional to shear-wave velocity ratio), structural and stratigraphic attributes (3D curvature, chaos, ISO-frequency) were generated and resampled into a 3D structural model. Then, these attributes and scaling seismic interval velocity were exported with geometric attributes information (IJK grid cell indices, XYZ grid cell coordinates) from proprietary E&P software platform to a web-based interactive computing platform to build the machine learning model.

To train the machine learning model, the collection features were divided into two parts, training data and test data. The training data was implemented to build up a machine learning model, while the test data was to validate it. K-fold cross-validation (K = 5) was

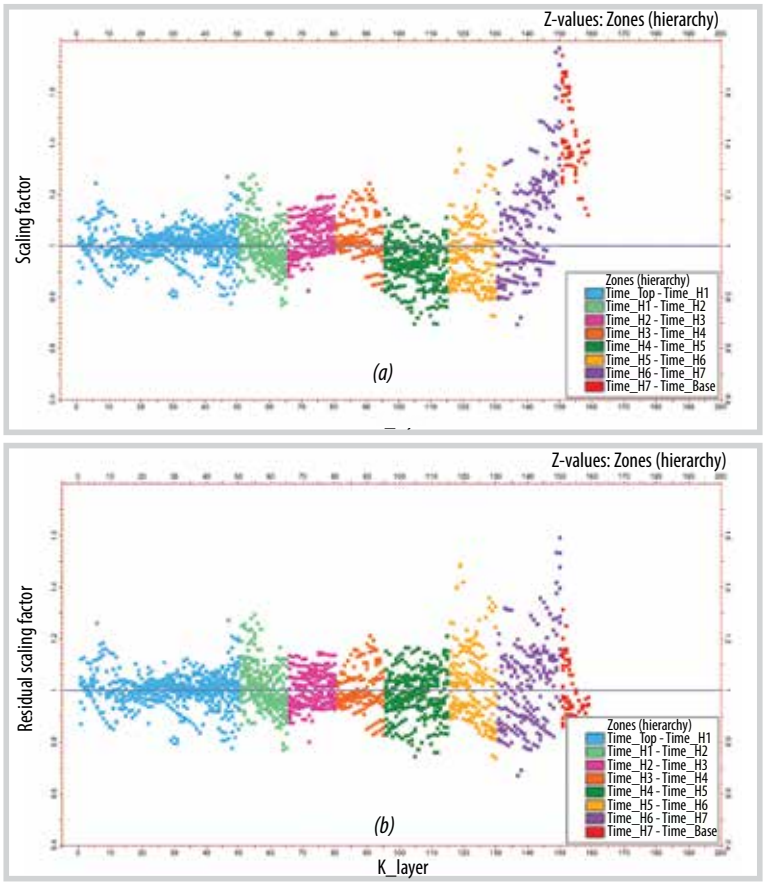

Figure 5. *The scaling factor (a) and the residual scaling factor (b).*

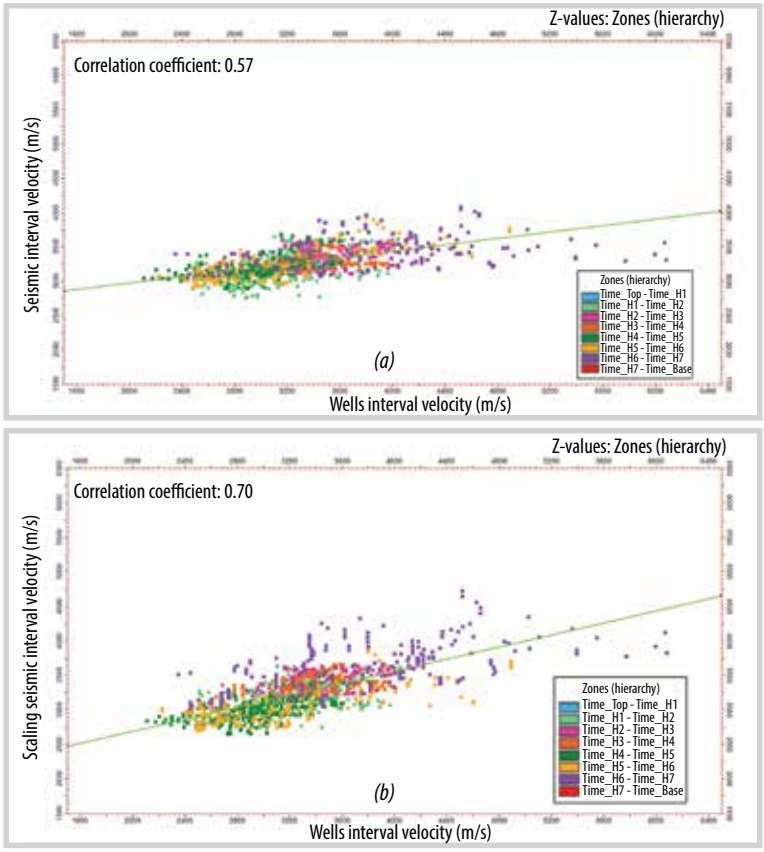

Figure 6. *The correlation between seismic interval velocity and well interval velocity (a), and the correlation between scaling seismic interval velocity and well interval velocity (b).*

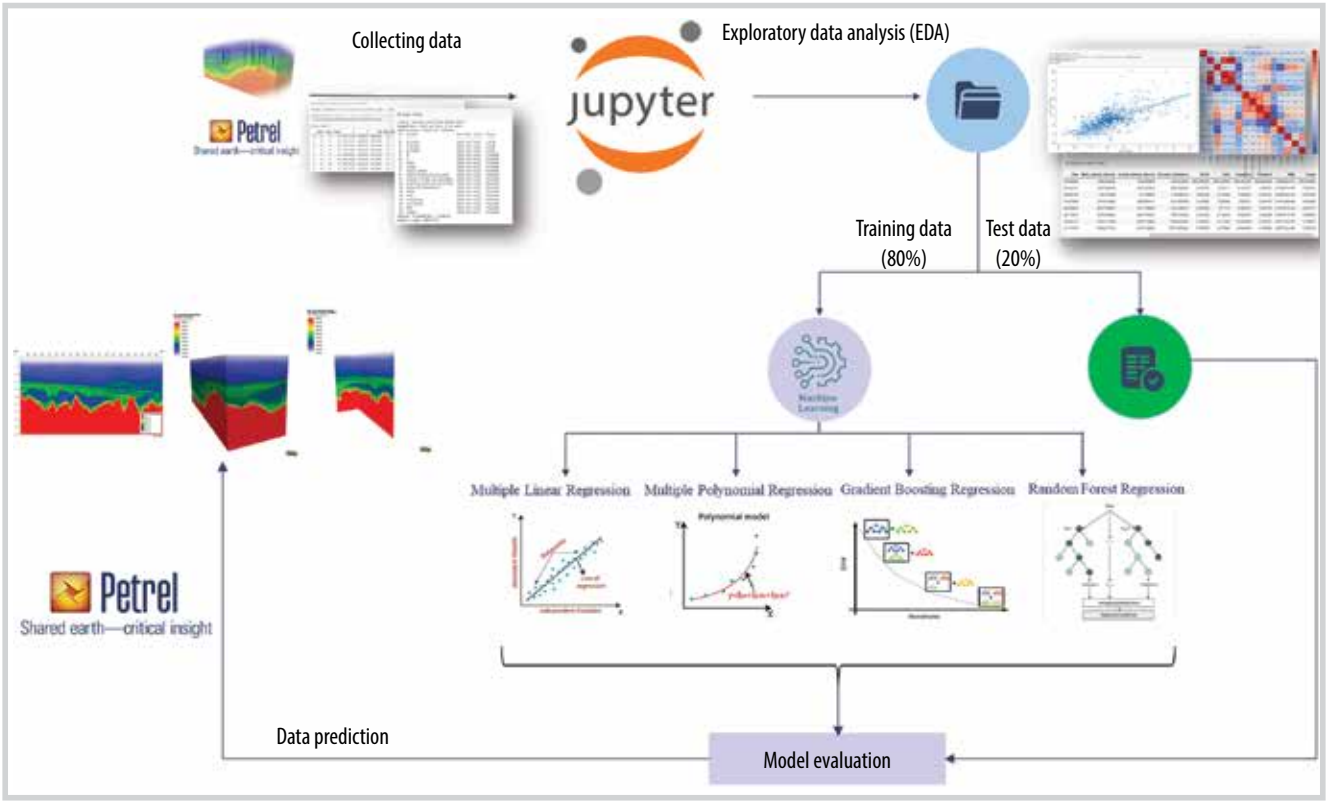

Figure 7. *The general workflow for predicting interval velocity using machine learning approach.*

Table 1. *The evaluation metrics for model evaluation*

Machine learning algorithm	R-squared (%)	Mean squared error	Mean absolute error
Random forest regression	80.5	55484.61	156.04
Gradient boosting regression	77.90	61728.01	180.55
Multiple polynomial regression	63.80	78214.99	202.47
Multiple linear regression	59.70	103826.06	236.28

also implemented to estimate the skill or performance of the machine learning model and avoid overfitting during the training process.

Model evaluation is an integral part of the model development process. It helps to find the best model that represents our data and how well the chosen model will work for predicting new datasets. Three evaluation metrics were used in this study, mean absolute error (MAE), mean squared error (MSE) and coefficient of determination (R2). The random forest regression algorithm [4] showed the best algorithm (the highest R-squared, the lowest mean squared error and mean absolute error) for predicting interval velocity in this study (Table 1).

The random forest regression model was used for predicting interval velocity for target zones from H1 to H7, the result of interval velocity prediction was re-imported to a proprietary E&P software platform to build the 3D velocity model for domain conversion.

2.4. Depth uncertainty analysis

The depth uncertainty analysis was performed for all 24 wells and 7 horizons in this study to estimate the depth uncertainty of the velocity model for both methods (scaling factor function and machine learning algorithm). The depth comparison between the actual horizons and the calculated horizons of each well (using adjusted velocities by excluding one well) was performed to understand the variation of depth error (depth residual).

For example, the new (partial) velocity model was rebuilt using calibrated seismic interval velocities of all wells (from well 1 to well 23, except well 24) to convert all the horizons of well 24 from time to depth. The actual horizons of well 24 were used to correlate with the calculated depth of horizons to estimate the depth residual of all horizons at well 24. The process was repeated for the rest of other wells (well 1 to well 23) to

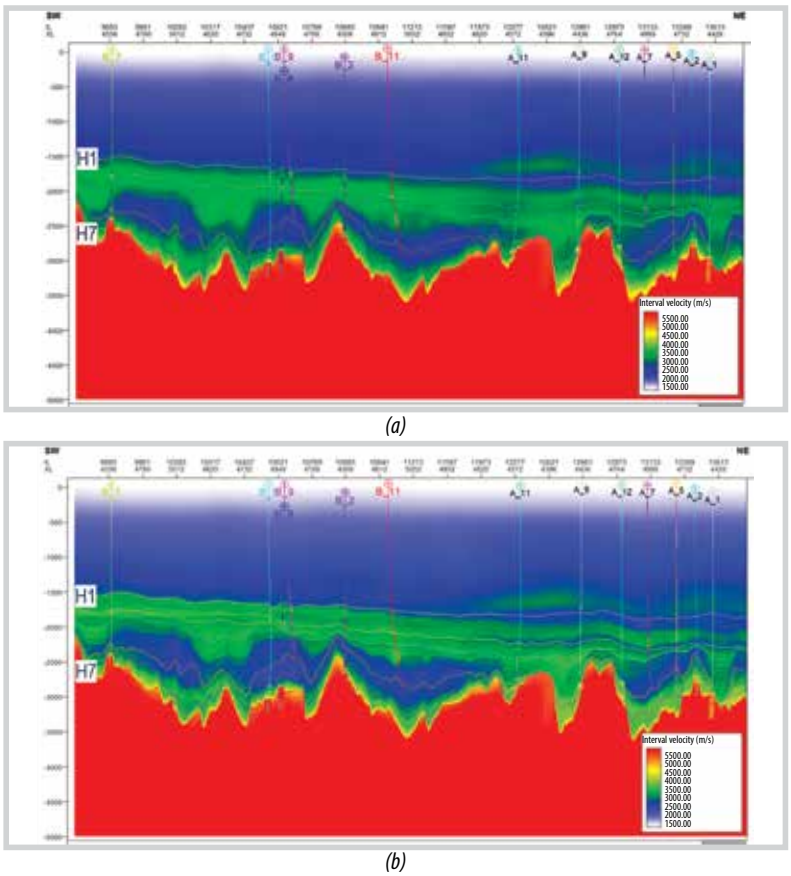

Figure 8. *The scaling seismic interval velocity using scaling factor function (a) and the final interval velocity using machine learning approach (b).*

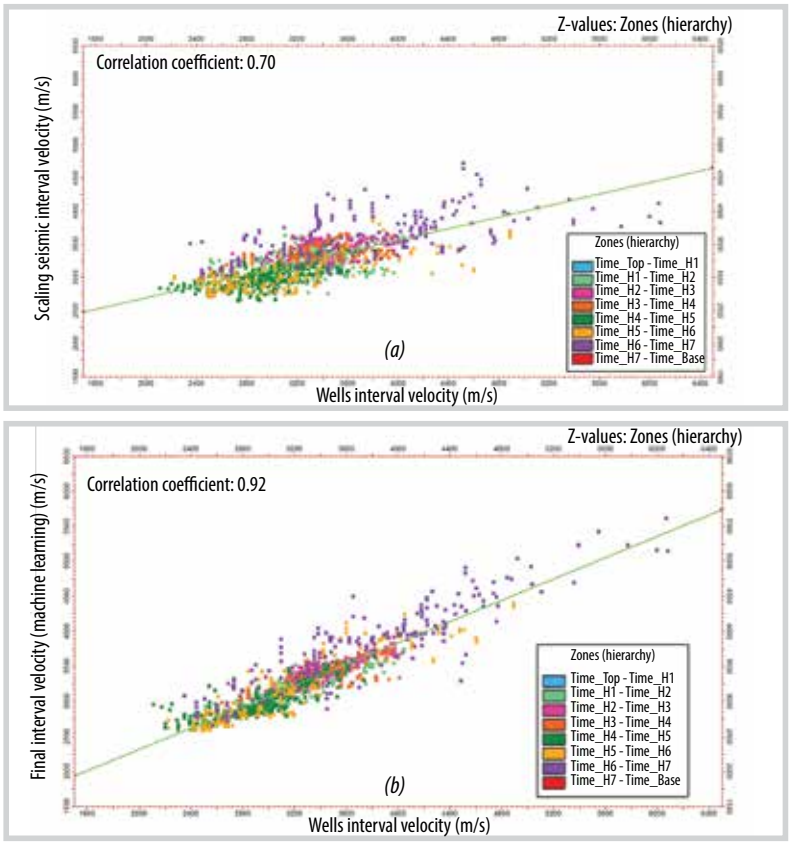

Figure 9. *The correlation between scaling seismic interval velocity and well interval velocity (a), and the correlation between final interval velocity (machine learning approach) and well interval velocity (b).*

obtain the depth residual range of horizons for all wells in this field.

3. Results and discussion

The final interval velocity using machine learning approach preserved high resolution velocity from the zone H1 to H7, reduced residual scale factor and improved significant correlation between final interval velocity with well interval velocity (Figures 8 and 9).

The residual scaling factor value is around 1 in the cross-plot, which indicates that the calibrated seismic interval velocity is approximate to the well interval velocity (Figure 10b). The range residual scaling factor of the machine learning approach was minimised compared to the single calibrating function approach below the zone H4.

The depth uncertainty results performed by 2 different approaches of the scaling factor function (traditional method) and machine learning algorithm (a new approach) (Table 2). The result proved that the machine learning algorithm can address the disadvantages of the conventional velocity calibration to preserve lateral and vertical velocity resolution while reducing the uncertainty of time-to-depth conversion. The depth uncertainty analysis shows the mean uncertainty prognosis is 15.56 m at the top horizon H1 (approximately 0.76% depth uncertainty vs. target depth) and the mean uncertainty prognosis is 19.64 m at the base horizon H7 (approximately 0.56% depth uncertainty vs. target depth).

Due to the complexity of the geological structure the residual range is increased at deeper parts (H5 to H7). However, by using machine learning algorithms, the mean uncertainty prognosis was reduced up to 37.33% compared to the conventional scaling factor function approach below the H4 because the range residual scaling factor was minimised in these zones.

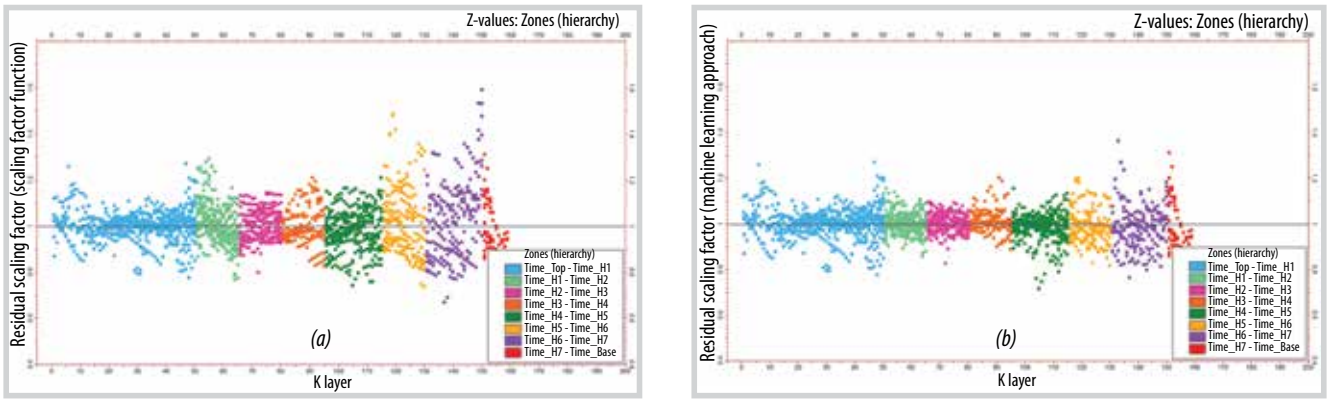

Figure 10. *The residual scaling factor using scaling factor function (a) and residual scaling factor using machine learning approach (b).*

Table 2. *The depth uncertainty analysis result*

Zone	Scaling factor function		Machine learning algorithm	
	Residual range (m)	Mean residual (m)	Residual range (m)	Mean residual (m)
H1	-25.58 - 32.21	15.43	-27.34 - 33.31	15.56
H2	-55.81 - 33.30	15.67	-56.29 - 29.67	13.91
H3	-30.99 - 35.84	16.42	-31.64 - 34.78	14.77
H4	-42.62 - 35.58	14.03	-26.96 - 33.66	12.47
H5	-34.64 - 54.29	22.55	-34.11 - 31.18	19.43
H6	-80.15 - 36.48	27.88	-41.01 - 18.51	21.10
H7	-89.75 - 24.40	31.34	-49.84 - 34.29	19.64

4. Conclusion

The study demonstrated the machine learning algorithm predicted accurate interval velocity including a measurement of the uncertainty. An accurate 3D velocity model is important not only for the converted depth surfaces but also the depth conversion of the seismic inversion results such as acoustic impedance, density, compressional and shear velocity cubes. The final calibrated interval velocity cube could be applied for 1D/3D pore pressure analysis and 1D/3D mechanical earth model (geomechanics) study, as well as basin modelling processes, etc.

In order to combine classic geo-statistics with quantile random forests algorithm in machine learning model, the embedded model estimator (EMBER) algorithm can be applied for predicting interval velocity with embedded estimations based on neighbouring well data using random forest algorithm in this field in the future. The used algorithm is a modified decision forest so that it trains the predictive ability of the spatial estimator as well as the standard data variables (embedding). Realisations with realistic geological texture can be performed by sampling from the envelope with an appropriate stationary random function allowing for additional hard conditioning at the data sample locations if required [5].

Acknowledgements

The authors would like to thank Vietsovpetro J/V and Schlumberger for their support and permission to publish this work.

References

[1] Laura Bandura, Adam D. Halpert, and Zhao Zhang, "Machine learning in the interpreter's toolbox: Unsupervised, supervised, and deep-learning applications", *SEG International Exposition and Annual Meeting, USA, 14 - 19 October 2018*. DOI: 10.1190/segam2018-2997015.1.

[2] Zhao Zhang, Adam D. Halpert, Laura Bandura, and Anne Dutranois Coumont, "Machine learning based technique for lithology and fluid content prediction – Case study from offshore West Africa", *SEG International Exposition and Annual Meeting, USA, 14 - 19 October 2018*. DOI: 10.1190/segam2018-2996428.1.

[3] Eduardo Lugo Flores, Marcos Victoria, and Guillermo Sanchez Roa, "Depth conversion: Application of an innovative methodology: Added value to a fractured carbonate reservoir interspersed with tertiary and Mesozoic salt bodies within a very complex structural setting", *EUROPEC/EAGE Conference and Exhibition, UK, 11 - 14 June 2007*. DOI: 10.2118/106650-MS.

[4] Leo Breiman, "Random forests", *Machine Learning*, Vol. 45, pp. 5 - 32, 2001. DOI: 10.1023/A:1010933404324.

[5] Colin Daly, "An application of an embedded model estimator to a synthetic nonstationary reservoir model with multiple secondary variables", *Frontiers in Artificial Intelligence*, Vol. 4, 2021. DOI: 10.3389/frai.2021.624697.

PETROVIETNAM JOURNAL
Volume 10/2022, pp. 19 - 27
ISSN 2615-9902

A SUCCESSFUL PILOT APPLICATION OF THE COMPLEX MIXTURE SURFACTANT POLYMER VPI SP TO ENHANCE OIL RECOVERY FACTOR FOR THE LOWER MIOCENE, BACH HO FIELD

Dinh Duc Huy[1], Nguyen Minh Quy[1], Pham Truong Giang[1], Hoang Long[1], Le Thi Thu Huong[1], Cu Thi Viet Nga[1]
Pham Xuan Son[2], Nguyen Lam Anh[2], Ho Nam Chung[2], Pham Trung Son[2], Nguyen Quynh Huy[2], Tran Thanh Nam[2]
[1]Vietnam Petroleum Institute
[2]Vietsovpetro
Email: huydd@vpi.pvn.vn
https://doi.org/10.47800/PVJ.2022.10-03

Summary

Enhanced oil recovery (EOR) implementation at field scale is complex. Therefore, pilot applications are usually conducted before field execution. This paper introduces a pilot project successfully applied for the Lower Miocene, Bach Ho field. Topics covered include: (i) pilot area selection, (ii) chemical preparation, (iii) specification and pilot design for execution, (iv) implementation, (v) pilot observation and interpretation, (vi) efficiency evaluation. The implementation of pilot projects is achieved on 23 January 2022. The evaluation shows that 2,700.2 tons of oil gained thanks to the application of the surfactant-polymer complex mixture (VPI SP).

Key words: Enhanced oil recovery, VPI SP, Lower Miocene, Bach Ho field.

1. Introduction

Bach Ho oil field started producing oil from the Miocene in 1986 while the south dome in 2011 on BH-441. The initial oil in place of the Miocene was approximately 80.05 million tons, of which 27.17 million tons came from the Lower Miocene, south dome (BK14/16). The reservoir in BK14/16 consists of 5 main sand bodies from layer 22 to layer 27 with an average depth of 2,300 mTVDss. The target layer in the pilot plan is layer 23, sandstone formation; the remaining oil volume in place is ~5 million tons. Layer 23 formation distribution is wide and thick, with medium to high permeability and support energy from the flank water (Figure 1).

2. Pilot area selection

The implementation of enhanced oil recovery plans at field scale is complex and difficult. Thus, before applying at field scale, the size of the solution should be first scaled down then increased step by step [1]. In addition, defining clear pilot objectives and execution will lead to a successful pilot. On the other hand, pilots carrying out need to weigh against the time and expense [2]. To minimise the uncertainty of chemical injections for increasing oil recovery of the Lower Miocene, Bach Ho field, a few key points need to be specified to prioritise the objects to consider.

- The preliminary screening evaluation in the pilot area is convincing technically and economically;

- Well pattern/well configuration is typical in the field with the extent of the communication between injector and producer, and effective water injection is preferable in this case;

- The volume of oil remains after the secondary stage;

- Available facilities in the pilot area are adaptable to the technology of EOR implementation.

The objective of the pilot plan is carefully selected. The results indicate that the location of injector 1609/BK16 is the likely area for EOR execution as follows:

- The results of dynamic model simulation and feasible study show the highest value [3];

- Distribution of the main reservoir (layer 23 sand body) is wide and fairly thick (23-0: 3.3 m, 23-1: 4.3 m, 23-2: 16.5 m) (Figures 1 & 3);

Date of receipt: 9/9/2022. Date of review and editing: 9/9 - 20/9/2022.
Date of approval: 5/10/2022.

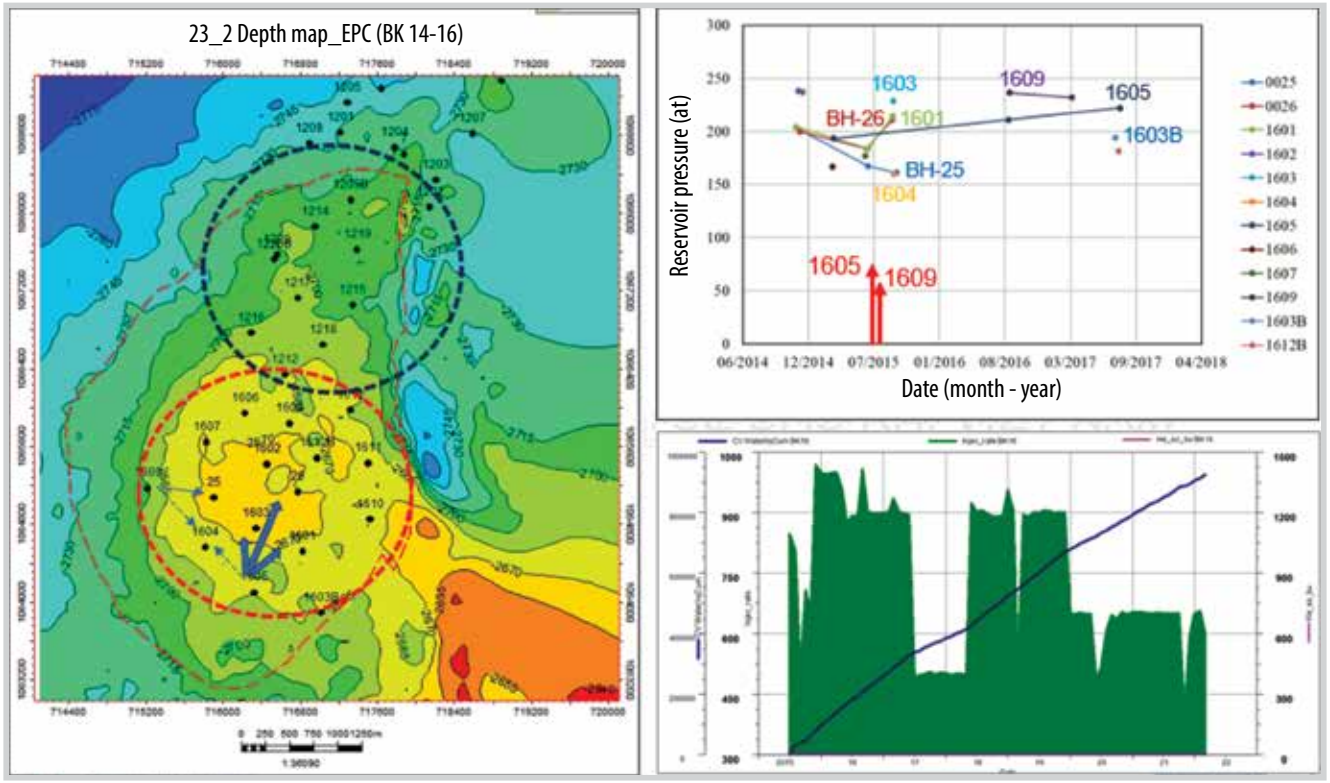

Figure 1. *Geology information and well parameters of BK16 area.*

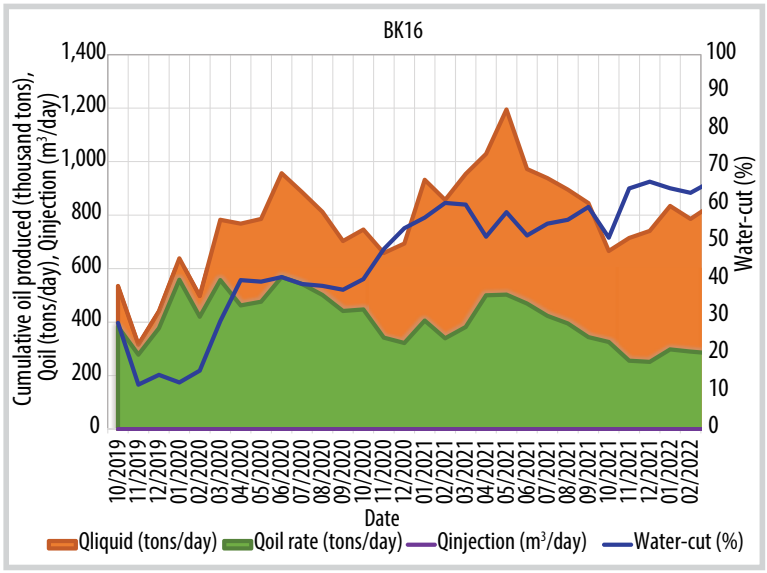

Figure 2. *The production performance of BK16.*

- Well spacing (500 x 500 m) and well pattern are typical for Bach Ho field while good communication between 1609 and the surrounding well is observed;

- The amount of remaining oil after production shows a high potential;

- Available facilities of BK16 are adaptable for injection chemical strategy.

Based on log interpretation results, mobile water is not observed at the initial condition of the interlayers 23_1 and 23_2, while it appears in the interlayers 23_3, 23_4 and 24, 25. In the western area (wells 1605, 1604, 1609), water saturation is higher than other locations in the interlayer 23_2. The net pay thickness of the interlayer 23_2 is quite good (12 - 16 m) but decreases rapidly toward the boundary. The net pay thickness of the interlayer 23_2 in the well area 1609 (16.5 m) is better than the well area 1605 (8.2 m).

BK16 was put into production in 2012, reaching an oil peak of 707 thousand tons per year in 2015. Producers are located at the top of the reservoir with favourable distances of 500 - 600 m to the injector. All producers have a high initial oil rate of 150 - 400 tons/day with water content less than 15% (Figure 2). In January 2022, total oil and liquid produced were 1.6 million tons and 2.8 million tons, respectively. The oil rate of all wells was lower than 20 tons/day with high water content in fluid streams (75 - 91%). The analysis of produced samples indicated that the ratio of water injection increased in water content. Survey results confirmed that all producers operated under a pressure regime which was higher than saturation pressure. Therefore, EOR is considered to maintain oil rate.

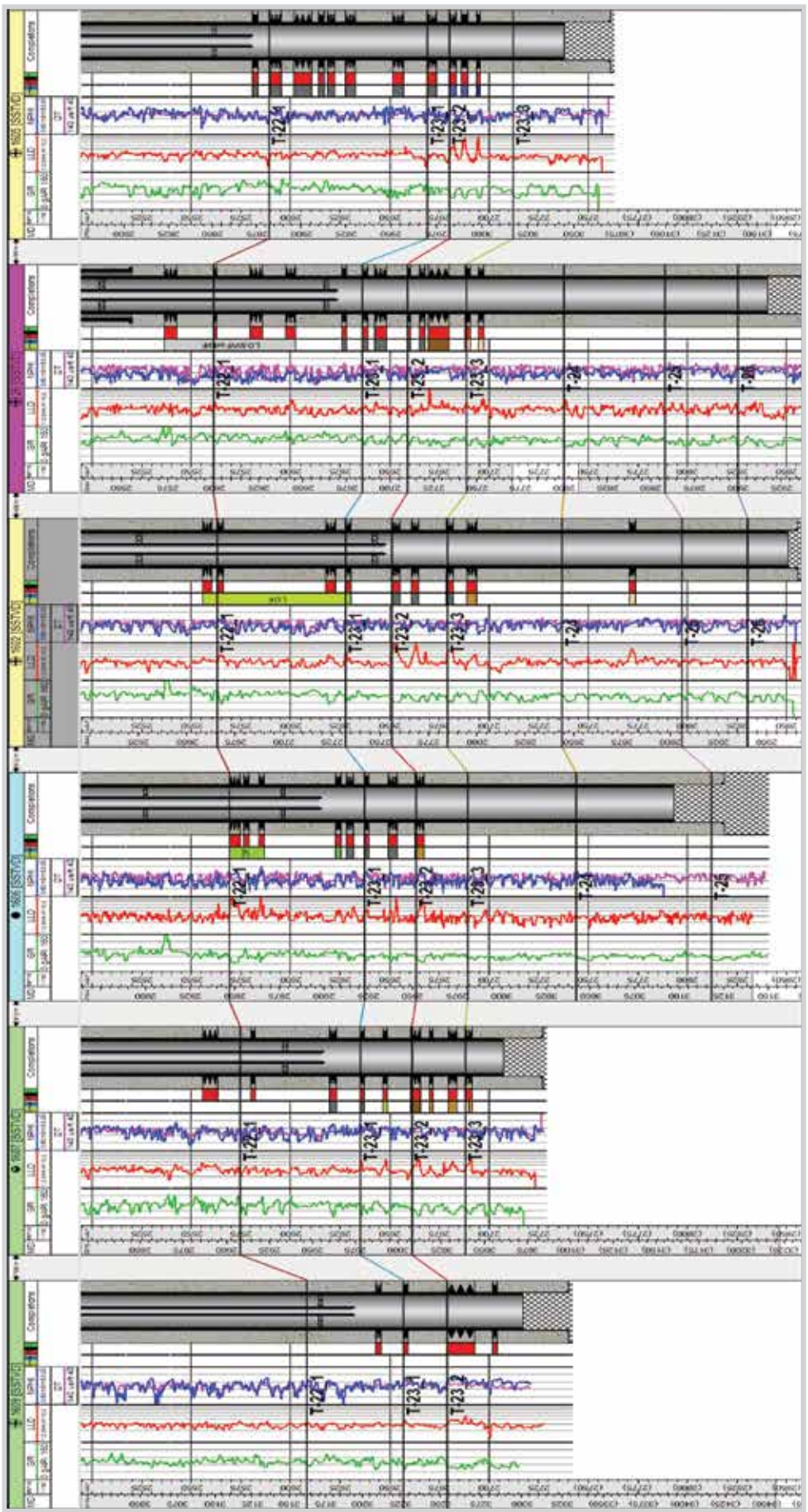

Figure 3. Well correlation of 1609/BK16 and the surrounding wells

3. Chemical preparation

The main components of the complex mixture surfactant-polymer made by VPI (VPI SP) consist of sodium olefin sulfonate (SOS), alkyl olefin sulfonate (AOS), and nonylphenol ethoxylate (NPEO) [4]. Before producing VPI SP at the pilot scale, the chemical is quality-checked in the laboratory at critical concentration with a stepwise increase in mixing volume (1 ton, 2 ton scale) [4, 5]. Laboratory results indicate that the complex chemical mixture is of high quality under tolerant reservoir conditions (110°C, 300 bar), maintaining properties for a long time (resistance ability and viscosity ~104 weeks), and increasing recovery factor in core flooding (21 - 32%) [5]. A dynamic model of the pilot selection is built in accordance with test results and the area sweep efficiency is evaluated. The simulation result indicates that with the reduction of capillary number Nc ($E10^{-8}$ to $E10^{-5}$) and IFT (20 - 35 mN/m to 0,07 - 0,01 mN/m), the produced oil is maximised [4]. In consideration of the chemical injection strategy in terms of both timing and expense, a matrix box is established to scale up the concentration and volume of the chemical. Consequently, 100 tons of VPI SP is optimally mixed

Figure 4. *VPI SP chemical in ISO IBC tank.*

Figure 5. *VPI SP stored in Vietsovpetro's base.*

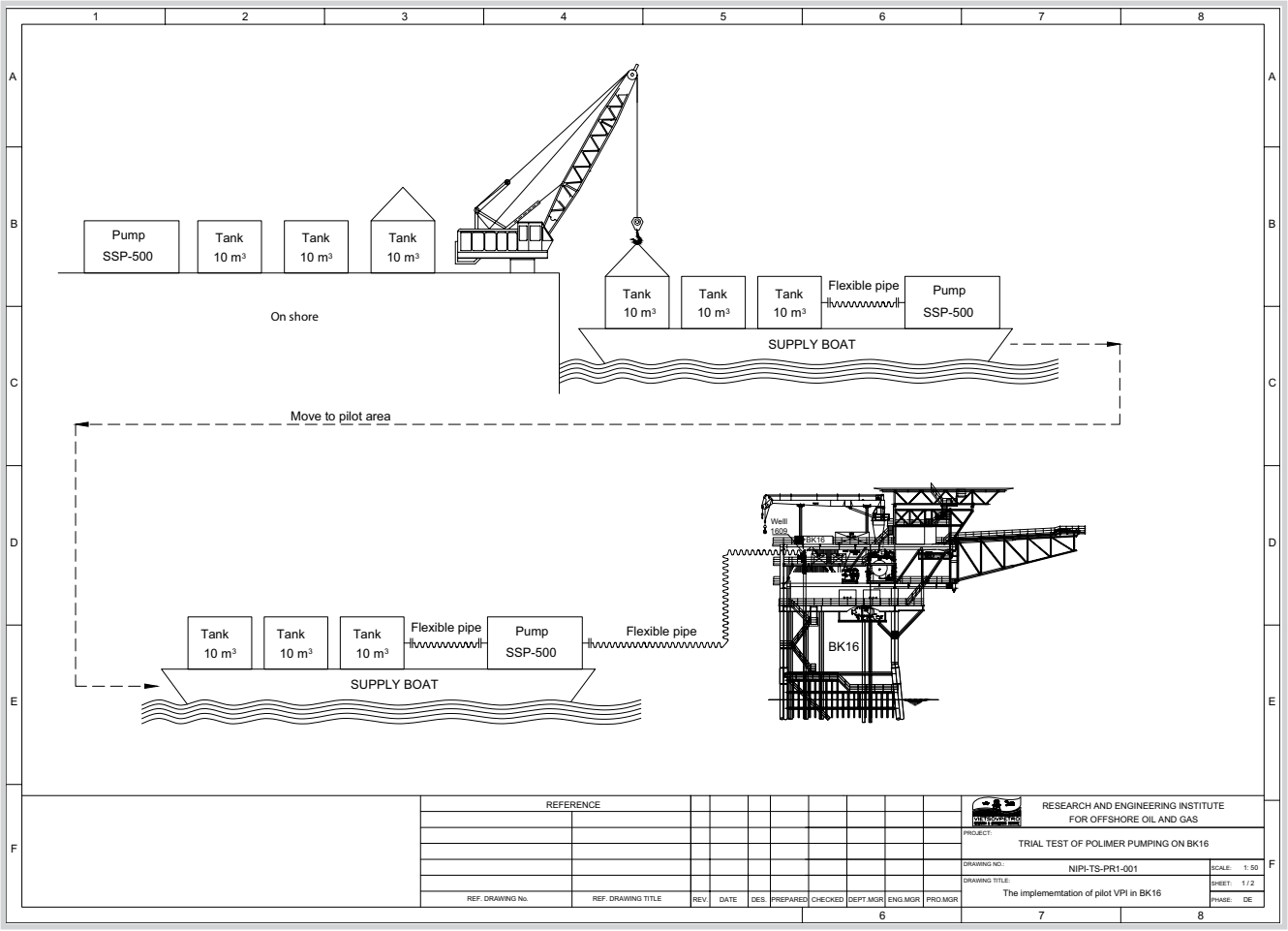

Figure 6. *The pilot implementation of VPI SP to enhance oil recovery factor.*

from the main ingredients surfactants and polymers (Figures 4 & 5) [4]. Additional tests of the new mixing are conducted to identify what happens during the interaction between oil and the chemical. The result shows that most of the products are emulsion-favoured, which is not only stable in the reservoir but also increases the sweep efficiency.

4. Pilot execution design

For more than 30 years of operation, Bach Ho field currently has offshore facilities supporting exploration, production, and transportation. According to preliminary site surveys, due to a long time of use, some equipment is reduced in operating capacity or broken during operation. The implementation using the current facilities shows

Figure 7. *Injection of VPI SP to 1609/BK16.*

some disadvantages, therefore, a system of equipment supporting the chemical injection is designed and made up. Being inspected and tested with the chemical, the obtained results show that the system satisfies the requirement.

In order to ensure operability and mobility during the implementation, the equipment system will be placed on floating devices or ships near marine structures. Besides, to ensure a smooth transportation and support from the existing system, the chemical will be mixed onshore with high concentration. High pressure pumps, ISO tanks, auxiliary equipment, equipment control devices, and spare parts are all placed on large service ships, moving to the pilot location (Figure 6).

By 2022, the chemical tanks and high-pressure pump will be installed directly in the ship and moved to BK16. The connection is established between the pump and well head injector 1609 via a flexible pipe. Pressure test is conducted up to 250 bar before injection to ensure the sealing of the system. The chemicals flow directly from the tank to the injector by high pressure pump.

5. Pilot implementation

All VPI SP in IBC tank was transferred to ISO tank of 10 m^3 and stored at room condition. During the process, properties of the chemical were observed to detect any abnormalities. Each ISO tank was covered after free gas was removed to eliminate the effect of oxygen to the quality of the chemical. To ensure the adaptability of the equipment to the injected fluid, a pumping trial was conducted with a small volume of the chemical. The procedure trial test is a scaled-down of the injectant strategy.

During 23 - 24 January 2022, the equipment system and the chemical were delivered to the pilot area (Figure 7). All of 100 tons VPI SP was successfully injected to 1609/BK16 in a strict compliance to the Vietsovpetro guidelines of safety and EOR chemical injection procedure. After the chemical injection, the injector was turned back working at the same condition as during water flooding. Pressure out of the VCO was recorded. It proved that the sealing between tubing and the reservoir was secured and all the volume of chemical was completely injected to reservoir. The implementation was carried out successfully without any safety issue.

6. Pilot observation

6.1. The well performance after VPI SP injection

After completing the implementation, a schedule of monitoring, sampling, and analysing fluid samples was jointly constructed by VPI and Vietsovpetro specialists. The post-injection observation is conducted in 6 months, in which the producer parameters and analysis results of the produced samples are tightly integrated. Production analysis is guided before and after chemical injection to compare the performance of the surrounding wells. Water analysis results confirm a clear effect of injector 1609 to the 1604, 25, 1607 and a fair effect to the 1602, 1606, 26.

Injector 1609 worked with a cycle of 10 days on and 10 days off before injection and then with the optimal cycle of 15 days on and 15 days off. Parameters of the injector are collected to evaluate the effect of the chemical to the near wellbore and the injectivity of the injection well. Data showed that the injectivity is stable and increases at the early time of the turnback. Furthermore, the wellhead pressure reduces when the injector turns back with the same injection rate (~400 m^3/day) as before. It suggests that the injector wellbore is not damaged by VPI SP (Figure 8).

Based on the analysis results, production performance was monitored carefully and analysed each week to predict any abnormal changes. Frequently, 1 sample of oil and 1 sample of water were taken from 6 production wells during monitoring. Samples were gathered in the VPI laboratory in Hanoi and analysed by a specialised device (UV-Vis). The fluid samples were carefully prepared, filtered to remove solid materials, and stored in a test tube. Then, the samples were analysed in series, each including 12 fluid samples.

Once again, the analyses confirmed the positive effect of injector 1609 to 6 wells. According to the results, the chemical appeared first in well 25 (1 March 2022), and then in wells 1604 (29 March 2022), 1607 (15 March 2022),

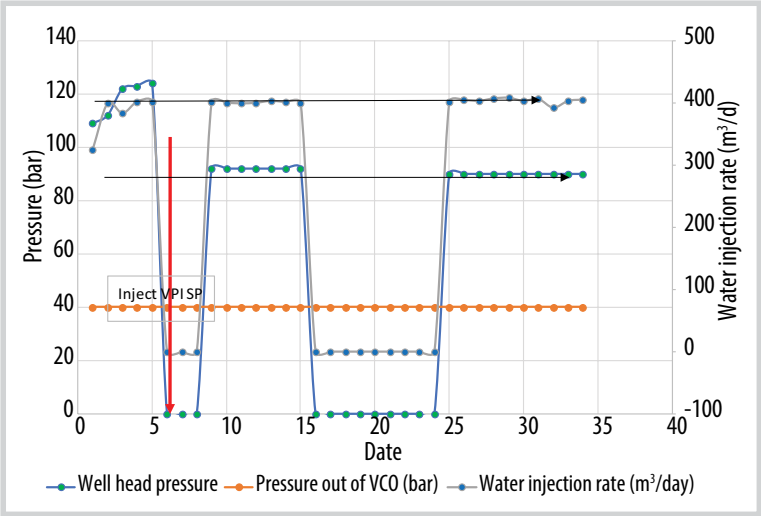

Figure 8. *Parameters of injection well 1609 after injecting VPI SP chemicals.*

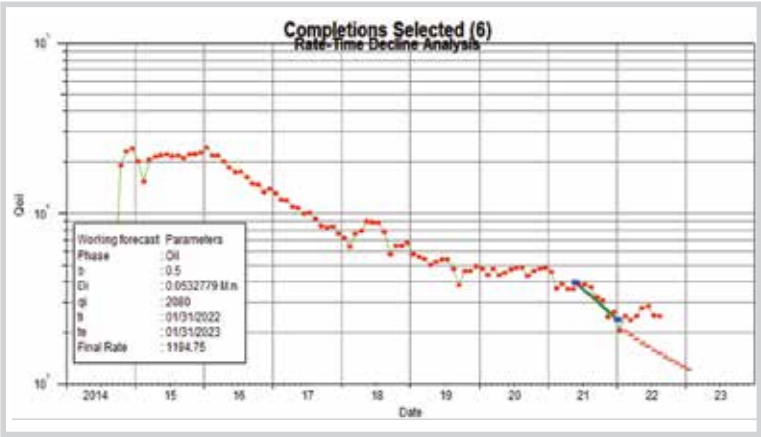

Figure 9. *Forecasting results of the DCA method.*

1602 (26 April 2022), 26 (17 May 2022) and 1606 (24 May 2022). The concentration of the chemical VPI SP at initial condition was observed to be high in wells 25 and 1067, it became less in well 1604 and very little in wells 1602, 26 and 1606. Parameters and chemical analysis confirm the positive effect of VPI SP to all producers.

6.2. Pilot interpretation

In order to evaluate the efficiency of injection to enhance oil recovery, it is necessary to predict the baseline oil rate assuming that all wells and the reservoir are maintained as before VPI SP injection. Based on suggestions from papers and experts [1, 2, 6], multiple methods are used to reduce the uncertainty during making a baseline oil rate. Tools used to predict baseline oil rate are OFM, VPI-KT-1 and simulation dynamic model.

6.2.1. EOR evaluation by decline curve analysis (DCA)

The DCA method is widely used in production forecast. This method has high reliability in some cases: Water cut is higher than 50%; number of wells, injection and production rate fluid, and the remaining reservoir energy are stable. The OFM software is applied in production forecasts given that the performance of the well is the same as before VPI SP is injected. Several adoptions are made to extrapolate the oil rate over time and results (Figure 9):

- Slope of prediction: recent history trendline
- Initial oil rate: oil rate in January 2022
- Declining factor "b": b = 0.5
- Prediction period: February - December 2022

6.2.2. EOR evaluation by advanced DCA using VPI-KT-01

Based on the same assumption, the VPI-KT-01 is used to evaluate the efficiency of the chemical. VPI-KT-01 is a production forecasting software in advanced DCA techniques with 5 declining main functions: power law exponential (PLE) decline, logistic growth model (LGM), stretched exponential production (SEP) decline, Duong, and ARP. It was developed by VPI in 2020, containing the interior-point algorithm to automate the process of history matching and forecasting [7]. The LGM (logistic function) is most used for history matching of the baseline oil rate and the SEP function has the most optimal correlation coefficient (R^2 > 0.8). Results of production forecast are shown in Figure 10.

6.2.3. EOR efficiency evaluation by simulation models

It is essential that details of the reservoir simulation model of the pilot are built in advance to optimise the pilot design, monitor the program and evaluate the EOR efficiency. Based on the UV-vis results, the geological and dynamic model is adjusted accordingly. The key points of geological formation that affect the results are identified. The model is optimised gridding to remove numerical dispersion before building and history matching.

Model of BK14/16 is history matching with data available until 23 January 2022.

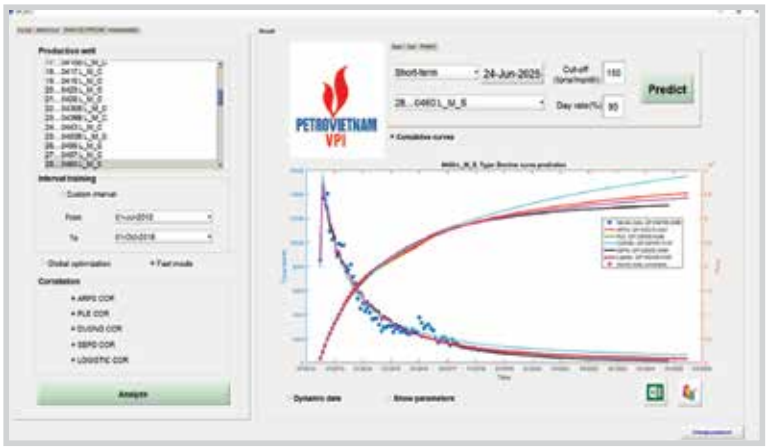

(a)

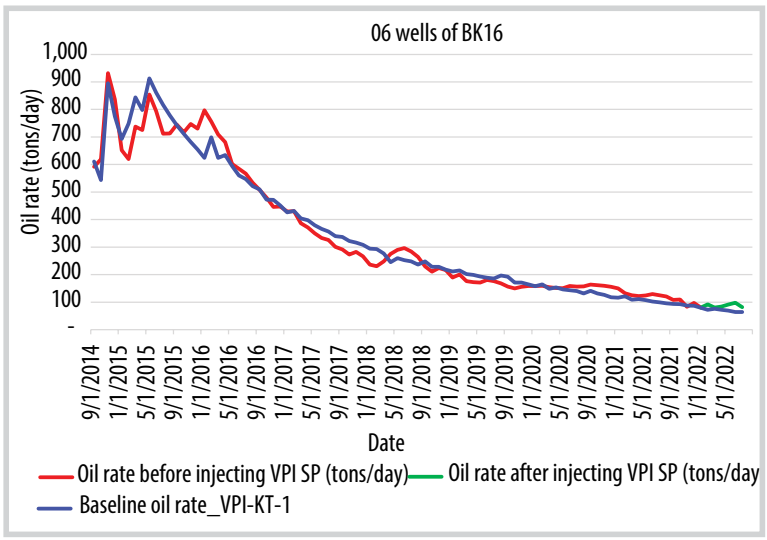

(b)

Figure 10. *The interface of VPI-KT-1 software (a) and the forecasting results (b).*

Results show that the discrepancy between the model and history is acceptable (Figure 11) and adequate for production forecast.

From April 2022, Vietsovpetro reduced the injection rates of wells 1605 (250 m^3/day) and 1609 (400 m^3/day) to 200 m^3/day and 250 m^3/day, respectively. Work cycle changed from 10 days on/10 days off to 15 days on/15 days off. According to the actual production performance in the period from February - July 2022, the lack of gas in the gaslift system and the increase of reservoir energy resulted in the gaslift active valve pushing up, causing most of the wells operating under capacity. After the operator conducted efficiency assessments, such as separating the gas pipeline in gaslift system and optimising the working regime, the wells started to operate stably again from the end of June 2022. Therefore, it is essential to evaluate separately the efficiency of each activity in the field. For that purpose, 4 options were proposed to assess the efficiency of water injection and gaslift optimisation:

- Option 1: Assuming the same condition as before 23 January 2022.

- Option 2: Simulating the water injection with decreasing rate and optimising the water injection process in the period from January - July 2022.

- Option 3: Simulating the gaslift optimisation and Option 2 in the period from January - July 2022.

- Option 4: Option 3 + Justification of chemical properties to match oil rate of observed wells from February - July 2022.

6.2.4. Efficiency evaluation of the EOR using VPI SP

Using several techniques to clarify the performance of each activity showed the consistency between the DCA method and Option 1 of the dynamic model. The reliable results prove that if the wells continue producing as before 23 January 2022, the produced oil is lower than actual 3067.2 tons in the period of February - July 2022. In addition, the efficiency of optimised water injection and gaslift in the period of February - July 2022 is evaluated subject to the actual data and the production forecast of the Options 2 and 3. Results show that oil production increased by 250 tons and 117 tons thanks to the optimised water injection and effort of gaslift regulation, respectively. Consequently, the oil gained from VPI SP application is 2700.2 tons (Table 1, Figure 12).

Due to optimisation activities simultaneously conducted by the operator, the dynamic model is a useful tool to simulate and evaluate separately the efficiency of each solution. Simulation results show high reliability and confidence. The incremental oil production in the period February - July 2022 is 2700.2 tons thanks to VPI SP, excluding the incremental production from gaslift regulation and water injection optimisation.

7. Conclusions

All 100 tons of VPI SP chemical is successfully injected to injector 1609/BK16 in the Lower Miocene, south dome of Bach Ho field. After injection, the results of production

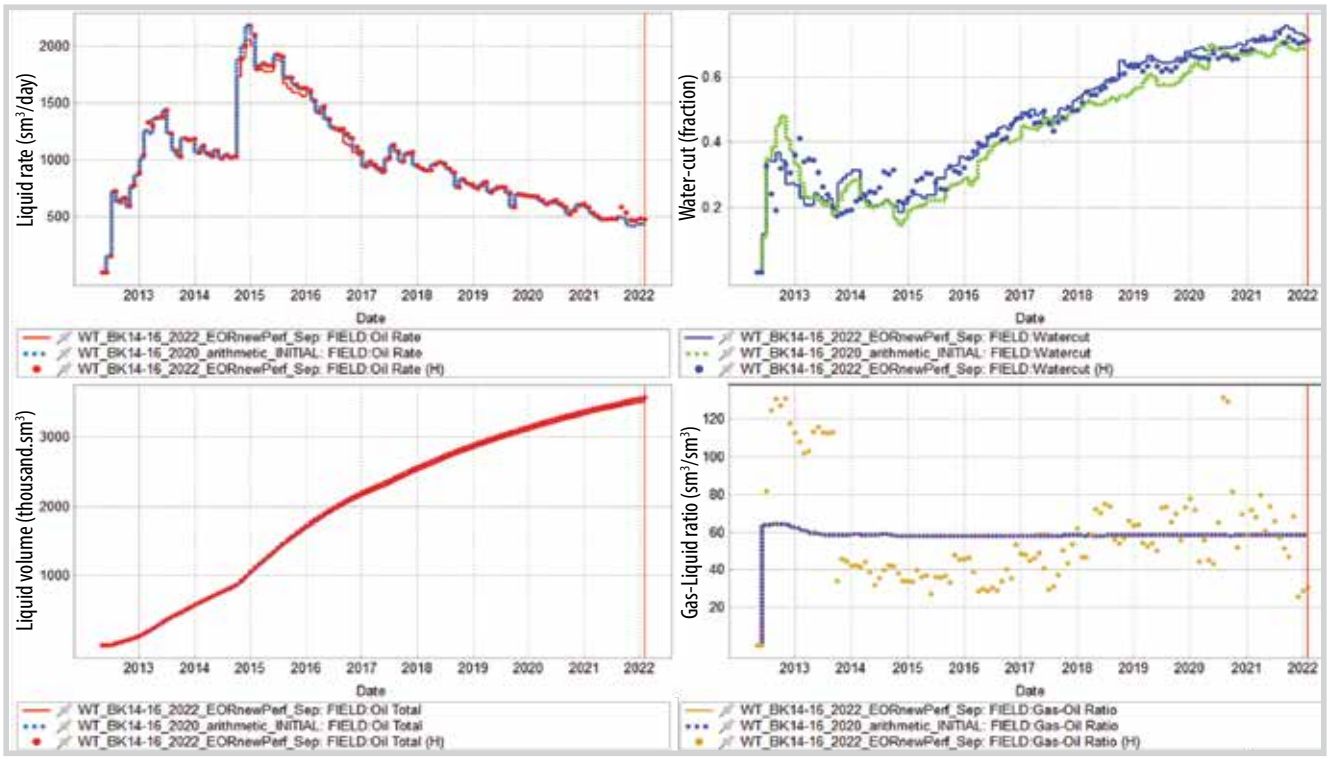

Figure 11. *Results of history matching BK16.*

Table 1. *Efficiency of incremental oil production of VPI SP*

Date	Producer	Injector	DCA		Option 3 of dynamic model (Water injection & Optimisation gaslift)			Actual data			Oil incremental (tons)
			OFM	VPI-KT-01	Oil rate (tons/day)	Oil produced per month (tons/month)	WC (%)	Oil rate (tons/day)	Oil produced per month (tons/month)	WC (%)	
January 2022	6	1			79.92	2,080.00	79.0	79.9	2,080	79.0	-
February 2022	6	1	77.09	72.05	75.52	2,114.68	82.9	91.86	2,494	80.3	379.3
March 2022	6	1	73.11	74.75	73.52	2,279.03	83.4	79.09	2,372	80.8	93.0
April 2022	6	1	69.56	71.05	75.85	2,275.56	83.0	84.09	2,512	80.8	236.4
May 2022	6	1	68.21	68.41	67.55	2,090.19	85.0	90.79	2,793	81.0	702.8
June 2022	6	1	64.9	64.94	67.71	2,020.43	84.9	98.08	2,870	82.3	849.6
July 2022	6	1	62.37	61.94	67.16	2,081.84	85.1	82.01	2,521	82.7	439.2
Sum											**2700.2**

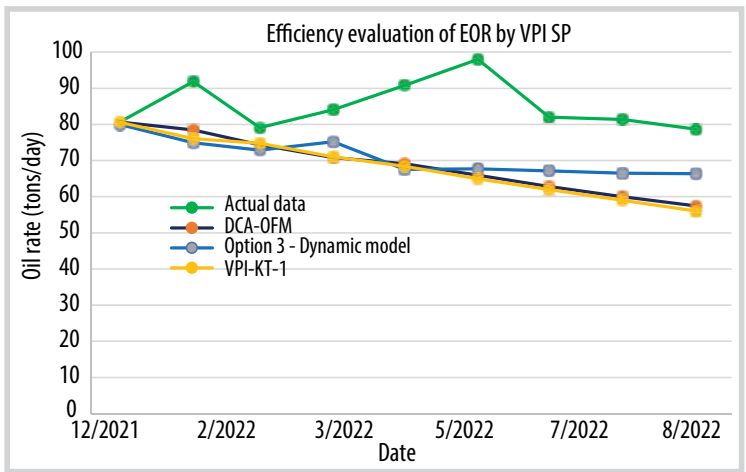

Figure 12. *Results of EOR efficiency evaluation of VPI SP.*

monitoring, sampling, and analysis of the produced fluids showed that the chemicals appeared first at well 25, and then at wells 1604, 1607, 1602, 26, 1606. Chemical concentration was observed to be high in fluids from 25 and 1067, less in fluid from 1604 and very little in those from 1602, 26 and 1606.

Analysis of injector performance parameters proved that VPI SP chemical did not cause any negative effect or damage near the wellbore of the injection well. The evaluation of VPI SP efficiency by various tools proved an incremental oil gain of 2,700.2 tons after 6 months, and the

performance of the surrounding producers continue showing positive effect.

The procedure of the pilot plan is proposed as a scaled-down of the full field EOR application. It can be used as a guide when considering similar applications in nearby fields.

Acknowledgement

This research is supported by the national EOR project ĐTĐLCN.28/19 "Research, industrial application and evaluation efficiency enhance oil recovery factor for the representative sediment in Cuu Long basin", Ref.No. 28/2019/HĐ-ĐTĐL.CN-CNN, date: 3 September 2019. We would like to express our thanks to Ministry of Science and Technology, and Vietnam Petroleum Institute (VPI) for supporting and funding this research.

Reference

[1] Alvarado Vladimir, *Enhanced oil recovery: Field planning and development strategies*. Gulf Professional Publishing, 2010. DOI: 10.1016/C2009-0-30583-8.

[2] G.F. Teletzke, R.C. Wattenbarger, and J.R. Willkinson, "Enhanced oil recovery pilot testing best practices", *SPE Reservoir Evaluation & Engineering*, Vol. 13, No. 1, pp. 143 - 154. DOI: 10.2118/118055-PA.

[3] Phạm Trường Giang, Lê Thế Hùng, Trần Xuân Quý, Nguyễn Văn Sáng, Lê Thị Thu Hường, Hoàng Long và Cù Thị Việt Nga, "Nghiên cứu đánh giá hiệu quả nâng cao thu hồi dầu bằng giải pháp bơm ép hệ hóa phẩm SP cho đối tượng Miocene dưới vòm Nam mỏ Bạch Hổ", *Tạp chí Dầu khí*, Số 7, trang 23 - 30, 2021. DOI: 10.47800/PVJ.2021.07-03.

[4] Phạm Trường Giang, Lê Thị Thu Hường, Cù Thị Việt Nga, Hoàng Long, Trần Thanh Phương, Phan Vũ Anh và Đinh Đức Huy, "Hoàn thiện công nghệ chế tạo hệ hóa phẩm nâng cao hệ số thu hồi dầu quy mô pilot áp dụng thử nghiệm công nghiệp cho đối tượng đại diện thuộc trầm tích Miocene mỏ Bạch Hổ", *Tạp chí Dầu khí*, Số 1, trang 49 - 55, 2022. DOI: 10.47800/PVJ.2022.01-02.

[5] Hoàng Long, Nguyễn Minh Quý, Phạm Trường Giang, Phan Vũ Anh, Lê Thị Thu Hường, Cù Thị Việt Nga, Trần Thanh Phương, Đinh Đức Huy và Lê Thế Hùng, "Nghiên cứu đánh giá, lựa chọn và chế tạo hệ hóa phẩm VPI SP để áp dụng thử nghiệm công nghiệp nhằm nâng cao hệ số thu hồi dầu cho mỏ dầu tại bể Cửu Long, thềm lục địa Việt Nam", *Tạp chí Dầu khí*, Số 11, trang 45 - 54, 2021. DOI: 10.47800/PVJ.2021.07-02.

[6] Hoàng Long, *"Nghiên cứu xây dựng cơ sở dữ liệu của 200 dự án trên thế giới và phần mềm chuyên ngành để đánh giá, lựa chọn các giải pháp nâng cao hệ số thu hồi dầu"*, Viện Dầu khí Việt Nam, 2020.

[7] Đinh Đức Huy, Trần Đăng Tú, Phạm Trường Giang, Trần Xuân Quý và Lê Thế Hùng, *"Xây dựng đường lưu lượng cơ sở nhằm đánh giá hiệu quả các giải pháp cải thiện hệ số thu hồi dầu IOR/EOR"*, Viện Dầu khí Việt Nam, 2021.

PETROVIETNAM JOURNAL
Volume 10/2022, pp. 28 - 34
ISSN 2615-9902

ANALYSING THE EFFECT OF BEDDING PLANE ORIENTATION ON THE WELLBORE FAILURE

Nguyen Van Hung[1], Luong Hai Linh[2]
[1]Phenikaa University
[2]Petrovietnam University
Email: hung.nguyenvan1@phenikaa-uni.edu.vn
https://doi.org/10.47800/PVJ.2022.10-04

Summary

The paper presents a theory of the "plane of weakness" modelling applied to a deviated borehole that penetrated through laminated shale containing numerous parallel weakness planes. The obtained results show that the strength envelope for anisotropic rock is characterised by a U-shaped reduction in strength for failure along the weakness plane, confining pressure from 20 MPa to 80 MPa whithout any change in the failure mechanism of the shale. In terms of borehole failure, there is a risk zone within the well, whose inclination varies between 60° - 90°, and the azimuth changes from 100° - 165°.

Key words: Wellbore stability, weakness plane, triaxial compression tests, geomechanics.

1. Introduction

Wellbore instability is a common problem in oil and gas exploration/production wells during drilling and leads to large expenses. Rock, a natural solid material, is characterised by its anisotropy due to various factors such as the age of formation, lithology, tectonic, deformation, texture and structure, etc. Particularly, weak bedding planes in a rock mass may affect mechanical properties of the rocks and wellbore stability because of its anisotropic strength [1].

Strength is considered as a major parameter to characterise the rock mechanical behaviour. Most of the studies indicate that the strength anisotropy is influenced by dual interaction of orientation of sample bedding plane with respect to the principal stress and the magnitude of confining pressure [2]. Hence, significant efforts have been paid to further understand the anisotropy behaviour in terms of engineering design and analysis to overcome the difficulties in construction of those projects in the anisotropic rock environments. During the last few years, the isotropic model used to determine the anisotropic rock properties revealed a significant uncertainty and unreliability [3 - 5]. In addition, research on wellbore instability was first conducted upon an assumption of linear elastic, isotropic rock, which does not reflect real condition of a rock mass [6].

Several experiments related to the effect of weak bedding planes on rock strength, pore pressure, wellbore instability analysis, etc. have been conducted, suggesting that the bedding plane orientations affected both the elastic constants and yield strength of the rock [4 - 9]. Okland and Cook [10] developed an anisotropic strength theory for wellbore instability problem in the North Sea oil/gas fields, showing that the wellbore instability became worse when drilling parallelly or sub-parallelly to the bedding planes. The plane of weakness theory has been used by Jin et.al. [11] to determine the stability of horizontal wellbores in a naturally fractured formation during well testing. The results showed that the strike of natural fractures could apparently affect the damage form of the sidewall rocks, and a sidewall adjacent to the area of minimum horizontal stress field orientation was the most ready to collapse. In the shale formation, Wu and Tan [12] illustrated that the strength along bedding planes was much weaker than the intact shale material. Effect of the bedding plane failure on wellbore stability in shale was assessed using a transversely isotropic poroelastic and single plane of weakness model. The obtained results showed that the shale bedding planes mainly affected high angle and horizontal wells, which were drilled close

Date of receipt: 8/9/2022. Date of review and editing: 8/9 - 4/10/2022.
Date of approval: 5/10/2022.

to the minimum horizontal stress direction. Other researchers [13 - 15] found that the analytical process of well drilling and completion in gas shale bearing weak bedding planes depended on logging data, real-time drilling data and in-situ stress tests.

Other elements can also affect wellbore instability when the well encounters weak bedding planes, e.g., the angle between the wellbore and the weak bedding plane. If the angle is high (~ 70° - 90°), the oblique loading on relatively weak laminations likely leads to premature shear failure. Depending on the relative magnitude of the anisotropic rock strength and borehole stress concentration, the breakouts may occur at positions around the borehole. This response is different from those conventionally found in isotropic rock. Due to overburdened diagenesis, shale commonly demonstrates high pore pressure, alignment of phyllosilicates. For this reason, instability of shale is a serious issue, which potentially causes costly problems in many foothills drilling operations, e.g., slip surfaces failing [7, 13]. Thus, a sufficient understanding of the mechanism for instabilities and lost circulation during drilling is needed to reduce the operation cost.

The results of uniaxial compressive, indirect tensile strength and triaxial tests were conducted based on a variety of failure criteria proposed for anisotropic materials. These theories were classified into three groups: mathematical continuous criteria, empirical continuous models, and discontinuous weakness plane theories. The empirical Hoek-Brown failure criterion was fitted to the triaxial data, the corresponding Mohr-Coulomb failure envelope using friction and cohesion parameters. The single plane of weakness theory proposed by Jaeger et.al. [1] is the most widely known. In this theory, the classic Mohr-Coulomb criterion is used to describe the failure of both the bedding planes.

In this paper, we will outline an anisotropic strength model, the effect of weak bedding plane parameters and in-situ stresses on wellbore failure analysis.

2. Modelling

The borehole failure analysis is conducted upon the following assumptions: (i) The rock is heterogeneous and anisotropic; (ii) a set of parallel weak bedding planes exists in which the strengths are low, but the strength of the rock in other directions is uniform; (iii) deformation of rock is low and linear.

2.1. Borehole stress

Before a well is drilled the rock is in a state of equilibrium and the stresses in the Earth under these conditions are known as the far field stresses. Once it is excavated, the static stress state becomes disturbed as the support originally offered by the drilled-out rock is replaced by the hydraulic pressure of the drilling mud and hence causing instability in the rock formation. The disturbed in-situ stress state therefore imposes a different set of stresses in excavation area. Figures 1 and 2 illustrate a schematic distribution of in-situ stresses existing in the formation around a wellbore. The stresses can be resolved into a vertical or overburden stress σ_v, the maximum horizontal in-situ stress σ_H, and the minimum horizontal in-situ stress σ_h, which are generally unequal. The direction of well is modelled as shown in Figure 3.

All of the stress components at the wellbore can be calculated in the following steps: (1) Identify the principal in-situ stress state (σ_v, σ_H, σ_h); (2) Transform the stress state (σ_v, σ_H, σ_h,) to the stress state (σ_x, σ_y, σ_z) defined with respect to the Cartesian coordinate system attached to the wellbore (Equations 1a - 1f); (3) Find the local stress state (σ_r, σ_θ, σ_a) with respect to the cylindrical coordinated system attached to the wellbore at the distance of a from the center of well, in terms of the stress state (σ_x, σ_y, σ_z) (Equations 2a - 2f); (4) Find the stress state at the wellbore (σ_r, σ_θ, σ_a) (a = r) as Figure 2. For a vertical well, the local stresses can be calculated from the Equations 3a - 3e, as Equations 4a - 4d below:

$$\sigma_x = (\sigma_H cos^2 a_w + \sigma_h sin^2 a_w) cos^2 i_w + \sigma_v sin^2 i_w \quad (1a)$$

$$\sigma_y = \sigma_H sin^2 a_w + \sigma_h cos^2 a_w \quad (1b)$$

$$\sigma_z = (\sigma_H cos^2 a_w + \sigma_h sin^2 a_w) sin^2 i_w + \sigma_v cos^2 i_w \quad (1c)$$

$$\tau_{xy} = \frac{1}{2}(\sigma_H - \sigma_h) sin2a_w cosi_w \quad (1d)$$

$$\tau_{xz} = \frac{1}{2}(\sigma_H cos^2 a_w + \sigma_h sin^2 a_w - \sigma_v) sin2i_w \quad (1e)$$

$$\tau_{yz} = \frac{1}{2}(\sigma_H - \sigma_h) sin2a_w sini_w \quad (1f)$$

$$\sigma_r = \frac{1}{2}(\sigma_x + \sigma_y)\left(1 - \frac{a^2}{r^2}\right) + \frac{1}{2}(\sigma_x - \sigma_y)\left(1 + 3\frac{a^4}{r^4} - 4\frac{a^2}{r^2}\right) cos2\theta + \tau_{xy}\left(1 + 3\frac{a^4}{r^4} - 4\frac{a^2}{r^2}\right) sin2\theta + \frac{a^2}{r^2} P_w \quad (2a)$$

$$\sigma_t = \frac{1}{2}(\sigma_x + \sigma_y)\left(1 + \frac{a^2}{r^2}\right) - \frac{1}{2}(\sigma_x - \sigma_y)\left(1 + 3\frac{a^2}{r^2}\right) cos2\theta - \tau_{xy}\left(1 + 3\frac{a^2}{r^2}\right) sin2\theta - \frac{a^2}{r^2} P_w \quad (2b)$$

$$\sigma_a = \sigma_z - 2\nu(\sigma_x - \sigma_y)\frac{a^2}{r^2}cos2\theta - 4\nu\tau_{xy}\frac{a^2}{r^2}sin2\theta \quad (2c)$$

$$\tau_{\theta z} = (\tau_{yz}cos\theta - \tau_{xz}sin\theta)(1 + \frac{a^2}{r^2}) \quad (2d)$$

$$\tau_{r\theta} = [\frac{1}{2}(\sigma_x - \sigma_y)sin2\theta + \tau_{xy}cos2\theta](1 - 3\frac{a^4}{r^4} + 2\frac{a^2}{r^2}) \quad (2e)$$

$$\tau_{rz} = (\tau_{xy}cos\theta + \tau_{yz}sin\theta)(1 - \frac{a^2}{r^2}) \quad (2f)$$

$$\sigma_r = P_w \quad (3a)$$

$$\sigma_t = (\sigma_x + \sigma_y) - 2(\sigma_x - \sigma_y)cos2\theta - 4\tau_{xy}sin2\theta - P_w \quad (3b)$$

$$\sigma_a = \sigma_z - 2\nu(\sigma_x - \sigma_y)cos2\theta - 4\nu\tau_{xy}sin2\theta \quad (3c)$$

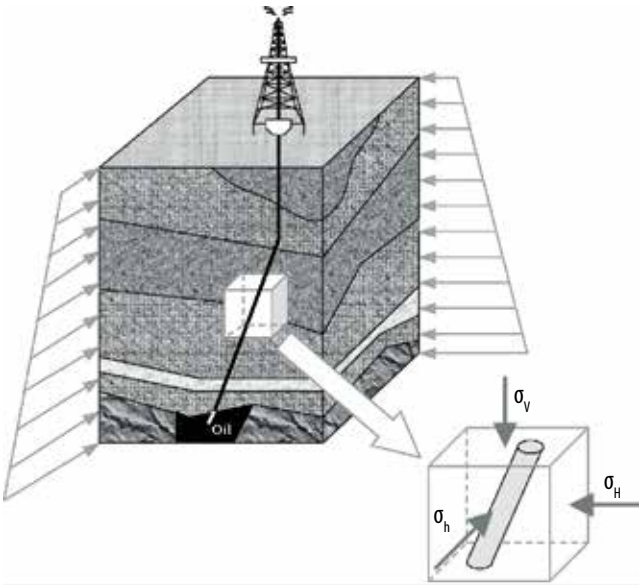

Figure 1. *A scheme showing in-situ stresses around a wellbore [13].*

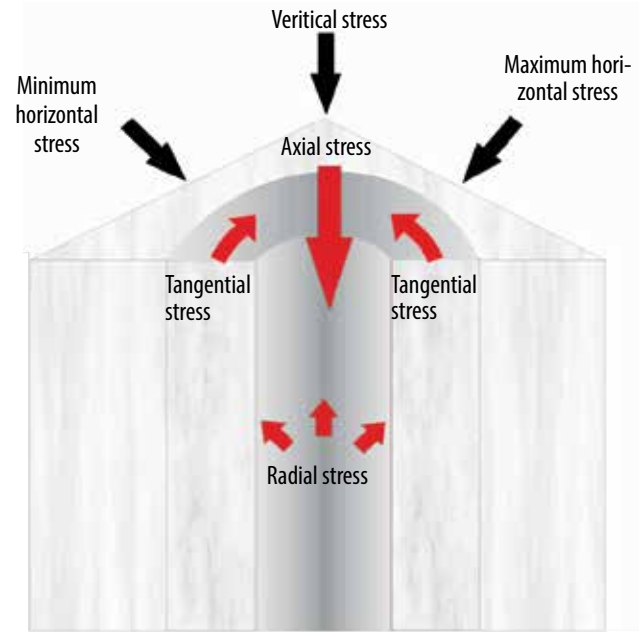

Figure 2. *Position of stresses around a wellbore in the rock formation [14].*

$$\tau_{\theta z} = 2(\tau_{yz}cos\theta - \tau_{xz}sin\theta) \quad (3d)$$

$$\tau_{r\theta} = 0;\ \tau_{rz} = 0 \quad (3e)$$

$$\sigma_r = P_w \quad (4a)$$

$$\sigma_t = (\sigma_x + \sigma_y) - 2(\sigma_x - \sigma_y)cos2\theta - P_w \quad (4b)$$

$$\sigma_a = \sigma_z - 2\nu(\sigma_x - \sigma_y)cos2\theta \quad (4c)$$

$$\tau_{\theta z} = 0;\ \tau_{r\theta} = 0;\ \tau_{rz} = 0 \quad (4d)$$

where:

σ_v: Vertical (overburden) in-situ stress (Pa, psi);

σ_H: Maximum horizontal in-situ stress (Pa, psi);

σ_h: Minimum horizontal in-situ stress (Pa, psi);

σ_x, σ_y, σ_z: stress state in the Cartesian coordinate system (Pa, psi);

τ: Shear stress (Pa, psi);

σ_t: Tensile stress (Pa, psi);

σ_r: Radius stress (Pa, psi);

P_w: Wellbore internal pressure (Pa, psi);

a: Borehole radius (m, in);

r, z, θ: Cylindrical co-ordinate system (m, in);

2.2. Anisotropic rock strength

According to the rock failure applied to planar anisotropy, which is known as "the single plane of

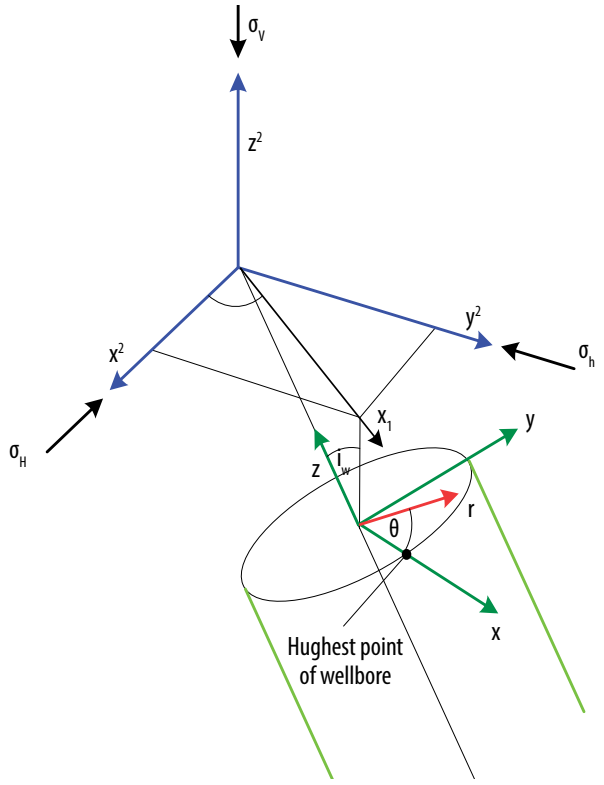

Figure 3. *The coordinate system for the in-situ stress display [14].*

weakness theory", the condition for sliding along these planes is given in Equation 5 [1]:

$$\sigma_1 = \sigma_3 + \frac{2(S_w + \mu_w\sigma_3)}{(1 - \mu_w cos\beta)sin2\beta} \quad (5)$$

where:

σ_1: Maximum principal stress (Pa, psi);

σ_3: Minimum principal stress (Pa, psi);

S_w: Inherent shear strength of the planes of weakness (Pa, psi);

$\mu_w = tan\varphi_w$: Coefficient of internal friction along weak planes;

φ_w: Friction angle of weak plane (degrees);

β: Angle between σ_1 and the normal to the planes of weakness.

Failure will occur in the bulk material based on the same failure criterion as the weak plane such that the maximum principal stress that can be sustained is:

$$\sigma_1 = 2\tau_0^b \frac{cos\varphi^b}{1 - sin\varphi^b} + \sigma_3 \frac{1 + sin\varphi^b}{1 - sin\varphi^b} \quad (6)$$

where:

τ_0^b: Cohesion;

φ^b: Friction angle of bulk material (degrees).

It is assumed that the bulk material has isotropic strength properties.

3. Case study

The data used in this study are derived from pre-existing works conducted by Crawford et.al. [17], with

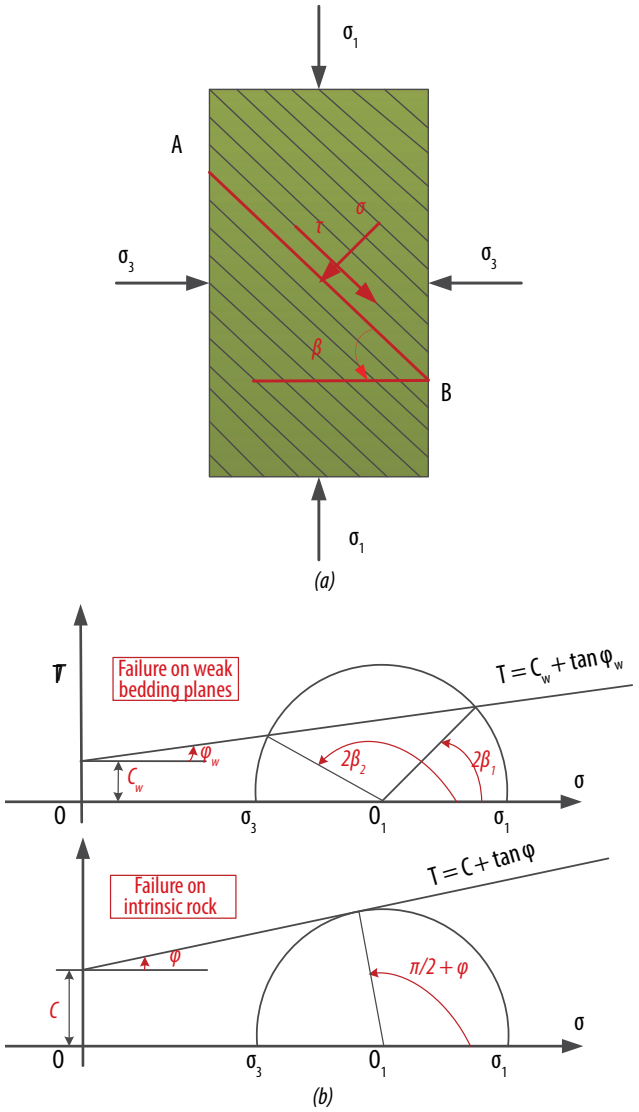

Figure 4. *(a) Stress state of rock containing weak bedding planes; (b) rock strength analysis of failure on weak bedding planes and intrinsic rock [16].*

Table 1. *Summary of 14 database lithologies used in anisotropic shear strength analyses [17]*

I.D		Lithology	Source		≠triaxial test (β)	Cohesive strength (MPa)	Friction angle (degrees)
Lst.	≠1	Laminated dolomitic limestone	Outcrop	McGill & Raney	40	93.9	29.9
Calcareous shales	≠2	Green River oil shale (lean)	Mine	McLamore & Gray	24	59.6	31.4
	≠3	Green River oil shale (rich)	Mine	McLamore & Gray	21	39.0	21.4
	≠4	Intra-reservoir marl	Cored well	In-house study	27	30.7	20.2
	≠5	Intra-reservoir marl	Cored well	In-house study	28	24.4	8.1
	≠6	Intra-reservoir marl	Cored well	In-house study	31	20.7	8.5
Sst.	≠7	Fine-grained highly cemented sandstone	Outcrop	Chenevert & Gatlin	17	38.4	56.4
Argillaceous shales	≠8	Outcrop shale	Outcrop	In-house study	35	29.1	29.7
	≠9	Top seal shale	Cored well	In-house study	31	18.7	9.1
	≠10	Top seal shale	Cored well	In-house study	30	17.6	5.7
	≠11	Top seal shale	Cored well	In-house study "	28	16.4	14.8
	≠12	Tournemire shale	Outcrop	Niandou et. al.	25	16.8	21.7
	≠13	Laminated silty mudstone	Mine	Attewell & Farmer	42	14.9	33.8
Coal	≠14	Barnsley Hards bituminous coal	Mine	Pomeroy et. al.	28	12.6	36.3

~400 triaxial compression testing on 7 individual lithologies (3 top seal shales, 3 intra-reservoir shales and 1 outcrop shale) [17], Narayanasamy et.al. [18], Chris et.al. [19]. Those studies used samples collected from Terra Novad, Yasar 2001 of the Upper Miocene - Pliocene Handere formation.

4. Determination of strength anisotropy

Based on the above models and laboratory data, the strength of rock is analysed first. Figure 5 presents a summary of the tests for shale in Table 1. The failure theory is used for interpretation of the test results for the anisotropic rocks, namely the single plane of weakness theory [1]. The failure stress can be computed by specifying cohesion and friction angle (for varying orientation of β). It is necessary to evaluate two cohesive strength parameters and two coefficients of internal friction for anisotropic materials. As shown in Figure 5, the strength envelope for anisotropic rock is a U-shaped reduction for failure along the weakness plane. At most confining pressures, the criterion overestimates the strength in the regions, where failure is predicted through the intact rock. It is clearly indicated that within the confining pressure varying from 20 MPa to 80 MPa, there is no change in the failure mechanism of the shale. In addition, the results evidently show the anisotropic strength slumped at supreme confining pressure besides, the theoretical method provides advantageous prevision of anisotropy behaviour at higher confining pressures.

5. Cohesive strength model

Cohesive strength or cohesion is the strength of bonding between the particles or surfaces that make up the material. In rock mechanics, the cohesive strength is more specifically the inherent shear strength of a plane across which there is no normal stress. In general, this strength parameter is determined in case of no distinction between failure of a weak plane and failure through the bulk material. In this case, the linearised Mohr failure line can be used, and cohesive strength is estimated by uniaxial tests or triaxial tests. According to experimental

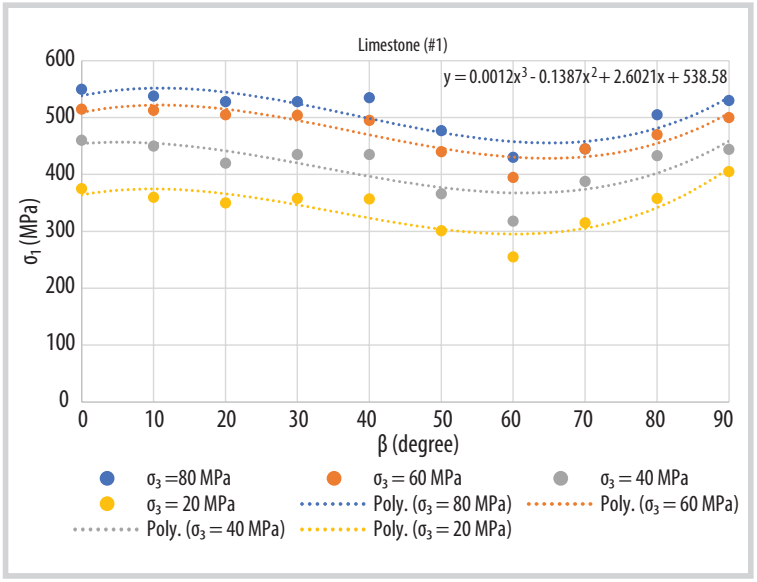

Figure 5. *Single plane of weakness model fits with testing data (solid lines - model, points - laboratory data).*

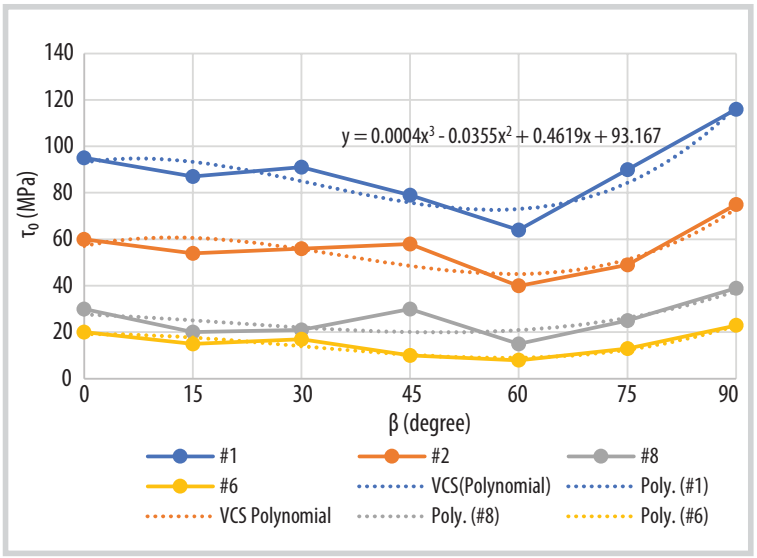

Figure 6. *The cohesive strength model.*

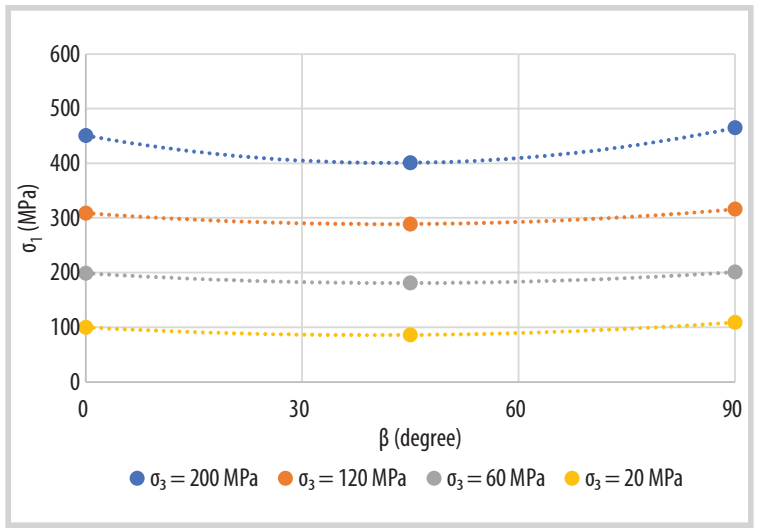

Figure 7. *Maximum principal stress prediction.*

Table 2. *Input data*

Property	Value
Depth (m)	6,000
Overburden stress (MPa/100 m)	2.4
Major horizontal stress (MPa/100 m)	2.08
Minor horizontal stress (MPa/100 m)	1.9
Pore pressure (MPa)	70
Cohesion of the weak planes (MPa)	3.5
Internal friction angle of weak planes (°)	14
Cohesion strength of rock (MPa)	18
Internal friction angle (°)	32
Poisson's ratio	0.22
Biot's coefficient	0.9
Wellbore diameter (mm)	140
Direction of the maximum horizontal principle in-situ stress (°)	115
Fluid density (g/cm^3)	1.22

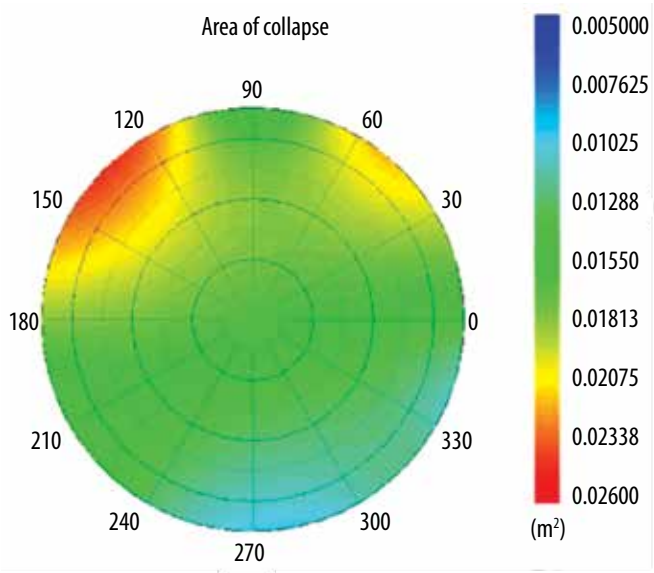

Figure 8. *Sanding onset in a well of shale formation.*

results (Table 1), the cohesive strength data is considered a function of the third-order polynomial of weak plane angle.

The cohesive strength of shale is determined as shown in Figure 6. The continuous variable cohesive strength criterion produces failure envelopes that predict a continuous change. The cohesion theory can be estimated correctly even with β = 0°, 90°, except at 45° and 75°. By using the polynomial technique, we constate that this technique can be used for predicting the maximum principal stress in function of β angle (Figure 7). This result is much better than the single plane of weakness model.

6. Borehole failure

Based on the above models (Equation 5), borehole failure is analysed by applying the data presented in Table 2. The sand production phenomenon is generally taking place through three stages: loss of mechanical integrity of rocks surrounding the borehole, separation of solid particles due to the hydrodynamic force, and transportation of the particles to the surface by production. Excessive sanding or solid production may damage the downhole and surface equipment. Drilling mud is normally chosen in such a way to resist the formation pore pressure, hence preventing the formation fluid from flowing into the wellbore. The drilling mud is not always able to resist the compressive stresses of the wellbore. In this case, shear failures of rock will occur due to the imbalance between stress and rock strength.

In this study, we investigate the possibility of sanding with the presence of weak plane. The returning results allowed us to constate that the field stress regime is normal ($\sigma_v > \sigma_H > \sigma_h$). Figure 8 reveals the possibility of sanding for this case study. As we can see from this figure, the most dangerous case is coded by the red color. In this case, there is a risk zone in the well with the trend angle of weak plane ranging between 60° - 90°, and the changes from 100° - 165°.

However, with any different range of weak plane, the well can be drilled in any azimuth without sanding problem. This result is vital which enables to recommend well plannings, and it is also a good solution for simulation to tackle the risk of drilling well.

7. Conclusions

Results are obtained from various tests applied to the anisotropic strength of shale associated with weak planes, and wellbore failure. This study allows us to draw the following conclusions:

The strength envelope for anisotropic rock shows a U-shaped reduction in strength for failure along the weakness plane.

No change in the failure mechanism of the shale is recorded within the 20 - 80 Mpa interval confining pressure.

The cohesion theory can be estimated correctly even with β = 0°, 90°, except at 45° and 75°. By using the polynomial technique, it is possible to provide a correctly prediction of the maximum principal stress in function of β angle.

There is a risk zone in the well with the trend angle of weak plane ranging between 60° - 90°, and the azimuth changing from 100° - 165°.

References

[1] John Conrad Jaeger, Neville G.W. Cook, and Robert Zimmerman, *Fundamentals of rock mechanics, 4th edition*. Blackwell Publishers, 2007.

[2] Yong Ming Tien, Ming Chuan Kuo, and Charng Hsein Juang, "An experimental investigation of the failure mechanism of simulated transversely isotropic rocks", *International Journal of Rock Mechanics and Mining Sciences*, Vol. 43, No. 8, pp. 1163 - 1181, 2006. DOI: 10.1016/j.ijrmms.2006.03.011.

[3] Shuai Heng, Yingtong Guo, Chunhe Yang, Jack J. K. Daemen, and Zhi Li, "Experimental and theoretical study of the anisotropic properties of shale", *International Journal of Rock Mechanics and Mining Sciences*, Vol. 74, pp. 58 - 68, 2015.

[4] Jingyi Cheng, Zhijun Wan, Yidong Zhang, Wenfeng Li, Syd S. Peng, and Peng Zhang, "Experimental study on anisotropic strength and deformation behavior of a coal measure shale under room dried and water saturated conditions", *Shock and Vibration*, 2015. DOI: 10.1155/290293.

[5] G. Duveau and J.F. Shao, "A modified single plane of weakness theory for the failure of highly stratified rocks", *International Journal of Rock Mechanics and Mining Sciences*, Vol. 35, No. 6, pp. 807 - 813, 1998. DOI: 10.1016/S0148-9062(98)00013-8.

[6] W.B. Bradley, "Failure of inclined boreholes", *Journal of Energy Resources Technology*, Vol. 101, No. 4, pp. 232 - 239, 1979. DOI: 10.1115/1.3446925.

[7] Brent S. Aadnoy, "Modeling of the stability of highly inclined boreholes in anisotropic rock formations", *SPE Drilling Engineering*, Vol. 3, No. 3, pp. 259 - 268, 1988. DOI: 10.2118/16526-PA.

[8] M.E. Chenevert and C. Gatlin, "Mechanical anisotropies of laminated sedimentary rocks", *SPE Journal*, Vol. 5, No. 1, pp. 67 - 77, 1965. DOI: 10.2118/890-PA.

[9] Vahid Dokhani, Mengjioa Yu, and Stefan Miska, "The effect of bedding plane orientation on pore pressure in shale formations: Laboratory testing and mathematical modeling", *47th U.S. Rock Mechanics/Geomechanics Symposium, San Francisco, 23 - 26 June 2013*.

[10] D. Okland and J.M. Cook, "Bedding related borehole instability in high angle wells", *SPE/ISRM Rock Mechanics in Petroleum Engineering, Norway, 8 - 10 July 1998*. DOI: 10.2118/47285-MS.

[11] Yuanlin Jin, Z. Qi, Mingqing Chen, F. Zhang, Y. Lu, and Bing Hou, "A mechanism study on the fractured reservoir instability during well testing of horizontal wells", *Shiyou Xuebao/Acta Petrologica Sinica*, Vol. 32, No. 2, pp. 295 - 298, 2011.

[12] Bailin Wu and C.P. Tan, "Effect of shale bedding plane failure on wellbore stability – example from analyzing stuck-pipe wells", *44th U.S. Rock Mechanics Symposium and 5th U.S. - Canada Rock Mechanics Symposium, Salt Lake City, Utah, 27 - 30 June 2010*.

[13] Bernt Aadnøy and Reza Looyeh, *Petroleum rock mechanics: Drilling operations and well design*. Gulf Professional Publishing, 2012. DOI: 10.1016/C2009-0-64677-8.

[14] Borivoje Pašić, Nediljka Gaurina-Medimurec, and Matanović Davorin, "Wellbore instability: Causes and consequences", *Rudarsko Geolosko Naftni Zbornik*, Vol. 19, No.1, 2007.

[15] Yufei Li, Yongqiang Fu, Geng Tang, Jianhua Guo, Jiyin Zhang, and Chaoyi She, "Effect of weak bedding planes on wellbore stability for shale gas wells", *IADC/SPE Asia Pacific Drilling Technology Conference and Exhibition, Tianjin, China, 9 - 11 July 2012*. DOI: 10.2118/155666-MS.

[16] Shiming He, Wei Wang, Jun Zhou, Zhen Huang, and Ming Tang, "A model for analysis of wellbore stability considering the effects of weak bedding planes", *Journal of Natural Gas Science and Engineering*, Vol. 27, pp. 1050 - 1062, 2015. DOI: 10.1016/j.jngse.2015.09.053.

[17] Brian Crawford, N.L. Dedontney, B. Alramahi, and S. Ottesen, "Shear strength anisotropy in fine grained rocks", *46th U.S. Rock Mechanics/Geomechanics Symposium, Chicago, Illinois, 24 - 27 June 2012*.

[18] Rajarajan Narayanasamy Naidu, D. Barr, A. MILNE, "Wellbore instability predictions within the Cretaceous mudstones, Clair field, West of Shetlands", *SPE Offshore Europe Oil & Gas Conference & Exhibition, Aberdeen, UK, 8 - 11 September 2009*.

[19] Chris Gallant, Jianguo Zhang, Christopher A. Wolfe, John Freeman, Talal Al-Bazali, and Mike Reese, "Wellbore stability consideration for drilling high-angle wells through finely", *SPE Annual Technical Conference and Exhibition, Anaheim, California, U.S.A., 11 - 14 November 2007*.

PETROVIETNAM JOURNAL
Volume 10/2022, pp. 35 - 45
ISSN 2615-9902

APPLICATION OF GAS-ASSISTED GRAVITY DRAINAGE (GAGD) TO IMPROVE OIL RECOVERY OF RANG DONG BASEMENT RESERVOIR

Nguyen Kien Trung, Ha Minh Dung
Japan Vietnam Petroleum Co., Ltd. (JVPC)
Email: nguyen.kien.trung@jvpc.com.vn
https://doi.org/10.47800/PVJ.2022.10-05

Summary

As an option to improve the ultimate oil recovery factor of the Rang Dong field, a feasibility study of gas-assisted gravity drainage (GAGD) application was carried out for the fractured basement reservoir with a single-well Huff 'n' Puff pilot test applied on a high water-cut producer. This paper aims to provide an in-depth understanding about such case study, which includes details on candidate selection, gas injection scheme, on-site execution, results of flow-back, post-job review and lessons learned.

The pilot test of GAGD was recorded with a good oil rate and low water-cut during flowing back after gas injection and shut-in for gas segregation, which suggests the positive effectiveness of GAGD to some degree. The expansion of the GAGD application to other wells and areas in the field would be encouraged in any similar situation. On the other hand, the results of this pilot test shed a light into further optimisation of the candidate selection and gas injection scheme by material balance analysis and reservoir simulation respectively.

Key words: Fractured basement, production, IOR, EOR, GAGD, pilot test, Rang Dong field.

1. Introduction

1.1. General information

Block 15-2 is located offshore of southern Vietnam, approximately 120 km off Vung Tau at the mouth of the Mekong River (Figure 1). After the production sharing contract (PSC) was signed in 1992, extensive exploration and development activities were carried out, and as a result, the first oils were achieved from the Rang Dong and Phuong Dong fields in 1998 and 2008 respectively.

As the largest field of this block, the Rang Dong field has achieved cumulative oil production of approximately 240 million barrels mainly from fractured basement and Lower Miocene sandstone reservoirs to date. The full field scale application of hydrocarbon gas enhanced oil recovery (HCG EOR) with water alternating gas injection (WAG) has been deployed at the Lower Miocene sandstone reservoir since 2014 while the basement reservoir has been produced mainly by the bottom water drive mechanism.

Date of receipt: 7/9/2022. Date of review and editing: 7/9 - 5/10/2022.
Date of approval: 5/10/2022.

1.2. Issues of the basement reservoir

The fractured basement reservoir of the Rang Dong field has been put into production since 1998 and passed the peak of 40,000 - 50,000 barrels of oil per day with intensive development activities in the period of 2002 - 2006. Since then, the production has been declining and remains at 5,000 barrels of oil per day with a water-cut of 80 - 90% recently.

The severest problem of the oil production is a rapid increase of the water-cut [1]. Figure 2 shows the water-cut trends in the individual wells. Many wells have problems of a high water-cut because the wells commence a rapid decline once the initial water-cut increase is observed.

Water injection had been implemented since 2003, however, it sometimes caused severe water breakthroughs. The cyclic production and production-injection patterns had been applied in several wells, but the impact was limited. Under such a situation, the estimated ultimate recovery factor (RF) of the basement reservoir was only 18%. Improvement of the recovery factor is critical for maximising the project value, but this is challenging due to the unique nature of the fractured basement reservoir.

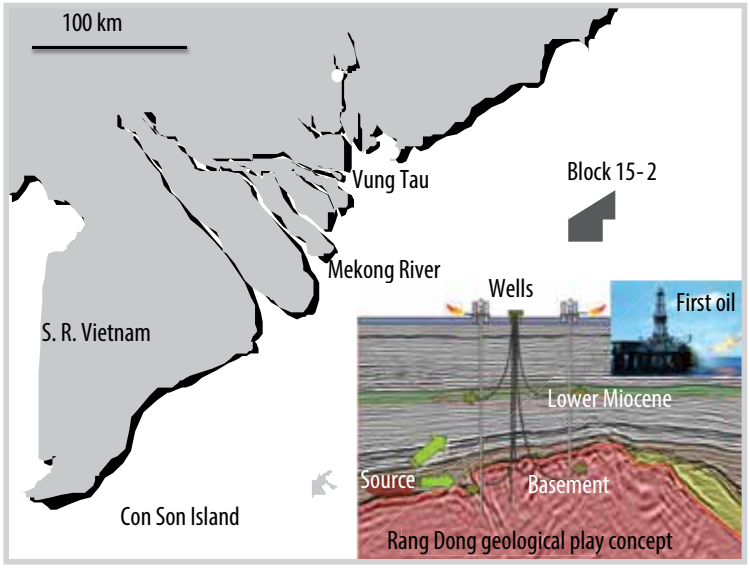

Figure 1. *Location map of Block 15-2 and geological play concept.*

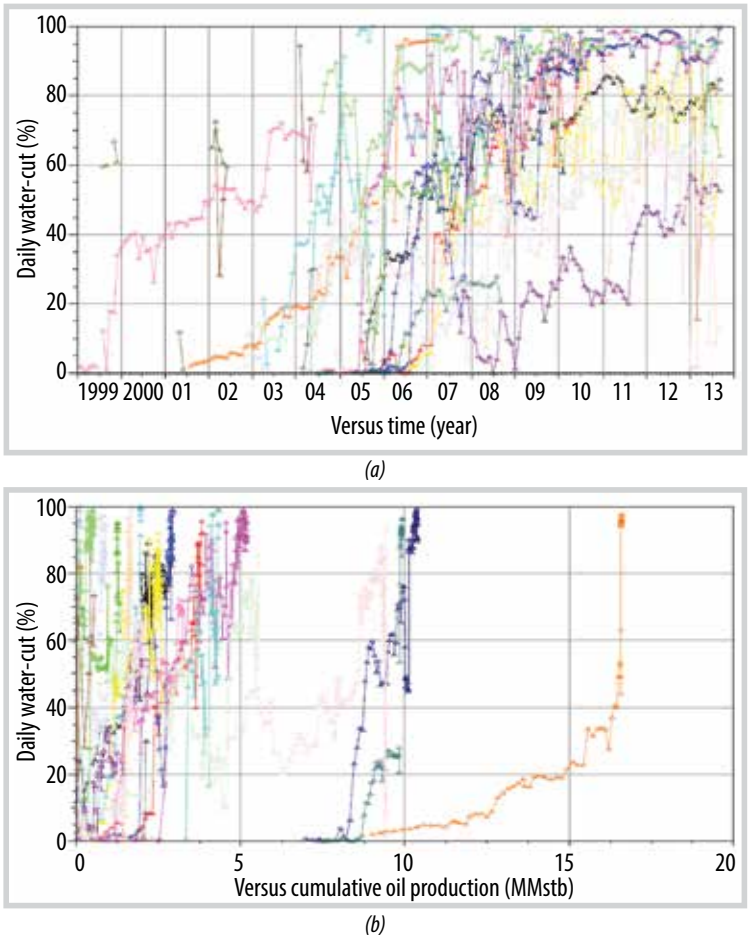

Figure 2. *Water-cut trends in the individual wells.*

For further improvement of the recovery factor, additional drilling for the attic potential remaining above the producing depth of the existing wells can be considered subject to technical and economical justifications. Meanwhile, the option of acid treatment, water shut-off and GAGD can be exercised and matured as one of the possible IOR techniques.

1.3. Gas-assisted gravity drainage concept

The GAGD process [3 - 8] is developed to overcome the limitations of conventional horizontal displacement such as water injection, gas injection, and WAG. The GAGD process attempts to flood the reservoir vertically by injecting gas at the top of the pay zone, using vertical wells and producing oil from horizontal wells placed near the oil-water-contact (OWC) (Figure 3).

Numerous projects have been initiated in the USA and Canada, and some have resulted in significant improvement of oil recovery. Most of the projects are established for dipped clastic or carbonate reservoirs of onshore fields.

In the Yates field (Midland, the USA), the GAGD process was applied to a naturally fractured carbonate reservoir in the 1970s and successfully enhanced oil production out of the matured field [3].

GAGD is a proven technology in terms of reservoir engineering for the improvement of oil recovery.

1.4. Applicability of GAGD for fractured basement

The existing producers of the Rang Dong basement reservoir were normally drilled horizontally at approximately 200 - 300 m deeper from top of the basement. In case of a rapid water breakthrough from the bottom, the attic above the wellbore might still have remaining oil potential (named as oil band). JVPC had applied water injection aiming at pressure maintenance and horizontal displacement of oil, but the impact on the improvement of oil recovery was limited. GAGD is probably one of the most effective techniques to displace the oil band to the producers.

The characteristics of the Rang Dong basement reservoir appear to be preferable, especially in terms of dominant gravitational force existing in high-angled permeable fractures. Some published papers [4, 5] introduce the empirical screening criteria of GAGD as shown in Table 1.

The properties of the Rang Dong basement reservoir mostly satisfy the above criteria. Furthermore, a source of high-pressure gas (as high as 3,200 psi at surface) is available through the operation of the HCG EOR program for the Lower Miocene sandstone reservoir, and it provides an advantage for this GAGD pilot test.

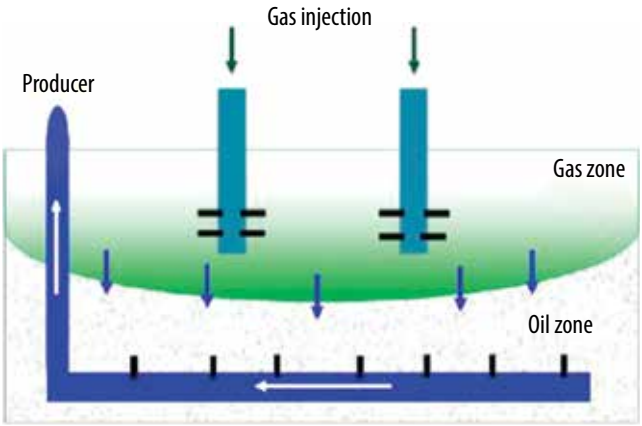

Figure 3. *Schema of GAGD application.*

2. Case study [1, 2]

2.1. GAGD Huff 'n' Puff pilot test

GAGD is probably one of the most effective techniques to improve oil recovery out of the basement reservoir. To ensure the effectiveness, the pilot test of GAGD was selected with minimised scope of work utilising the existing water out producer and with minimum facility modification for low implementation cost. The GAGD Huff 'n' Puff process (Figure 4) consists of 3 steps as i) gas injection, ii) gas migration and stabilisation, then iii) production.

2.2. Well candidate selection

Initially, there were 3 candidates nominated out of all the basement producers relating to the fact that the high-pressure gas injection system and test separator for appropriate monitoring are available with a minimum facility modification needed for those wells.

Table 1. *Screening criteria of GAGD*

Parameter	Rang Dong basement	Screening criteria
Vertical reservoir permeability	> 1,000 mD	> 300 mD
Bed dip angle	60 ~ 80 degree	> 10 degree
Oil viscosity	Free flow	Free flow
Spreading coefficient	Positive	Positive
Waterflood residual-oil satuation	Not specified	Substantial (range not specified)

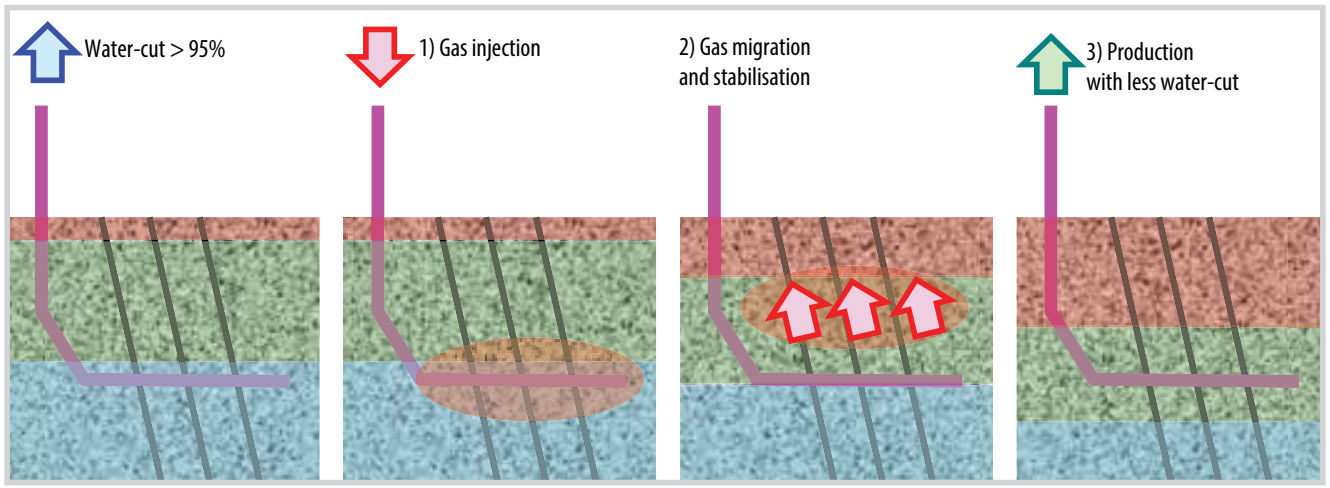

Figure 4. *Schema of GAGD pilot test.*

Table 2. *Well selection criteria for GAGD pilot test*

Selection criteria	Well A	Well B	Well C
High water-cut	70 - 100%	90 - 95%	95 - 100%
Expected oil/gas above wellbore	253 m	227 m	64 m
Reservoir pressure below injection pressure of 4,000 psi	Yes	Yes	Yes
Isolated segment for minimised injection volume	Yes	Possible	No
Gravity segregation expected	Yes	Unknown	Yes
Final ranking	I	II	III

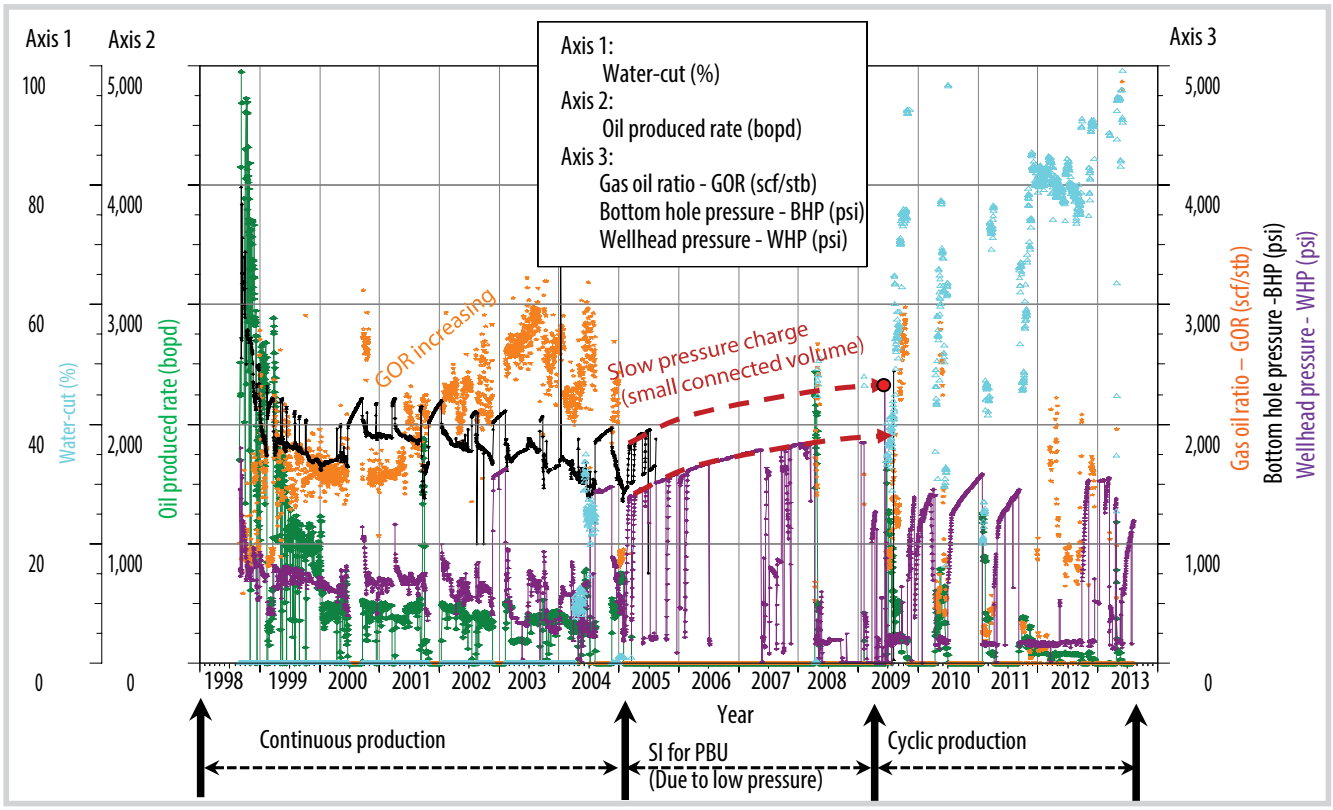

Figure 5. *Production performance of well A.*

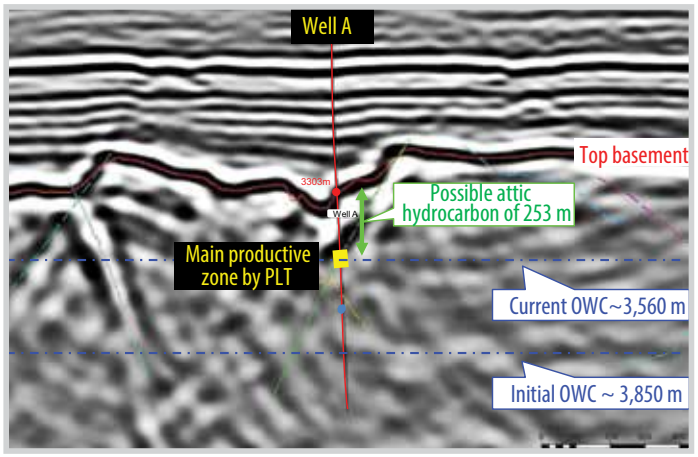

Figure 6. *Seismic section along well A and relating sub-surface information.*

Well selection criteria: These candidates were reviewed through production performance. Well profile and rank are shown in Table 2 for final selection.

Being ranked as the most preferable candidate, Well A was selected for the GAGD Huff 'n' Puff pilot test. The well performance (Figure 5) indicated the existence of oil band and the impact of gravity segregation during cyclic production (i.e., the water-cut was reduced right after opening the well, giving a period of shut-in due to high water-cut). The slow pressure build-up (PBU) suggests a small volume connected to the well, and subsequently, a small volume of gas injection is required.

The well trajectory and seismic section along well A (Figure 6) show a remaining oil/gas column of 253 m still expected above the producing fracture depth level.

2.3. Simulation study for pilot test design

The reservoir simulation was utilised for pre-GAGD design of the pilot test including the prediction of the gas injection scheme.

- Sector model and history matching

The seismic faults or fractures connected to the well were geologically modelled, and as a result, a sector model for an area of around 0.6 km^2 was built for simulation and history matching. The settings of the model are described as follows.

+ Initial OWC is assumed at 3,850 m (as mid-depth in-between oil-down-to and structural spill point), and no gas cap exists initially for the undersaturated oil reservoir.

+ Saturation pressure of 4,800 psi, oil formation volume factor of 1.678 reservoir barrel/stock tank barrel (rb/stb), and solution gas-oil ratio (GOR) of 1,204 scf/stb are set in the model.

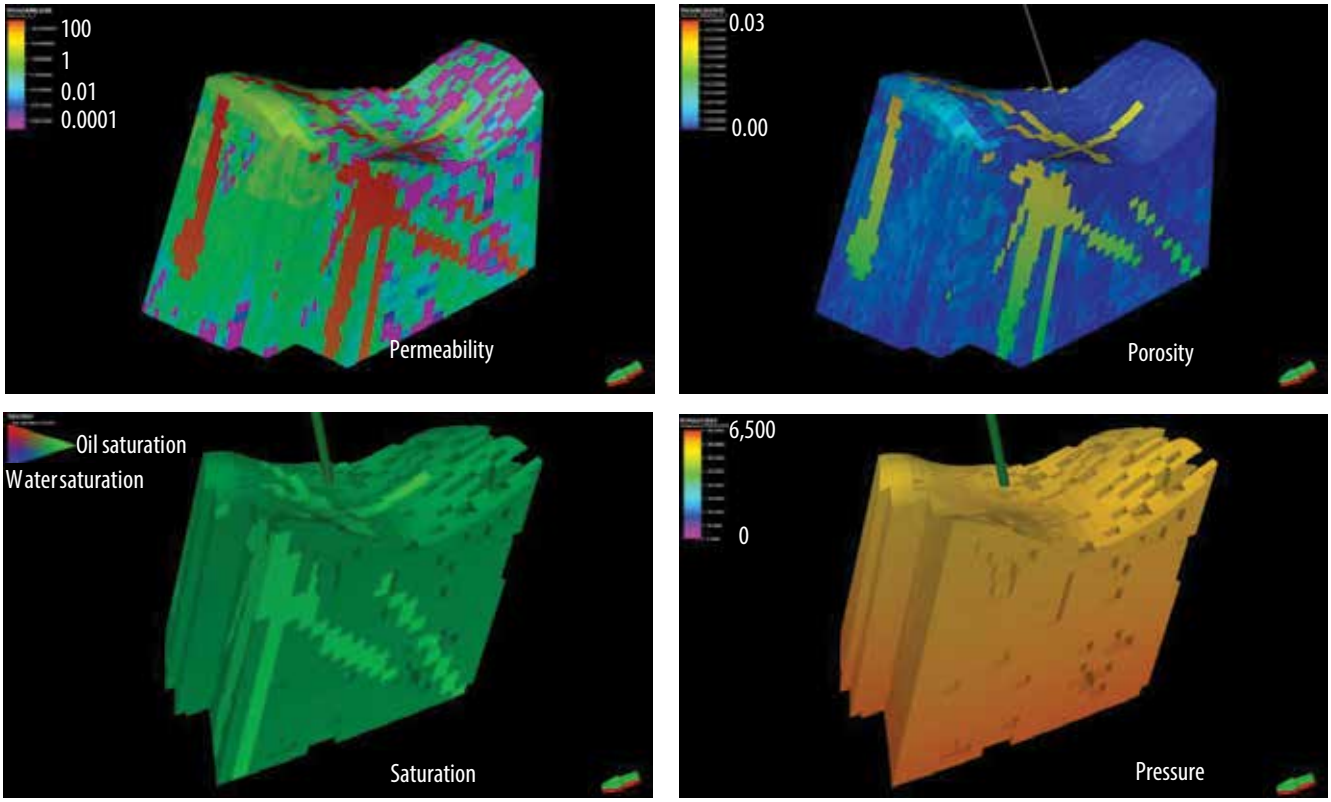

Figure 7. *Reservoir properties of sector model.*

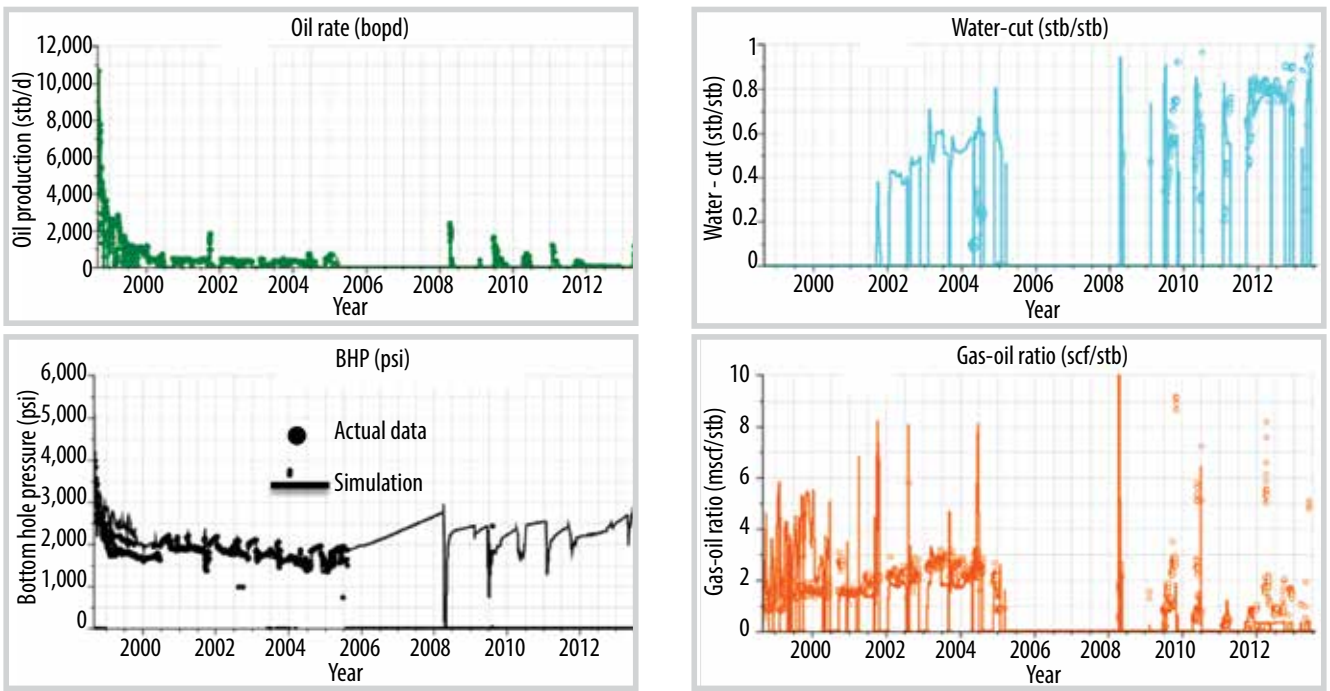

Figure 8. *History matching of well A.*

+ Initial reservoir pressure is at 5,320 psi at datum depth of 3,500 m in vertical depth.

+ Straight X-shaped relative permeability for cells of highly permeable fractures, and a curve shaped one for the others are assumed for fractured basement reservoir.

+ Carter Tracy aquifer is set at the bottom.

+ Modelling OIIP of 5.0 MMstb (1.27 MMstb in primary fracture cell, and 3.78 MMstb in others) is matched with OIIP estimated by material balance analysis.

The result of properties modelling for the connected seismic faults based on the above-mentioned settings is demonstrated in Figure 7.

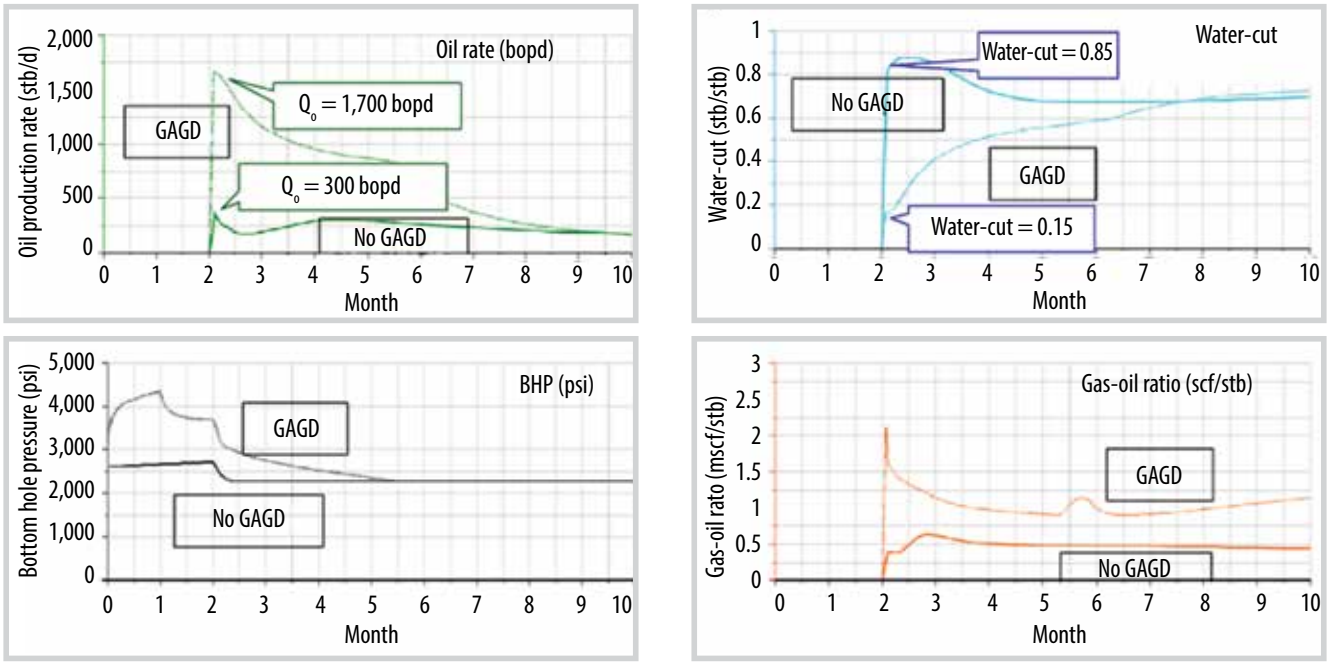

Figure 9. *Prediction of GAGD Huff 'n' Puff.*

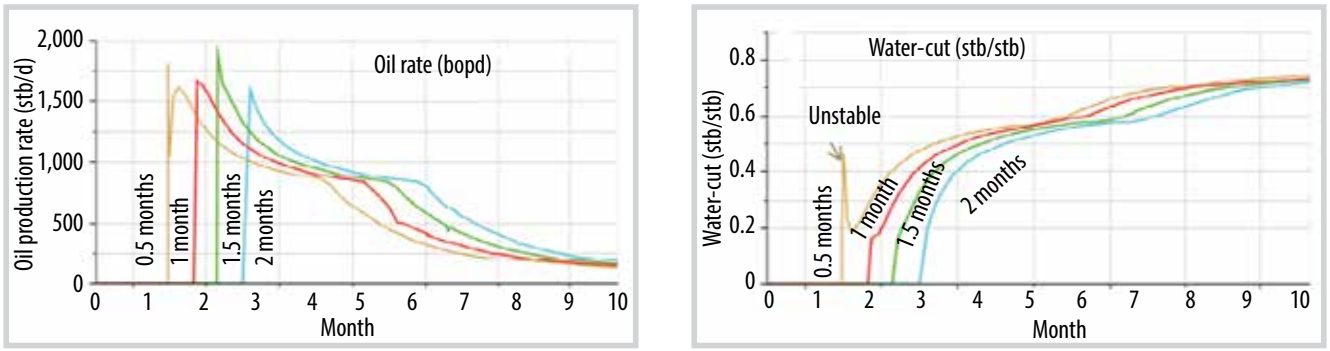

Figure 10. *Sensitivity check for shut-in period.*

The history matching was then carried out, and its result is shown in Figure 8.

+ The history run is controlled by the oil production rate (history data).

+ Simulated water breakthrough is earlier than actual, but the current water-cut at 95% is well converged.

+ Simulated GOR fluctuates, but its increase trend from 2001 to 2005 is matched. Simulated GOR in cyclic operation period is slightly deviated.

+ Flowing and shut-in bottom hole pressure (BHP) are reasonably matched.

- Preliminary injection scheme of GAGD

Based on the obtained result of the modelling and history matching, the preliminary design of the pilot test can be defined by prediction from the model. Three major steps of GAGD schema are set including 1) gas injection (total volume of 0.3 Bcf, injection rate at 10 MMscfd for 1 month), 2) shut-in (1 month for gas migration and stabilisation) and 3) flowing back. A reference case (without GAGD) is also simulated with 2 months shut-in (instead of applying Step 1 and 2 with GAGD), then flowing back. The flow-back is controlled by a liquid rate of 2,000 barrels of oil per day in the simulation.

The results of prediction with GAGD and without GAGD (Figure 9) are summarised below:

+ Oil-rate increases from 300 barrels of oil per day without GAGD to 1,700 barrels of oil per day with GAGD, showing the positive effect of GAGD application.

+ Water-cut reduces from 85% without GAGD to 15% with GAGD.

+ Cumulative oil increment of 0.104 MMstb is predicted with GAGD in the simulated period (10 months after the gas injection).

+ Cumulative gas increment of 0.137 Bcf, approximately 46% of injected gas volume, is recovered after GAGD.

+ Expected oil-water-contact moves down to the producing depth of the existing wells after gas injection and stabilisation.

- Sensitivity check for the design

To finalise the scheme of the pilot test, sensitivity runs of the gas injection volume and a shut-in period are carried out. For example, the sensitivity runs of the shut-in period (Figure 10) shows a fluctuated oil rate and water-cut in the initial flowing period with a 0.5-month shut-in, and a minimum 1-month shut-in would be necessary to let the injected gas migrate and stabilise.

- Finalised injection scheme of GAGD

The design of GAGD pilot test is fine-tuned by a sensitive check and finalised as follows.

+ Execution of the GAGD pilot test has 3 major steps including 1) gas injection of 0.3 Bcf (injection rate of 10 MMscfd for 1 month), 2) shut-in (1 month for gas migration and stabilisation) and 3) flowing back.

+ A contingent plan is prepared for 1) extending the gas injection period for 1 more month in case of a negligible positive response by the initial gas injection, 2) conducting a gradient survey for well monitoring, 3) repeating the Huff 'n' Puff operation in case of success (which could be optimised by the result of the initial test), 4) there is an option of postponing the test if the well declines rapidly.

2.4. Consideration of the applicability for the entire basement reservoir

This first pilot test is considered to provide a critical understanding of the effectiveness of the GAGD technique with a minimal cost of USD 65,000 for facility modification providing the availability of a high-pressure compressor for EOR of the Lower Miocene sandstone reservoir, and a deferment of 0.162 Bcf (54% of total gas injection) as predicted by the reservoir simulation. Subject to the result of the pilot test, the way-forward would be defined accordingly.

3. Implementation of GAGD pilot test [2]

3.1. Gas injection operation

The GAGD Huff 'n' Puff pilot test commenced the gas injection and a stable injection rate of 10 MMscfd was initially achieved as designed (Figure 11). After injecting a total gas volume of approximately 40 MMscf, the well-head

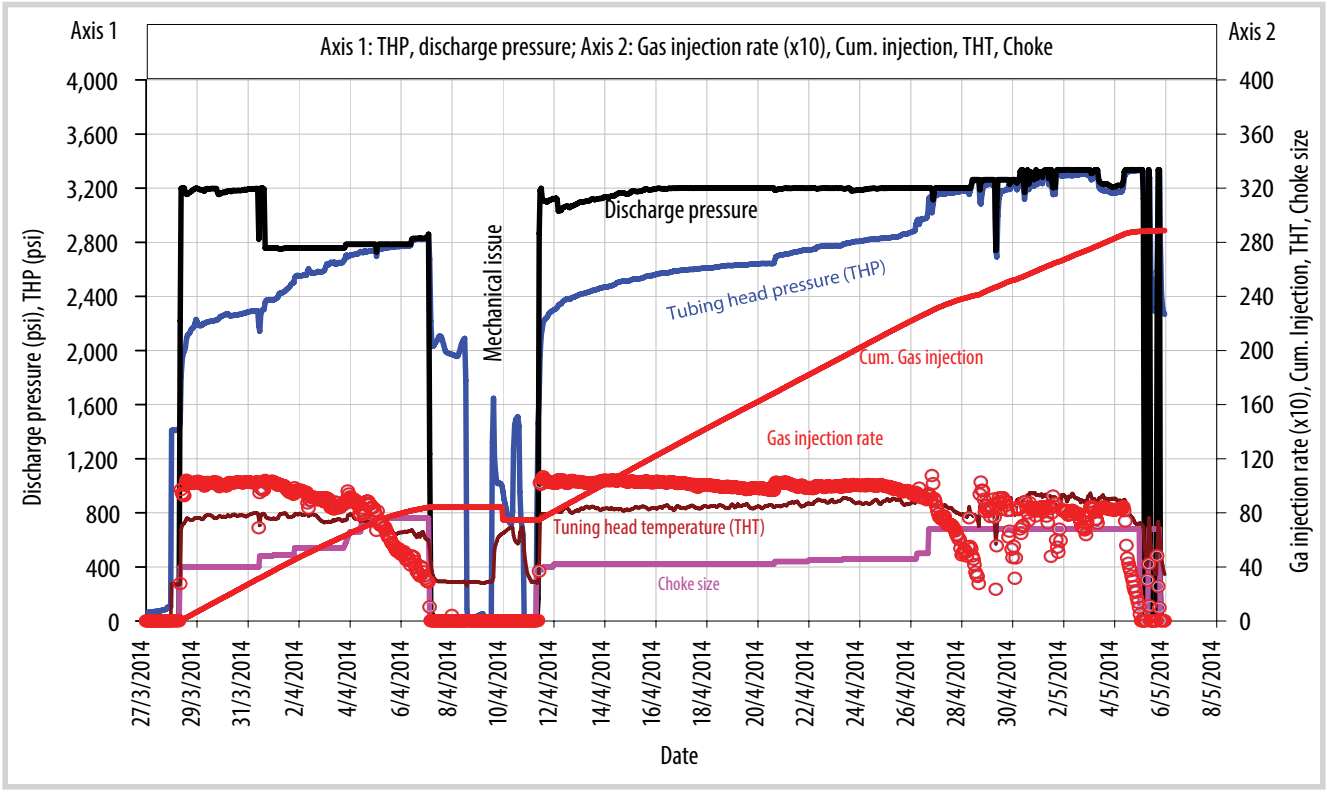

Figure 11. *Operation of gas injection.*

pressure started to increase, and the injection rate declined accordingly. The flow-back of 10 MMscf injected gas was performed, the gas injection was then resumed. It is noted that due to the exiting pack-off in the shallow section in the well, it was impossible to run the gauge cutter to check the tubing condition, and therefore, this reduction of gas injectivity was assumed to be a possible mechanical restriction inside the tubing and/or gas trapped near the wellbore reservoir zone caused by the gas injection, and it was released by flow-back. For the remaining injection period until the end of the injection phase, the gas injectivity was maintained at an almost stable rate.

A total of 298 MMscf of gas was injected into the reservoir (including 10 MMscf bled off). The designed injection target volume of 300 MMscf (0.3 Bcf) was almost achieved.

3.2. Performance of flow-back

- First flow-back cycle

After the gas injection and shut-in, the well was reconnected to the production line and re-opened on for flow-back. The initial flow was worse than the prediction. A total of 40 MMscf of gas was produced together with condensate during the first cycle of flow-back.

- Second flow-back cycle

The well was shut-in for a few days, and then re-opened with flowing gas and condensate. A total of 15 MMscf of gas was produced in this cycle.

- Third flow-back cycle

After a few days of shut-in, the well was re-opened, and it was still producing gas and condensate. A total of 35 MMscf of gas was produced in this cycle.

- Fourth flow-back cycle

The well was shut in for approximately 3 weeks, then re-opened, but still producing only gas and condensate. A total of 60 MMscf of gas was produced in this cycle.

A total of 50% of injected gas was produced from the above-mentioned 4 cycles of flow-back, i.e., 150 MMscf produced versus 300 MMscf of injected gas.

- Fifth flow-back cycle

The well was re-opened after 2 months of shut-in. Improvement was observed in this cycle with a higher oil rate and low water-cut in the first week. Water-cut then started increasing and quickly resumed to a high level (90 - 95%) as before the gas injection.

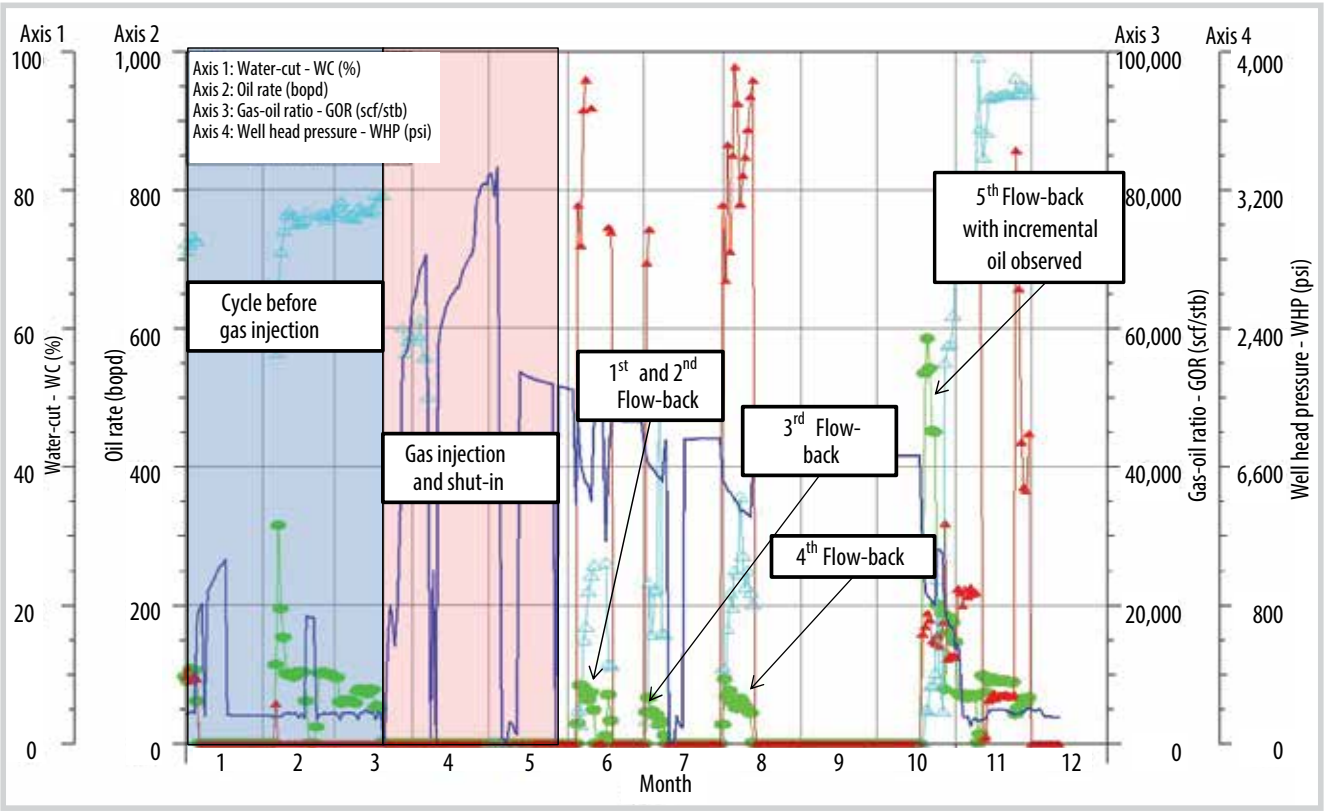

Figure 12. *Performance of gas injection and flow-back.*

A total of 106 MMscf of gas and 6,244 stb of oil were produced in this cycle.

The summary of flow-back performance is shown Figure 12.

4. Post-operation review and lessons learned

4.1. Reservoir simulation

The pre-GAGD sector model predicted a maximum oil rate of 1,700 barrels of oil per day with slow water-cut increasing in several months but the actual result turned out to be less with the oil rate of 600 barrels of oil per day observed in the fifth cycle and water-cut rising rapidly in one week. Such a model captured one of the possible scenarios in its prediction, but it did not fully reflect all the different scenarios relating to the below uncertainties:

+ Current water and gas contacts (OWC, GOC);

+ Permeability and size of aquifer;

+ Vertical (Kv) and horizontal (Kh) permeability for each fracture zone.

To address such uncertainties, sufficient sensitivity analysis would be required during the pre-job design as per the lessons learned from this GAGD pilot test.

4.2. Review of material balance analysis [2]

To better explain the actual performance of the well, the material balance analysis using the multi-tank model was applied in consideration of the difficulty to fully represent uncertainties by the reservoir simulation. The conceptual model of the multi-tank system for material balance analysis is illustrated in Figure 13.

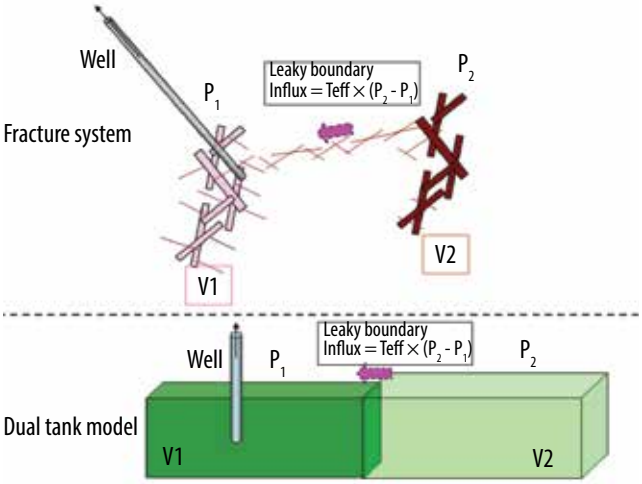

Figure 13. *Concept model of the multi-tank system applied for fractured basement.*

The material balance analysis during pre-job was optimistic in terms of the remaining oil in the main tank (which is connected directly to the wellbore) even though the pressure was well matched. Actual data showed that the remaining oil might be lower than predicted. Therefore, the designed gas injection volume (0.3 Bcf) was too much, and GOC was pushed down below the producing depth level. This is possibly the main reason why only gas was produced until 50% of the injected gas volume was bled off.

The detailed material balance analysis of pre-GAGD is shown in Figure 14. The material balance analysis of post-GAGD was re-evaluated with the pessimistic scenario (less

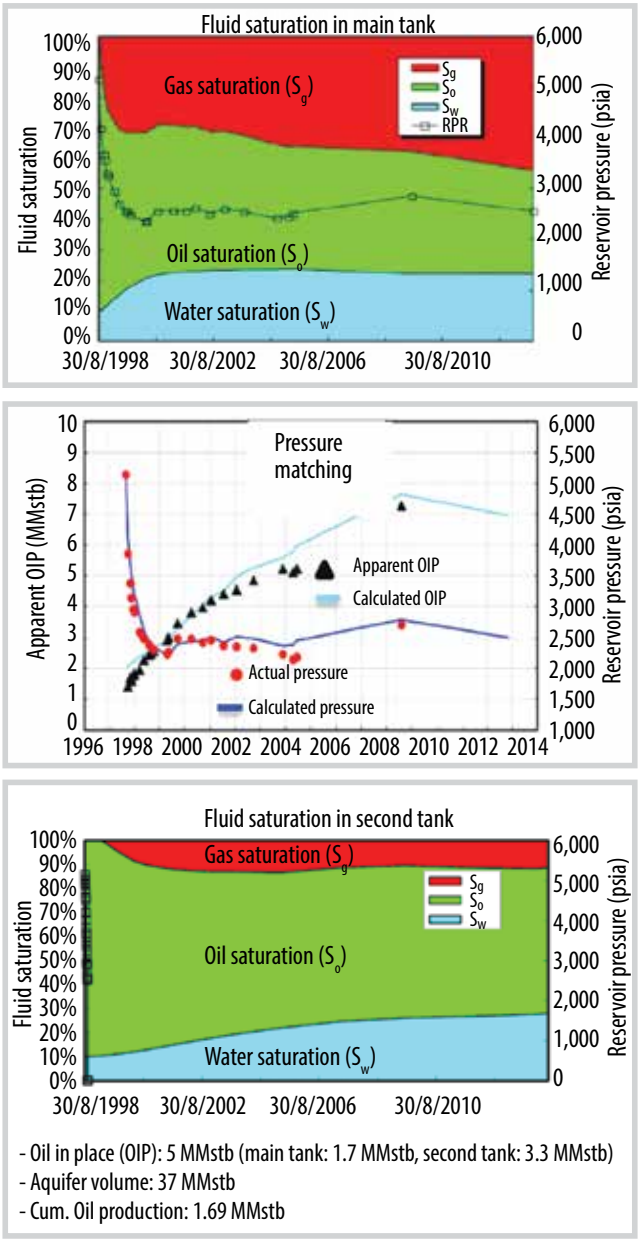

Figure 14. *Pre-GAGD material balance analysis.*

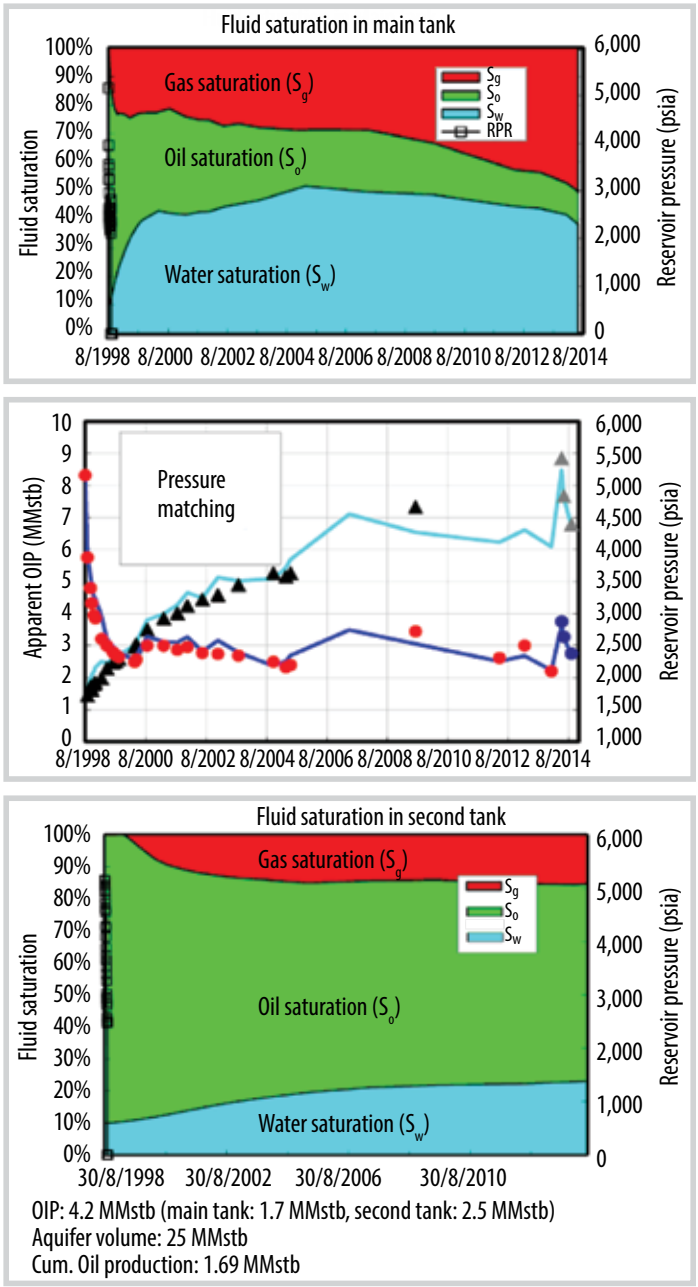

Figure 15. *Post-GAGD material balance analysis.*

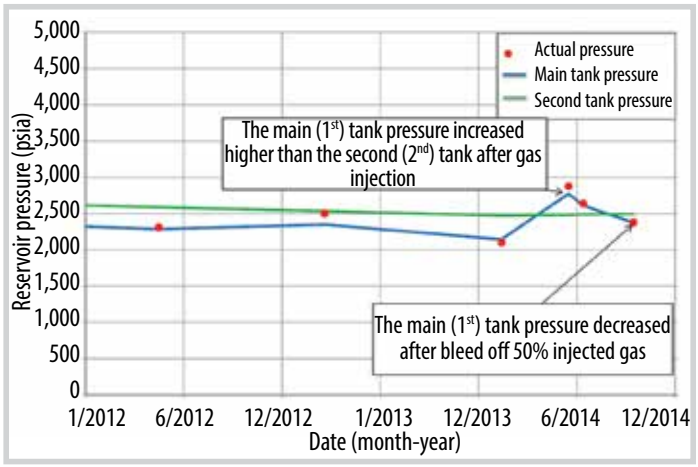

Figure 16. *Pressure profile of the multi-tank system.*

oil remaining). The pressure data (including data after gas injection and flow-back) was re-matched and the detailed result is shown in Figure 15.

Based on the behaviour and analysis of the matched multi-tank system model, the main oil production was supported by influx from the second tank having higher pressure and more remaining oil. After the gas injection phase, the pressure in the main tank increased immediately and became higher than the pressure in the second tank, and then, the influx from the second tank to the main tank was stopped. This could be the other important reason that caused only gas production in several flows back cycles.

To reduce pressure in the main tank below the second tank pressure and to resume the influx of oil, it is necessary to bleed off around 150 MMscf (50% of the injected volume). In fact, the actual performance in the fifth cycle was better after a flow-back of approximately 150 MMscf of injected gas. This is supported by the material balance analysis. The pressure profile of the multi-tank is shown in Figure 16.

4.3. Lessons learned and recommendations

The key lessons learned from this GAGD pilot test are listed below:

- Comprehensive reservoir modelling and simulation for full realisation of uncertainties are essential to design the scheme of gas injection and soaking time robustly.

- It is recommended to apply GAGD IOR in the wells having sufficient remaining oil in the first tank. This will mitigate the risk of high pressure in the main tank caused by gas injection, which then stops oil influx from the second tank.

5. Conclusions

The GAGD pilot test was implemented successfully with the indication of positive effectiveness of gas-assisted gravity drainage. A total of 298 MMscf of hydrocarbon gas was injected into the reservoir and the well was shut-in for oil/gas segregation. The flow-back was then monitored with several cycles (re-opened/closed) applied until the positive impact of GAGD was observed during the fifth cycle with a good oil rate and low water-cut, but water-cut increased quickly after only 1 week.

The simulation model was reasonably matched with production data, but the prediction was a failure. The model couldn't reflect the characteristics of reservoir heterogeneities due to a lack of sufficient sensitivity analysis during the pre-job design.

The material balance analysis was reviewed, showing the root-cause of the failure of prediction regarding the well performance after gas injection attributed to heterogeneities of the reservoir (multi-fracture system). Given such findings, for further application of GAGD, it is recommended to focus on the well/area with good remaining oil in the main fractures (directly connected to the well) and more homogeneous reservoirs.

The result of the pilot test provided a significant insight into the process optimisation of further pilot tests prior to proceeding to large-scale application for the entire basement reservoir.

Acknowledgements

The authors would like to acknowledge the support from JVPC, Partners (PVEP, Perenco Rang Dong) and the Vietnam Oil and Gas Group (Petrovietnam) for allowing use of the data and results of the pilot test as well as the permission to publish the paper.

References

[1] JVPC, *"Investigation of gas assisted gravity drainage applicability for basement reservoir - Pilot test proposal"*, 12/2013.

[2] JVPC, *"Gas assisted gravity drainage - Pilot test result"*, 12/2014.

[3] R. Valdez, S.P. Pennell, A. Cheng, T. Farley, and P.A. Boring, "Miscible hydrocarbon GOGD pilot in the Yates field unit", *SPE Improved Oil Recovery Conference, Tulsa, Oklahoma, USA, 14 - 18 April 2018*. DOI: 10.2118/190248-MS.

[4] M.M. Kulkarni and D.N. Rao, "Characterization of operative mechanisms in gravity drainage field projects through dimensional analysis", *SPE Annual Technical Conference and Exhibition, San Antonio, Texas, USA, 24 - 27 September 2006*. DOI: 10.2118/103230-MS.

[5] B. Lepski, Z. Bassiouni, and J.M. Wolcott, "Screening of oil reservoir for gravity assisted gas injection", *SPE/DOE Improved Oil Recovery Symposium, Tulsa, Oklahoma, USA, 19 - 22 April 1998*. DOI: 10.2118/39659-MS.

[6] H.K. Dinh, N.V. Le, M.G. Peter, V.T. Nguyen, T.S. Dang, V.Q. Nguyen, N.D. Hoang, T.A. Truong, H.M. Tran, and K.B. Nguyen, "Gas-assisted gravity drainage GAGD Huff n puff application for fractured basement reservoir - Case study", *SPE/ATMI Asia Pacific Oil & Gas Conference and Exhibition, Jakarta, Indonesia, 17 - 19 October 2017*. DOI: 10.2118/186210-MS.

[7] A.M. Saidi and S. Sakthikumar, "Gas gravity drainage under secondary and tertiary conditions in fractured reservoir", *Middle East Oil Shows, Bahrain, 3 - 6 April 1993*. DOI: 10.2118/25614-MS.

[8] Watheq J. Al-Mudhafar, and Dandina N. Rao, "Optimization of gas assisted gravity drainage (GAGD) process in a heterogeneous sandstone reservoir: Field-scale study", *SPE Asia Pacific Enhanced Oil Recovery Conference, Kuala Lumpur, Malaysia, 11 - 13 August 2015*. DOI: 10.2118/174579-MS.

PETROVIETNAM JOURNAL
Volume 10/2022, pp. 46 - 52
ISSN 2615-9902

VPI-MLOGS: A WEB-BASED MACHINE LEARNING SOLUTION FOR APPLICATIONS IN PETROPHYSICS

Nguyen Anh Tuan
Vietnam Petroleum Institute
Email: tuan.a.nguyen@vpi.pvn.vn
https://doi.org/10.47800/PVJ.2022.10-06

Summary

Machine learning is an important part of the data science field. In petrophysics, machine learning algorithms and applications have been widely approached. In this context, Vietnam Petroleum Institute (VPI) has researched and deployed several effective prediction models, namely missing log prediction, fracture zone and fracture density forecast, etc. As one of our solutions, VPI-MLogs is a web-based deployment platform which integrates data preprocessing, exploratory data analysis, visualisation and model execution. Using the most popular data analysis programming language, Python, this approach gives users a powerful tool to deal with the petrophysical logs section. The solution helps to narrow the gap between common knowledge and petrophysics insights. This article will focus on the web-based application which integrates many solutions to grasp petrophysical data.

Key words: Petrophysics, outliers removing, log prediction, interactive visualisation, web application, VPI-MLogs.

1. Introduction

Understanding data is a crucial step in any aspect of technological fields and research domains. In data science, clearly and precisely understanding data always requires time. In the petroleum field, petrophysics data has several unique features that require users to have not only domain knowledge but also specialised software to deal with data problems.

The most notable programming languages (such as Python) give developers tools to address issues and validate data without any special softwares or payments. In addition, some valuable functions could be designed to fit the user's machine learning requirements such as data processing, data cleaning, exploratory data analysis and model deployment.

The dashboard is basically fulfilled by charts, model results, and data insights. For example, Power BI and Tableau take a lot of advantages by their powerful organised abilities. However, because of their limited modification, several innovative ideas cannot be presented. Alternatively, many Python libraries appeared to support presentation and graphic user interface functions. Streamlit.io is one of these answers, combined with interactive visualisation by Altair library helping improve display features and data exploration.

In the end, a solution integrating interactive visuals and web applications has completely erected to deal with petrophysical log data which include several steps from data preprocessing (LAS files loading and re-organising, EDA, outliers removal, etc.) to model deployment (missing log forecast or fracture prediction). A web-based application is also more friendly than rigid coding lines.

2. Recent work and new approach

Traditionally, most of petrophysical tasks require custom software such as Petrel, Techlog (Schlumberger), IP Interactive Petrophysics (Lloyd's Register)...

During log interpretation, interactive function is performed beside advanced operations to provide information for exploration progress. On the other hand, recently, machine learning algorithms have become more and more popular and embedded in almost all industrial sectors. However, updating the latest technology always faces many restrictions, especially in financial aspect. From the user's perspective, VPI's team has researched and experienced applications of machine learning to address missing log data or erect fracture predictive models.

Date of receipt: 11/9/2022. Date of review and editing: 11 - 25/9/2022.
Date of approval: 5/10/2022.

In operation perspective, professional software runs locally in user's devices. It always requires a computer with high performance, and in some cases, it needs a workstation. This traditional approach retains several limitations such as high cost or immobility.

To solve these issues, the web-based application is considered. The new approach focuses on execution velocity and convenience with many advantages, namely the ability of implementing on medium performance computation, online availability, easy to access and ease-of-use. Following to the solution, users can upload their log data to the application host then predictive models are performed to return results back to users.

3. Research method

Python has grown to be one of the most popular programming languages in the world and is widely adopted in the data science community. Python contains a wide range of tools such as Pandas for data manipulation and analysis, Matplotlib for data visualisation, and Scikit-learn for machine learning, all aimed towards simplifying different stages of the data science pipeline.

Python supports a lot of visualisation libraries that allow users to generate data insights. There are prominent libraries with unique features such as matplotlib, seaborn, plotly, etc.. Recently, the performance has been further enhanced with the emergence of interactive visualisation tools.

To adapt for a web-based approach, several libraries in Python have been used namely Pandas, NumPy, Matplotlib, Altair, Streamlit, Vega-Lite.

3.1. Interactive visuals

In recent petrophysical log interpretation process, the main activities are handled by interactive windows such as histogram, cross-plot charts, curve view, etc. Therefore, interaction function always plays an important role. Instead of using merely traditional visual libraries (matplotlib, seaborn, etc.), the new approach focuses on a novel visual technique which is optimised to deal

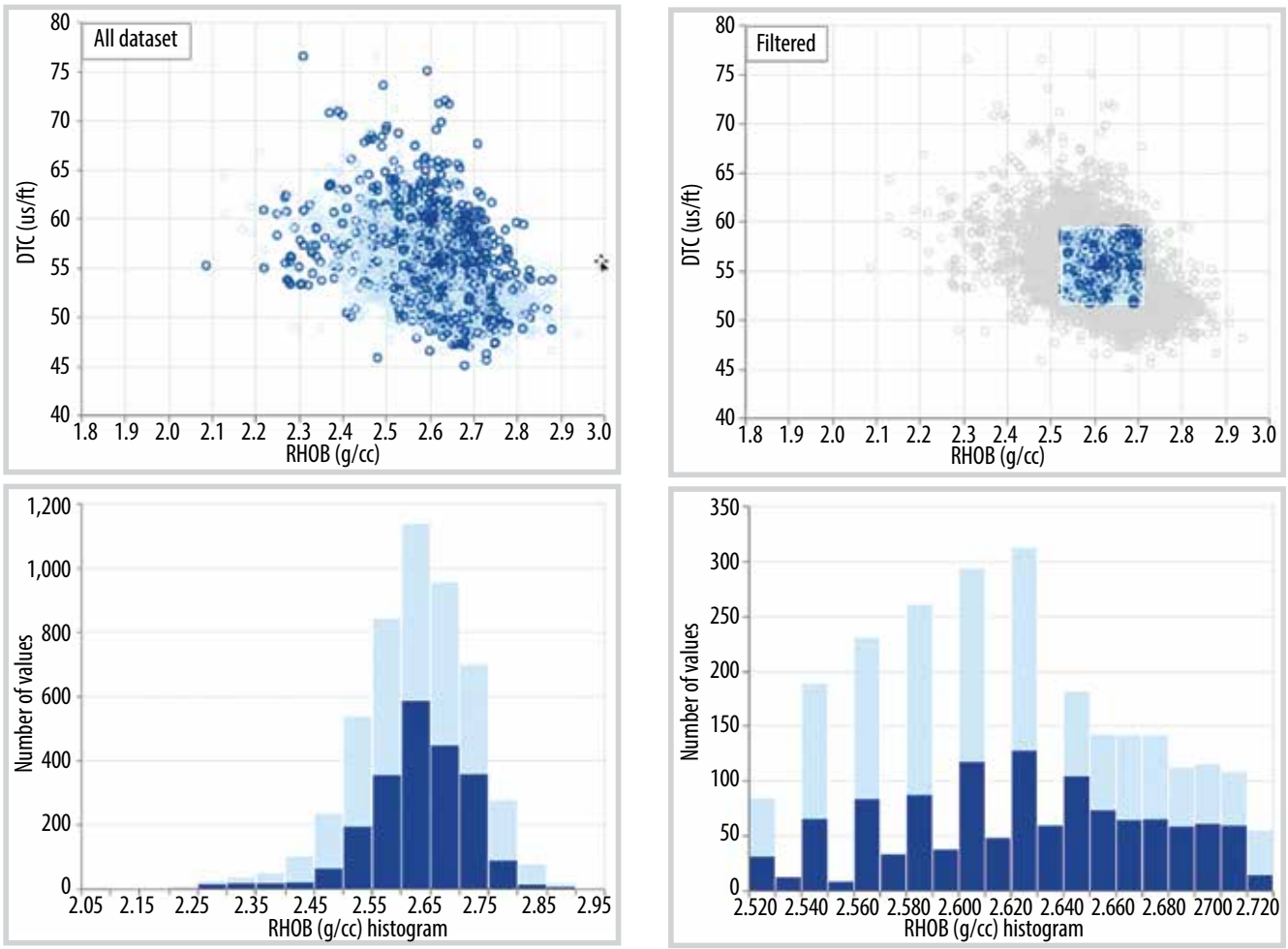

Figure 1. *Scatter plot and histogram chart interact with user selection.*

with hundreds of thousands dataset instances, and the most important, it possesses supreme interaction functions.

Altair is a visualisation Python library based on the Vega-Lite grammar, which allows a wide range of statistical visualisations to be expressed using a small number of grammar primitives. Vega-Lite implements a view composition algebra in conjunction with a novel grammar of interactions that enables users to specify interactive charts in a few lines of code. Vega-Lite is declarative; visualisations are specified using JSON data that follows the Vega-Lite JSON schema [1].

Altair allows users to directly interact with charts and connect to different visualisations. In Figure 1, a cross-plot between DTC and RHOB is represented simultaneously with the RHOB histogram chart. By interaction from the cross-plot view, selected points are immediately filtered in the histogram charts. It brings a convenient approach to understand petrophysical data as well as interpret initial mutual relation between logs.

3.2. Web-based framework to deploy our machine learning model

Beyond a visual dashboard, the model deployment solution should be considered. PowerBI or Tableau seems to be limited. The appearance of Streamlit in 2020 swiftly received great attention thanks to its many advantages in terms of speed, readability, ease-of-use and the ability of operating predictive models on the web-base.

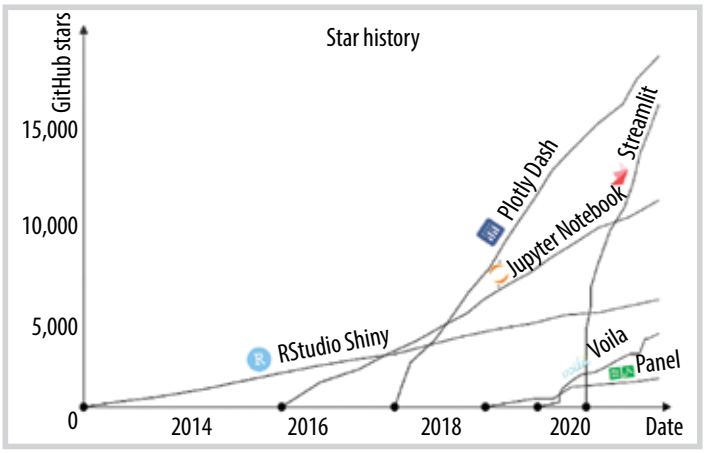

Firgure 2. *Streamlit has surged in popularity in recent years.*

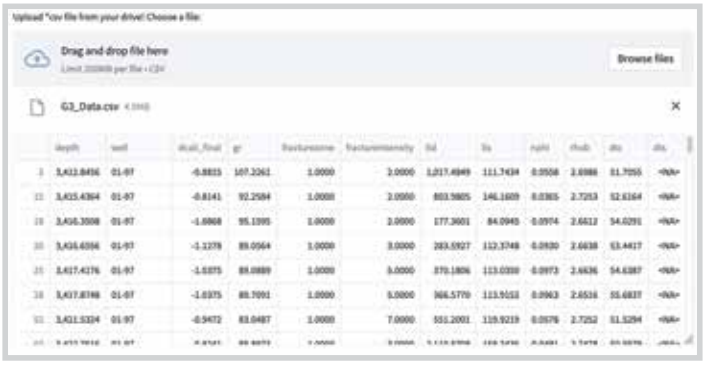

Figure 3. *Application interface and loading data section.*

Generally, Streamlit is an open-source Python library that is used to build powerful, custom web applications for data science and machine learning. Streamlit is compatible with several major libraries and frameworks such as Latex, OpenCV, Vega-Lite, seaborn, PyTorch, NumPy, Altair, and more. Streamlit is also popular and used among big industry leaders, such as Uber and Google X.

Besides, Streamlit has a wide range of UI components. It covers almost every common UI component such as checkbox, slider, a collapsible sidebar, radio buttons, file upload, progress bar, etc. Moreover, these components are very easy to use.

Streamlit has made it thoroughly simple to create interfaces, display text, visualise data, render widgets, and manage a web application from inception to deployment with its convenient and highly intuitive application programming interface [2].

4. VPI-MLogs for petrophysics

The application named VPI-MLogs includes full steps of a machine learning project to deal with petrophysical log problems. It can be summarised in 4 main stages: Data collection, data cleaning/ processing, EDA, Model&Prediction. The solution is deployed on a web-based platform thus avoiding the requirements of specialised software and technical expertise.

4.1. Data collection

Every petrophysical log data is stored as Log ASCII Standard (LAS) format with tabular structure. In Python, Lasio library allows users to access information directly from LAS files and transfer it to tabular data (pandas DataFrame). All calculations and modifications are made conveniently after this conversion.

In the first step, data in the LAS extension can be collected and loaded to the dashboard. The system automatically converts it to pandas DataFrame. Several functions are also provided for users' modification, namely curves name changing, setting the limited values, saving selected curves, merging multiple LAS files to CSV file…

Then, a preprocessed database has been formed and ready for the upcoming stages. A download button allows users to save the revised file to their storage.

4.2. Data cleaning/processing

During model preparation, it is important to clean the data sample to ensure that the observations best represent the problem. Outliers are unusual values in the dataset, and in general, machine learning modelling and modelling processes can be improved by understanding and even removing these values. In petrophysical logs, outliers can be resulted from many reasons: measurement errors, drilling fluid impact, bore well collapse, etc.

Even with a thorough understanding of the data, outliers can be hard to define. Great care should be taken

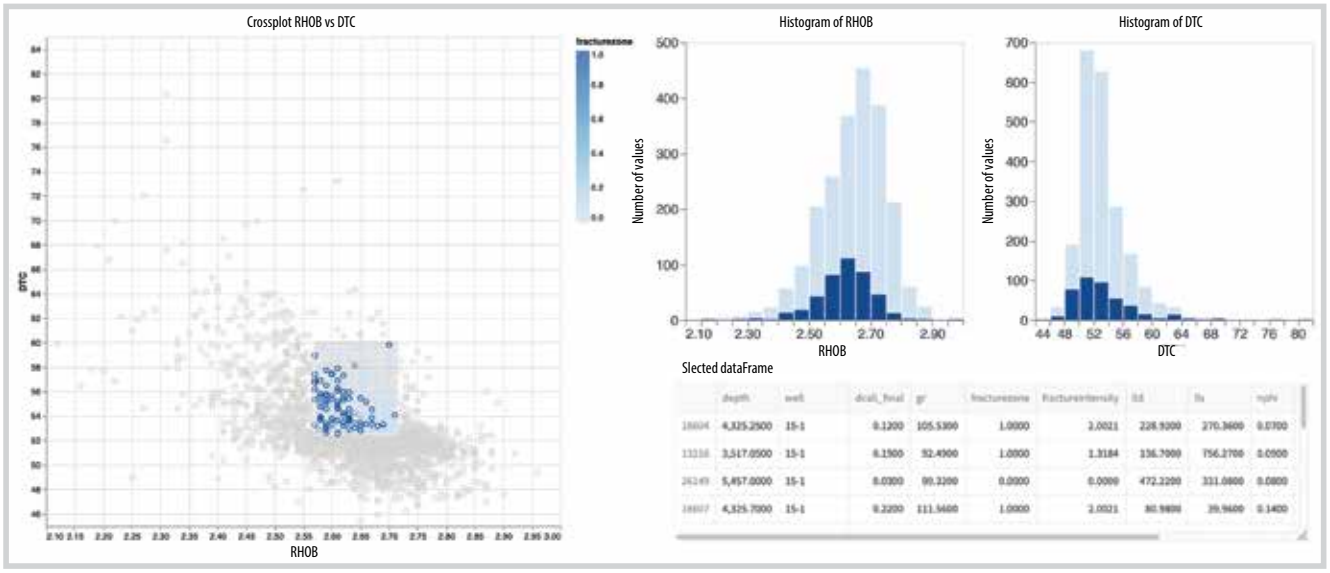

Figure 4. *Streamlit selection integrated with cross-plot and histogram chart to highlight the outliers. The outlier data points showed by selection (right-bottom).*

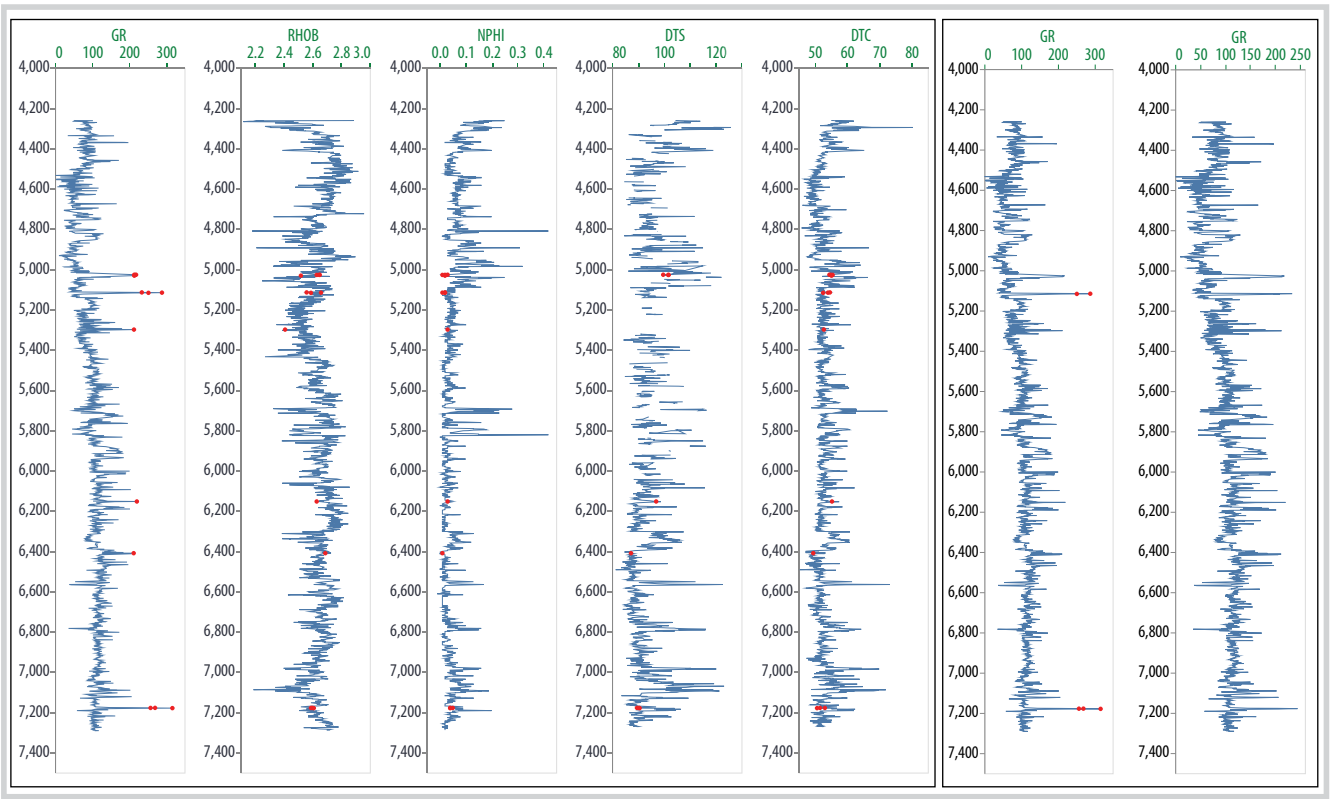

(a) *(b)*

Figure 5. *Curves and the highlight of selected point in log view (a). Outliers removing (b).*

not to remove or change values hastily, especially if the sample size is small [2].

On the web-based solution, many types of functions such as histogram chart, cross-plot 2 curves, logs view provide a basic tool to detect outliers. By user's selection of wells and curves to plot, they can proactively interact with data and deal with the skeptical points.

Combined with cross-plot, selection is an important tool to detect suspicious outliers (Figure 4). Simultaneously, the skeptical points are indicated in the dataset and highlighted on the curve view charts. Expert users using analytical techniques will decide whether to remove the outlier or keep it as good data points. The result can be saved to the local disk by a download button.

4.3. Exploratory data analysis

Exploratory data analysis is the stage where we actually start to understand the message contained in the data. EDA examines what data can tell us before actually going through formal modeling or hypothesis formulation. It should be noted that several types of data transformation techniques might be required during the process of exploration [3].

Several visuals have been equipped and integrated to support the EDA process:

- Scatter graphs: Scatter plots are used when we need to show the relationship between two variables. These plots are powerful tools for visualisation, despite their simplicity.

- Histogram: Histogram plots are used to depict the distribution of any continuous variable. These types of plots are very popular in statistical analysis.

- Bar charts: Bar charts are frequently used to distinguish objects between distinct collections to track variations over time. Bars can be drawn horizontally or vertically to represent categorical variables.

- Box plot: A type of descriptive statistics chart, visually shows the distribution of numerical data and skewness through displaying the data quartiles (or percentiles) and averages.

- Pair plot: A simple way to visualise relationships

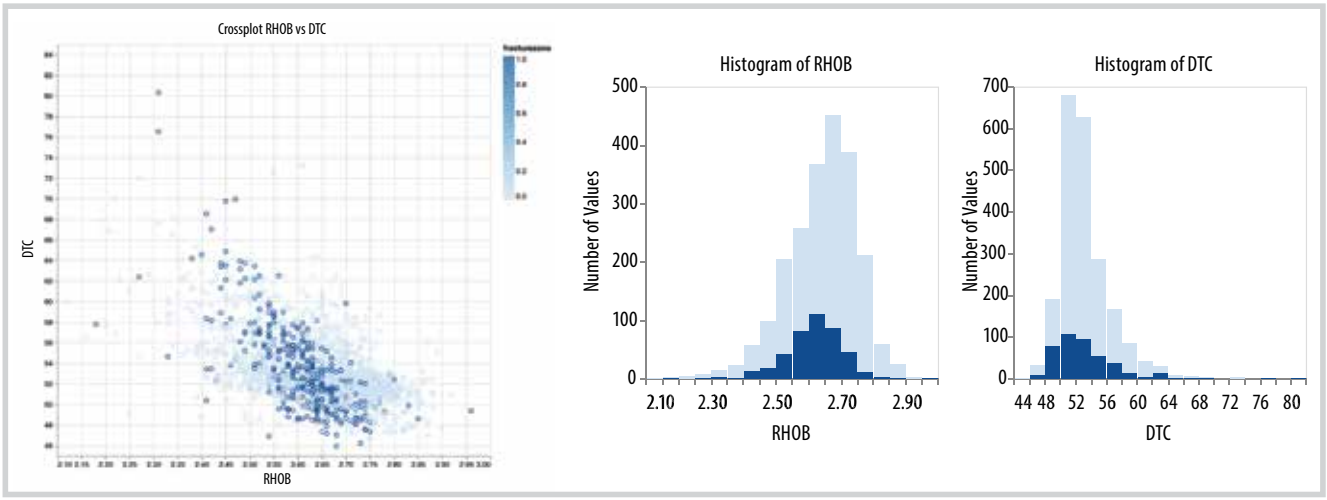

Figure 6. *Scatter and histogram charts.*

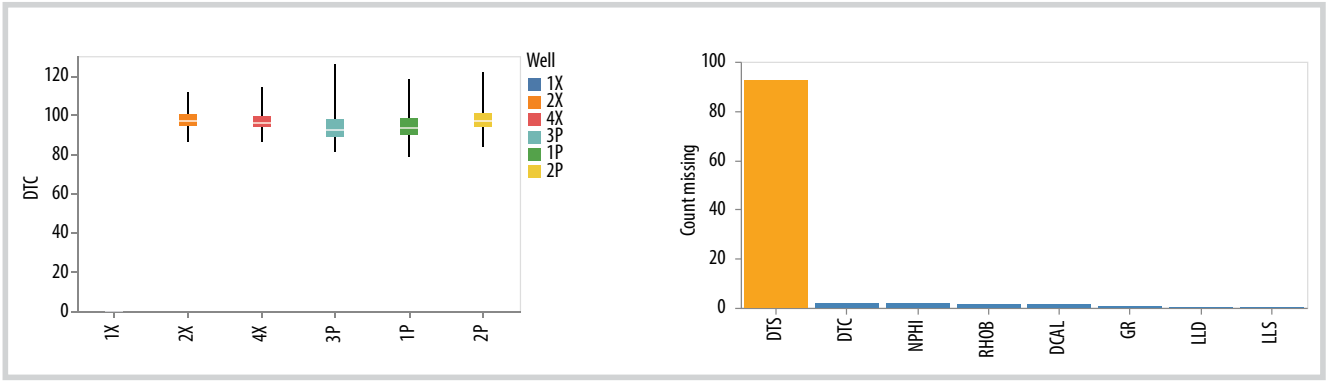

Figure 7. *Bar chart and box plot.*

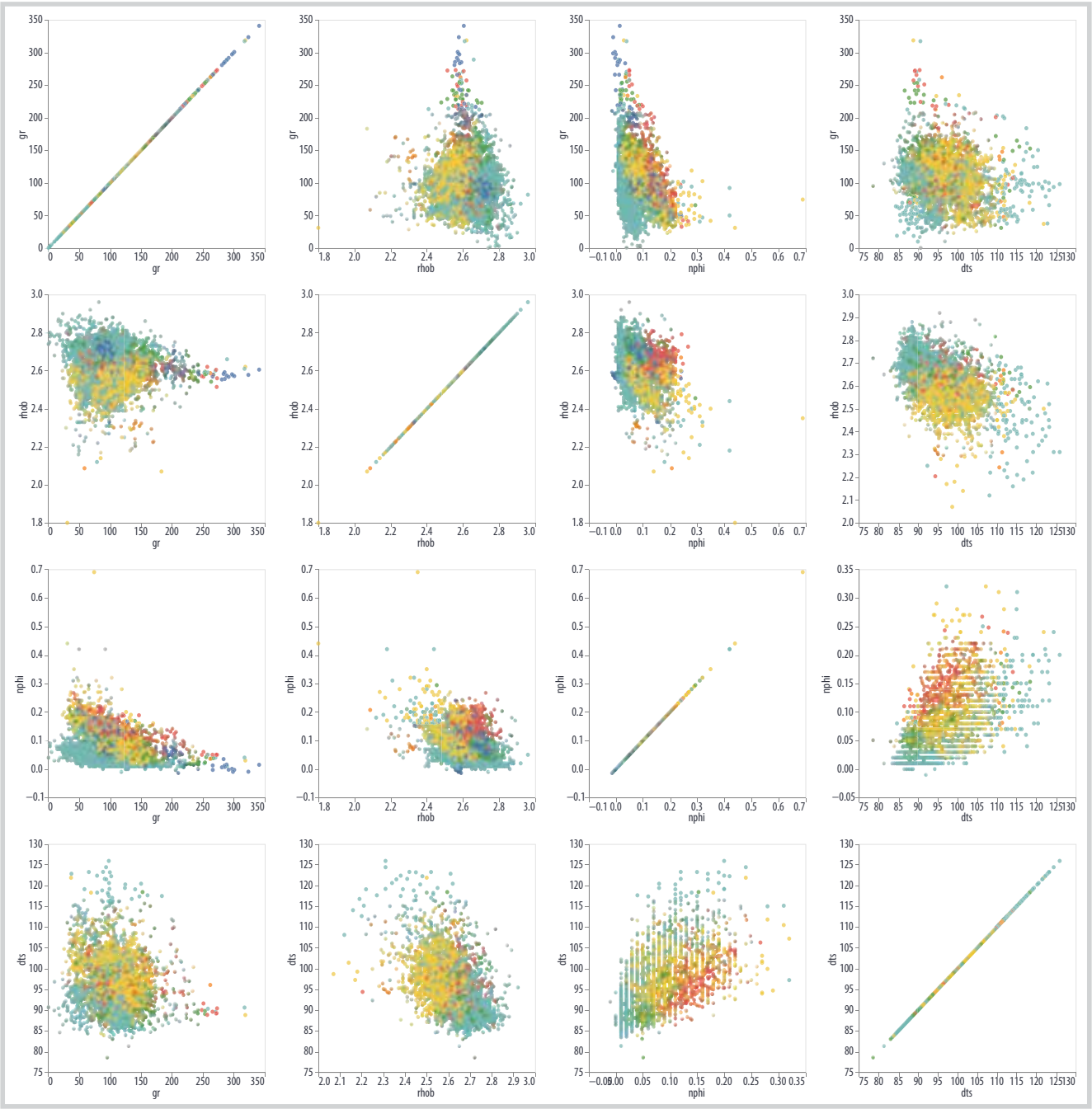

Figure 8. *Pair plot shows the duo relationship among logs.*

between each variable. It produces a matrix of relationships between each variable in the data for an instant data examination.

- Correlation heatmap: A type of plot that visualises the strength of relationships between numerical variables. Correlation plots are used to understand which variables are related to each other and the strength of this relationship.

4.4. Model deployment and prediction

Model deployment is the process of putting machine learning models into production. This makes the model's predictions available to users, developers or systems.

Streamlit is an alternative to Flask for deploying the machine learning model as a web service. The biggest advantage of using Streamlit is that it allows users to use HTML code within the application Python file. It doesn't essentially require separate templates and CSS formatting for the front-end UI [4].

In this section, a fitting predictive model is added under the code. Following that, the cleaned data

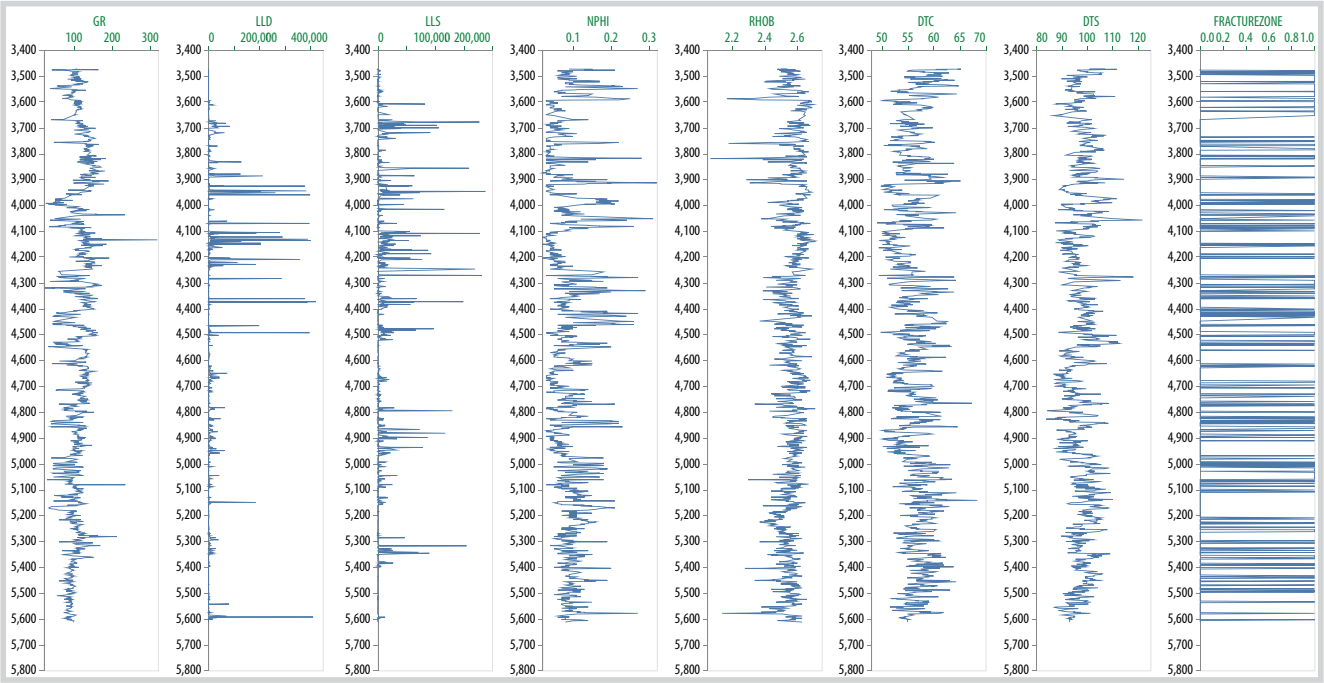

Figure 9. *Curves view with predicted values.*

containing features, which can be loaded by users, will be used as input of the model. By click the prediction button on the interface, the prediction process can be operated. The output is a dataset with predicted values. In addition, visual curves will appear.

In Figure 9, data uploaded from users include GR, LLD, LLS, NPHI, RHOB, DTC and DTS used as features which have been put to the fracture predictive model. Besides, the prediction result depicted next to features graphs. Through this visualisation, users can evaluate the predicted value by cross-checking with other curves concurrently.

The results can be downloaded and saved as petrophysical logs (LAS) or CSV file.

5. Conclusion and future outlook

The main objective of this application is to provide a solution for petrophysical log visualisation, modification, and predictive model deployment. Python and several libraries are used to perform the functions. Altair has been used as the main tool of observation and selection. Furthermore, a web-based system has been chosen as a fast and friendly method of model deployment. In which, Streamlit stands out with the advantages of simplicity, readability. Eventually, the whole solution covers from data loading, curves modification, outliers removal and model prediction.

In upcoming stages, training progress will be included in the VPI-MLogs final solution. Then, users can use their data as training input. VPI-MLogs will allow users to change the hyperparameters and select algorithms to optimise their model. In the end, users can entirely modify their data, build their model, and finally make their prediction.

References

[1] Jacob VanderPlas, Brian E. Granger, Jeffrey Heer, Dominik Moritz, Kanit Wongsuphasawat, Arvind Satyanarayan, Eitan Lees, Ilia Timofeev, Ben Welsh, and Scott Sievert, "Altair interactive statistical visualizations", *Journal of Open Source Software*, Vol. 3, No. 32, 2018. DOI: 10.21105/joss.01057.

[2] Mohammad Khorasani, Mohamed Abdou, and Javier Hernández Fernández, *Web application development with streamlit: Develop and deploy secure and scalable web applications to the cloud using a pure Python framework*. Apress, 2022.

[3] Suresh Kumar Mukhiya and Usman Ahmed, *Hands-on exploratory data analysis with Python*. Packt Publishing, 2020.

[4] Pramod Singh, *Deploy machine learning models to production: With Flask, Streamlit, Docker, and Kubernetes on Google Cloud Platform*. Apress, 2021.

PETROVIETNAM JOURNAL
Volume 10/2022, pp. 53 - 58
ISSN 2615-9902

OMNIPHOBIC CARBON STEEL SURFACE WITH GOOD WAX-REPELLENT PERFORMANCE

Nguyen Van Kiet[1], Nguyen Thi Phuong Nhung[1], Tran Thu Hang[2], Nguyen Hoang Luong[1]
[1]Petrovietnam University
[2]Petrovietnam College
Email: kietnv@pvu.edu.vn; and nhungntp@pvu.edu.vn
https://doi.org/10.47800/PVJ.2022.10-07

Summary

In this report, superhydrophobic and omniphobic coatings were produced by a combination of creating a ZnO micro/nanostructure on the carbon steel surface and coating a low surface energy material. Before reducing the surface energy with 1H, 1H, 2H, 2H-perflu orodecyltriethoxysilane, the steel surface was electrodeposited by a micro/nanostructured ZnO layer for a controlled deposition time. The process resulted in the steel surfaces being superhydrophobic (contact angle of 165 ± 2°) and omniphobic with white oil, diesel oil (contact angle of 135 ± 2°) and paraffin (contact angle of 127 ± 2°). The properties of superhydrophobic/omniphobic steel surfaces were then fully analysed by SEM, XRD, FTIR and contact angle measurements.

Key words: Steel surface, superhydrophobic, omniphobic, paraffin, ZnO thin film, micro/nanostructure.

1. Introduction

The precipitation of waxes containing mainly paraffinic compounds is a serious problem in low-temperature crude oil production, such as reduced oil transportation efficiency, increased manufacturing cost, even causing pipelines to be blocked, etc. [1, 2]. To predict wax deposition, there are various methods based on two main ways of adding additives and using appropriate pipeline surface materials. Additives are categorised into different kinds depending on its activating mechanism: anti-sticking agents, dispersants, or inhibitors. Among them, adding additives is mostly used because of its effectiveness in preventing the wax precipitation, however it is costly and not environmentally friendly [3]. Therefore, in recent years, many research groups have made great efforts on pipeline surface materials, especially focusing on wax-repellent coatings for pipelines [4, 5].

In fact, the fabrication of wax-repellent surfaces is a kind of making liquid-repellent surfaces. It is based on the wetting property of the surface, which is determined by a contact angle (CA) between the liquid and the solid surface. The value of contact angle depends on the characteristics of the surface (such as composition, chemical finishing, roughness, etc.) and the interfacial surface tension (solid - liquid - vapor) [6 - 8].

When a liquid droplet is deposited on a perfected smooth and chemical homogeneous surface, the contact angle is derived from Young's equation (θ) [9 - 11]:

$$Cos\theta = \frac{\gamma_{SV} - \gamma_{SL}}{\gamma_{LV}}$$

where γ refers to the interfacial tension; S, L, and V refer to the solid, liquid and vapor phases, respectively. Based on the water contact angle, a surface can be classified as superhydrophilic if the contact angle ≈ 0, hydrophilic if the contact angle is less than 90°, hydrophobic if the contact angle is greater than 90°. Note that the maximum water contact angle on "a perfected smooth and chemical homogeneous surface" is about 130° [8]. Similar to water, based on the contact angle of liquid having a low surface tension (such as oil, alcohol, or another organic solvent), the surface can be categorised as superomniphilic, ominiphilic and omniphobic [6, 10].

In fact, the surface always illustrates both physical defects (or roughness) and chemical inhomogeneity. In this case, the contact angle between the liquid and the

Date of receipt: 12/9/2002. Date of review and editing: 12 - 19/9/2022.
Date of approval: 5/10/2022.

surface is defined as the apparent contact angle that has a strong bond with the contact angle by Young's equation (as described in "wetting on rough surfaces - the Cassie-Baxter state and the Wenzel state).

According to some reports [8, 12, 13], the fabrication of liquid-repellent surfaces has been studied based on creating a re-entrant structure or a combination between textured surface and chemically modified surface. The textured surface increases the surface roughness while the chemical modification of the surface leads to a decrease in the surface energy [14, 15].

To create the textured surface, there are several methods such as sandblasting, particle coating, plasma treatment, chemical treatment, lithography, deep coating, and vapor deposition. However, it may be noted that the large-scale commercial applications of these techniques are limited due to the required special equipment, expensive material, complex and long fabrication process [4].

Chemically, there are two main methods for surface treatment: the first one is the deposition of hydrophobic material (via physisorption) such as fluorocarbon polymer, teflon or cytop by spin coating, plasma coating, etc. The other way is the covalent immobilisation of a low surface energy via chemisorption: silanisation for oxide surfaces, thiol alkylation for noble metal surfaces [6].

In recent years, a few omniphobic and superhydrophobic steel surfaces have been fabricated [16], but they are mesh steel surfaces and have not been wax-tested yet [2, 3, 5,17]. In this article, we introduce a simple process to fabricate wax-repellent steel surfaces. First, the steel substrate is polished by sandpaper, then it is coated with a micro/nanostructured ZnO layer. Finally, this surface is modified with fluoro substance. The preparation of wax-repellent steel surface is analysed by Scanning Electron Microscopy (SEM), energy dispersive X-ray spectroscopy (EDX), X-ray diffraction (XRD), Fourier transform infrared spectroscopy (FTIR) and contact angle measurements for water, oil liquid, diesel, and paraffin.

2. Experimental

2.1. Materials

Methyltrichlorosilane, ethanol, acetone, H_2SO_4, H_2O_2, NH_3, and $Zn(CH_3COO)_2$ and white oil are obtained from Sigma-Aldrich. In this study, CT3 steel substrate is bought from China and consists of Fe (42.89%), C (0.14%), Mn (11.12%), Si (0.13%), Cr (0.02%), and Zn (0.51%). Paraffin wax is from China and crude oil is from Vietnam (Bach Ho crude).

2.2. Preparation of superhydrophobic steel surface

2.2.1. Formation of micro/nanostructured ZnO coating

The steel surfaces are cut into 1.5 cm × 3.0 cm × 3.0 cm for the CT3. The substrates are then polished by sandpaper (100, 200, and 600 grit) and subsequently degreased in acetone and ethanol, and finally rinsed with distilled water.

The steel substrate is firstly dipped into 0.1 M HCl solution for 30 seconds before the zinc electrodeposition process is conducted for different time durations: 5 minutes, 15 minutes, 30 minutes, 45 minutes, and 60 minutes. More details concerning this process are described in our previous article [10, 18].

A 2-electrode cell is used, in which cathode is the steel substrate, anode is a Zn metal sheet (0.2 cm × 2 cm × 5 cm) and the electrolyte is deionised water. A constant voltage of 1 V is applied between the two electrodes to grow the Zn layer for different durations. After electrolysis, the substrate is cleaned with deionised water and then dried. Finally, the substrate is annealed in a furnace at 250°C for 120 minutes to form a ZnO thin film coating on the steel surface.

2.2.2. Surface functionalisation by silanisation

The ZnO-coated steel substrates are UV/O3 treated for 30 minutes to remove any organic contaminants and to generate surface hydroxyl -OH groups. The activated surface is then directly dipped into a 50 mL hexane containing 50 microliters 1H, 1H, 2H, 2H-perfluorodecyltri ethoxysilane. The substrate is rinsed 3 times with hexane, 3 times with ethanol, and then dried under a gentle nitrogen flow.

Morphology and composition of the thin film is checked by JEOL JSM-7600F SEM and an Oxford Instruments EDS X-ray microanalyser.

The chemical surface is analysed by FTIR, XRD and EDX while the wetting properties of all substrates are determined by measuring static contact angle of water, white oil, diesel and melting paraffin with OCA - DataPhysics Instruments at 3 positions on each surface using 5 µl distilled water or oil.

3. Results and discussion

3.1. SEM observation

To consider the effect of structure on superhydrophobic and omniphobic properties, in this study, the steel substrate is coated a micro/nanostructured ZnO layer by electrodeposition using acetate zinc solution for various time durations: 5, 15, 30, 45 and 60 minutes. All these surfaces then are treated with 1H, 1H, 2H, 2H-perfluorodecyltriethoxysilane.

Figure 1 shows SEM images of steel substrate before and after ZnO coating by electrodeposition method: (a) steel substrate without ZnO coating (M_0), (b) steel substrate with ZnO electrodeposition for 5 minutes (M_1), (c) steel substrate with ZnO electrodeposition for 15 minutes (M_2), (d) steel substrate with ZnO electrodeposition for 30 minutes (M_3), (e) steel substrate with ZnO electrodeposition for 45 minutes (M_4) and (f) steel substrate with ZnO electrodeposition for 60 minutes (M_5).

The cathodic electrochemical deposition reactions to grow the nano/microstructure ZnO layer are proposed as follows [19].

$$O_2 + 2H_2O + 4e^- \rightarrow 4OH^- \quad (1)$$

$$Zn^{2+} + xOH^- \leftrightarrow Zn(OH)_x^{2-x} \quad (2)$$

$$Zn(OH)_x^{2-x} \leftrightarrow ZnO + H_2O + (x-2)OH^- \quad (3)$$

First, OH^- ions are generated on the substrate by reducing O_2 precursor (reaction 1). Secondly, Zn^{2+} ions and OH^- are combined to generate $Zn(OH)_x^{2-x}$ ions (reaction 2). Finally, ZnO is formed by dehydration of $Zn(OH)_x^{2-x}$ ions (reaction 3).

As shown in Figure 1a, the ZnO-uncoated surface of CTs-1 is rough with some minor scratches, holes, and other defects. However, after a 5-minute electrodeposition, the ZnO particles having diameters of about 500 nm appear on the substrate (Figure 1b). The deposition time lasting more than 15 minutes results in the formation of a pattern with flower shapes, each with a spherical particle inside, which increases the roughness of the surface.

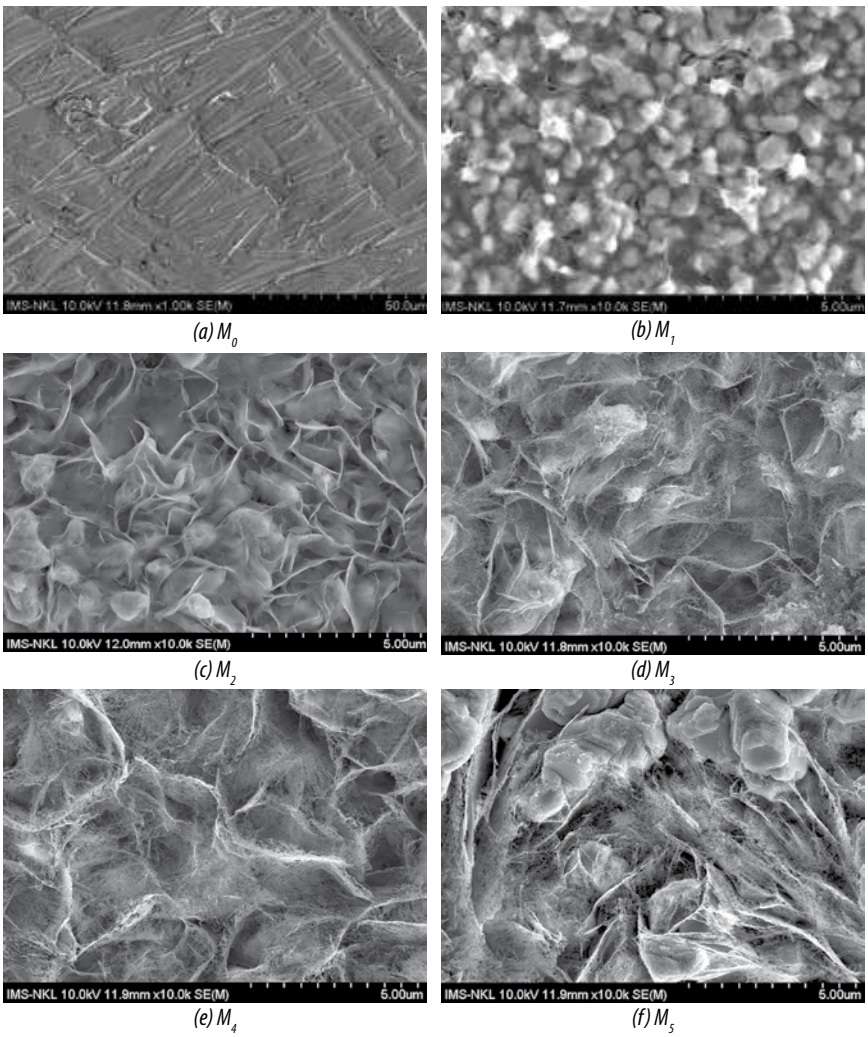

(a) M_0 (b) M_1 (c) M_2 (d) M_3 (e) M_4 (f) M_5

Figure 1. *SEM images: (a) steel substrate without ZnO coating (M_0), (b) steel substrate with ZnO electrodeposition for 5 minutes (M_1), (c) steel substrate with ZnO electrodeposition for 15 minutes (M_2), (d) steel substrate with ZnO electrodeposition for 30 minutes (M_3), (e) steel substrate with ZnO electrodeposition for 45 minutes (M_4) and (f) steel substrate with ZnO electrodeposition for 60 minutes (M_5).*

3.2. XRD analysis

Figure 2 presents the X-ray diffraction (XRD) pattern of steel substrate and of micro/nanostructured ZnO-coated steel substrate. The peak in the XRD spectra in Figure 3 can belong to the (100), (002), (101), (110), (112), and (201) crystallographic planes of wurtzite hexagonal ZnO crystal structure. The diffraction pattern indicates pure crystallinity of ZnO micro/nanostructure.

3.3. EDX analysis

The chemical compositions of steel surfaces without and with ZnO coating are also measured by energy-dispersion X-ray (EDX spectroscopy) as shown in Figure 3.

From Figure 3, before coating with the ZnO layer, the steel surface mostly contains C and Fe atoms with proportions of 30.1% and 69.2%, respectively. Meanwhile, the ZnO-coated steel surface presents a high amount of Zn and O atoms with 33.7 and 46.4%, respectively.

From those results, it might confirm that the micro/nanostructured ZnO layer has been coated on the steel surface by electrodeposition method.

3.4. Effect of micro/nanostructured ZnO coating to the superhydrophobicity and omniphobicity of the steel surface

In this section, four liquids (water, white oil, diesel oil and paraffin) are used to test the superhydrophobic/omniphobic properties of the steel surfaces. For each liquid, the contact angles (CA) on steel surface and micro/nanostructured ZnO coated-steel surface are measured and plotted in Figure 4.

On the steel surface without ZnO coating (M_0), the surface is hydrophobic (contact angle = 126°), omniphilic with white oil (contact angle = 78°, total spreading diesel and paraffin). When a steel surface is deposited with ZnO nanoparticles (M_1), it becomes superomniphobic for all oils (contact angle = 0) and less hydrophobic (contact angle = 110°). Although the surface M_0 is less rough than M_1 and has omniphilic properties with contact angle < 90°, the surface M_1 is more omniphilic and water easily enters among the particles at Wenzel state.

For other surfaces (M_2, M_3, M_4 and M_5) that are electrodeposited longer, their roughness increases dramatically, resulting in these surfaces being superhydrophobic with a contact angle of more than 160° and omniphobic (contact angle > 110°). Particularly, the surfaces M_4 and M_5 having the electrodeposition time of more than 45 minutes are the highest omniphobic; the contact angle value of white oil, diesel and paraffin are around 130°.

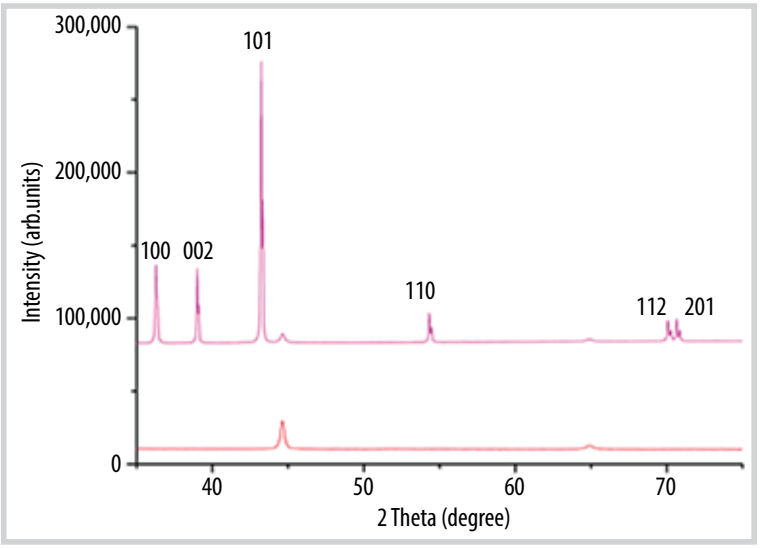

Figure 2. *X-ray diffraction spectra of steel substrate without ZnO coating (orange line), and micro/nanostructured ZnO-coated steel substrate (purple line).*

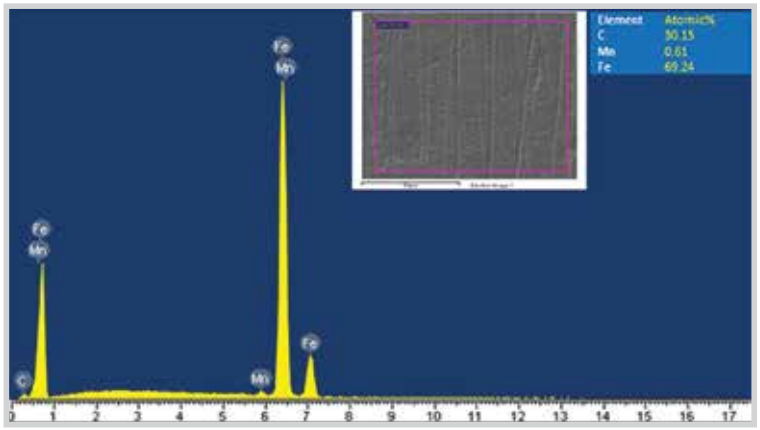

(a)

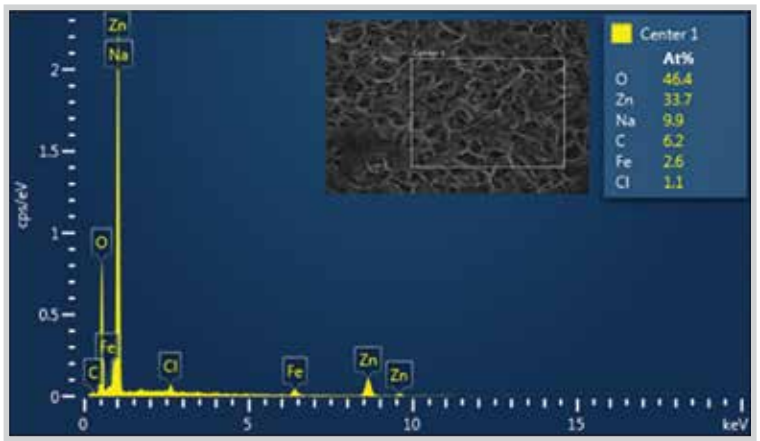

(b)

Figure 3. *EDX spectroscopy of steel surface without ZnO coating (a) and with ZnO coating (b).*

3.5. Effect of time chemical reactions on superhydrophobicity and omniphobicity of the micro/nanostructured ZnO-coated steel surface

In this section, time silanization reactions between 1H,1H, 2H, 2H-perfluorodecyltriethoxysilane and micro/nanostructured ZnO-

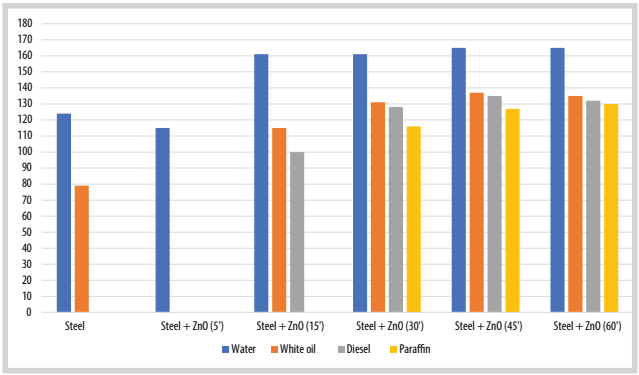

Figure 4. *Contact angle of water, white oil, diesel and paraffin on steel surface and different ZnO-coated steel surface.*

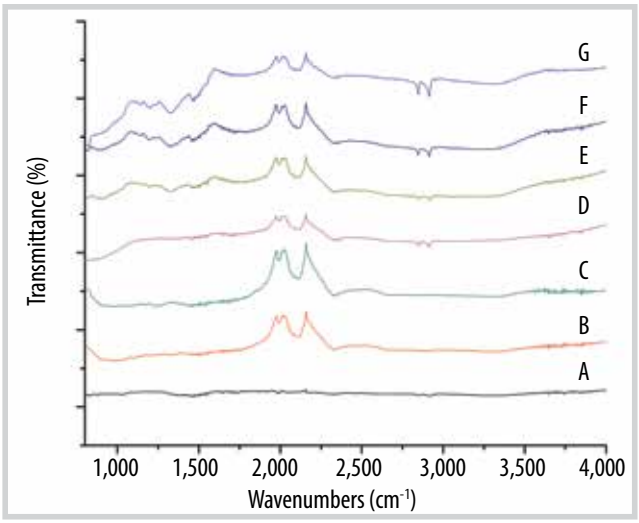

Figure 5. *FTIR spectra of the as-prepared steel surface (curve A), ZnO-coated steel surface (B), ZnO-coated surface are modified with silane for 0.5 hours (C), 1 hour (D), 2 hours (E), 6 hours (F), and 16 hours (G).*

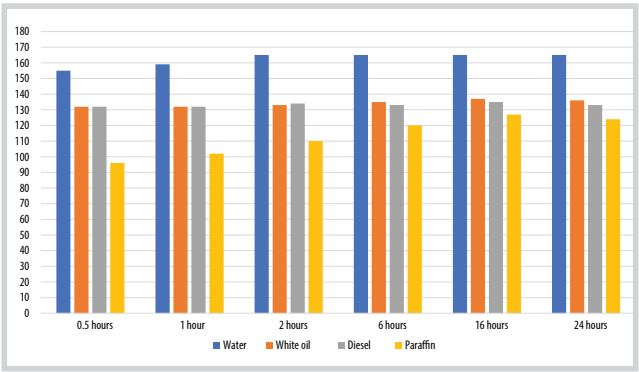

Figure 6. *Contact angle of water, white oil, diesel and paraffin on ZnO-coated steel surface with silanisation treatment.*

coated steel surface are investigated to show how it affects the wettability of substrate. In fact, the surface M4 (with 45 minutes of ZnO electrodeposition) reacts with that silane for various time durations: 0.5 hours, 1 hour, 2 hours, 6 hours , and 16 hours.

From Figure 5, the FTIR spectrum of steel sample (line A) does not show any functional group pick. When the steel surface is coated with a micro/nanostructured ZnO layer, two picks at 1,993 cm^{-1} and 2,110 cm^{-1} appear and relate to ZnO stretching. Further, this surface is modified with silane, the intensity of picks at 1,993 cm^{-1} and 2110 cm^{-1} decreases, and two picks appear at 2,847 cm^{-1} and 2,914 cm^{-1}, which correspond to the $C\text{-}H_x$ stretching modes and have density increasing with the reaction time. If the silanisation reaction takes place for 0.5 hours, the pick of $C\text{-}H_x$ stretching modes still does not appear, however, it occurs after a one-hour reaction.

In this section, the contact angle of the four above-mentioned liquids is also measured (Figure 6). It is obvious that all samples become superhydrophobic (contact angle > 150°) and omniphobic after 0.5 hours of chemical treatment. However, the contact angle values of four liquids are stable after 6 hours of silanisation treatment (with contact angle of water about 160°, contact angle of oil about 135° and contact angle of paraffin about 128°).

4. Conclusion

In this project, we have successfully studied superhydrophobic and omniphobic steel surfaces. A simple electrodeposition method has generated micro/nanostructured ZnO layer coating on the steel surface. From the SEM analysis, it shows that different electrodeposition times produced different ZnO layer structures. In addition, the results by EDX and XRD also illustrated that the micro/nanostructured ZnO layer was crystal. The modification with 1H, 1H, 2H, 2H-perfluoro decyltriethoxysilane for 6 hours gave the best results in terms of static contact angle with the values of 160 ± 2° and 130 ± 2° for water and oil, respectively. However, this result has presented good wax-repellent properties.

Acknowledgment

The current project was financially supported by PetroVietnam University under grand code GV2103.

References

[1] Jinghao Yang, Yingda Lu, Nagu Daraboina, and Cem Sarica, "Wax deposition mechanisms: Is the current description sufficient?", *Fuel*, Vol. 275, 2020. DOI: 10.1016/j.fuel.2020.117937.

[2] Yuzhen Guo, Weiping Li, Liqun Zhu, Zhiwei Wang, and Huicong Liu, "Phosphoric chemical conversion coating with excellent wax-repellent performance", *Applied Surface Science*, Vol. 259, pp. 356 - 361, 2012. DOI: 10.1016/j.apsusc.2012.07.051.

[3] A. L. Sousa, H. A. Matos, and L. P. Guerreiro, "Preventing and removing wax deposition inside vertical wells: A review", *Journal of Petroleum Exploration and Production Technology*, Vol. 9, No. 3, pp. 2091 - 2107, 2019. DOI: 10.1007/s13202-019-0609-x.

[4] Yuzhen Guo, Weiping Li, Liqun Zhu, and Huicong Liu, "An excellent non-wax-stick coating prepared by chemical conversion treatment", *Materials Letters*, Vol. 72, pp. 125 - 127, 2012. DOI: 10.1016/j.matlet.2011.12.079.

[5] Zhiwei Wang, Liqun Zhu, Huicong Liu, and Weiping Li, "A conversion coating on carbon steel with good anti-wax performance in crude oil", *Journal of Petroleum Science and Engineering*, Vol. 112, pp. 266 - 272, 2013. DOI: 10.1016/j.petrol.2013.11.013.

[6] Nguyen Thi Phuong Nhung, Philippe Brunet, Yannick Coffinier, and Rabah Boukherroub, "Quantitative testing of robustness on superomniphobic surfaces by drop impact", *Langmuir*, Vol. 26, No. 23, pp. 18369 - 18373, 2010. DOI: 10.1021/la103097y.

[7] Nguyen Thi Phuong Nhung, Renaud Dufour, Vincent Thomy, Vincent Senez, Rabah Boukherroub, and Yannick Coffinier, "Fabrication of superhydrophobic and highly oleophobic silicon-based surfaces via electroless etching method", *Applied Surface Science*, Vol. 295, pp. 38 - 43, 2014. DOI: 10.1016/j.apsusc.2013.12.166.

[8] Arun K. Kota, Gibum Kwon, and Anish Tuteja, "The design and applications of superomniphobic surfaces", *NPG Asia Materials*, Vol. 6, pp. 1 - 16, 2014. DOI: 10.1038/am.2014.34.

[9] N. Valipour Motlagh, F.Ch. Birjandi, J. Sargolzaei, and N. Shahtahmassebi, "Durable, superhydrophobic, superoleophobic and corrosion resistant coating on the stainless steel surface using a scalable method", *Applied Surface Science*, Vol. 283, pp. 636 - 647, 2013. DOI: 10.1016/j.apsusc.2013.06.160.

[10] Nguyen Thi Phuong Nhung, Nguyen Thi Ngoc Tien, Nguyen Hoang Luong, Tran Thu Hang, Nguyen Van Kiet, and Nguyen Phan Anh, "Micro/nanostructured ZnO-based superhydrophobic steel surface with enhanced corrosion protection", *Petrovietnam Journal*, Vol. 6, pp. 59 - 66, 2022. DOI: 10.47800/PVJ.2022.06-07.

[11] Nan Wang, Dangsheng Xiong, Yaling Deng, Yan Shi, and Kun Wang, "Mechanically robust superhydrophobic steel surface with anti-icing, UV-durability, and corrosion resistance properties", *ACS Applied Materirals and Interfaces*, Vol. 7, No. 11, pp. 6260 - 6272, 2015. DOI: 10.1021/acsami.5b00558.

[12] Nguyen Thi Phuong Nhung, Rabah Boukherroub, Vincent Thomy, and Yannick Coffinier, "Micro-and nanostructured silicon-based superomniphobic surfaces", *Journal of Colloid and Interface Science*, Vol. 416, pp. 280 - 288, 2014. DOI: 10.1016/j.jcis.2013.10.065.

[13] Tianqi Guo, Liping Heng, Miaomiao Wang, Jianfeng Wang, and Lei Jiang, "Robust underwater oil-repellent material inspired by columnar nacre", *Advanced Materials*, Vol. 28, No. 38, pp. 8505 - 8510, 2016. DOI: 10.1002/adma.201603000.

[14] Hong-Liang Li, Yingchun Zhu, Dongsheng Xu, Yong Wan, Linhua Xia, and Xiu-song Zhao, "Vapor-phase silanization of oxidized porous silicon for stabilizing composition and photoluminescence", *Journal of Applied Physics*, Vol. 105, No. 11, 2009. DOI: 10.1063/1.3133209.

[15] Lichao Gao and Thomas J. McCarthy, "A perfectly hydrophobic surface (θA/θR = 180°/180°)", *Journal of the American Chemical Society*, Vol. 128, No. 28, pp. 9052 - 9053, 2006. DOI: 10.1021/ja062943n.

[16] HaoYang, Xingjuan Zhang, Zhi-Qi Cai, Pihui Pi, Dafeng Zheng, Xiufang Wen, Jiang Cheng, Zhuo-ru Yang, "Functional silica film on stainless steel mesh with tunable wettability", *Surface and Coatings Technology*, Vol. 205, No. 23 - 24, pp. 5387 - 5393, 2011. DOI: 10.1016/j.surfcoat.2011.05.049.

[17] Sirong Yu and Hao Li, "Fabrication of superhydrophobic and oleophobic zinc coating on steel surface", *Materials Science and Technology*, Vol. 33, No. 11, pp. 1290 - 1297, 2017, DOI: 10.1080/02670836.2017.1288675.

[18] Nguyen Thi Phuong Nhung, Nguyen Viet Chien, Nguyen Dang Nam, Tran Phuong Huy, Nguyen Van Kiet, and Nguyen Van Duy, "Simple method to fabricate superhydrophobic carbon steel surface", *Petrovietnam Journal*, Vol. 10, pp. 44 - 47, 2016. [Online]. Available: http://pvj.vn/index.php/TCDK/article/view/349.

[19] Hui Lu, Xiangyang Zhai, Wenwu Liu, Mei Zhang, and Min Guo, "Electrodeposition of hierarchical ZnO nanorod arrays on flexible stainless steel mesh for dye-sensitized solar cell", *Thin Solid Films*, Vol. 586, pp. 46 - 53, 2015. DOI: 10.1016/j.tsf.2015.04.056.

PETROVIETNAM JOURNAL
Volume 10/2022, pp. 59 - 69
ISSN 2615-9902

A STUDY ON FINANCIAL MECHANISMS TO DEVELOP THE POWER SYSTEM IN VIETNAM

Ha Duong Minh
Vietnam Initiative for Energy Transition
Email: minh.haduong@vietse.vn
https://doi.org/10.47800/PVJ.2022.10-08

Summary

Vietnam's commercial electricity demand grew by 9.6% per year during 2011 - 2020. The Ministry of Industry and Trade (MOIT) forecasts that the average annual investment cost for the power system over 2021 - 2030 will be around USD 9.0 billion to USD 12.6 billion per year for generation sources and USD 1.5 billion to USD 1.6 billion for the grid. This article discusses the financial options to mobilise this capital. The private sector interest in financing new thermal power projects is low for coal and uncertain for gas; the current energy price crisis suggests deferring any new LNG power plant openings until after 2026. There, the state-owned sector takes the lead. For renewable energy, private investors have shown eagerness to finance new solar and onshore/nearshore wind projects under the feed-in-tariff regime. The subsequent mechanisms will be market-based: auctions and direct power purchase agreements. Offshore wind projects allow the state-owned oil and gas industry to invest jointly with international private developers and reorient its strategy in response to the energy transition. Developing the green bond market is an opportunity for Vietnamese banks. State-owned enterprises can use them to raise money through non-sovereign debt. Finally, a gradual increase in electricity prices will improve the sector's ability to finance the necessary power system expansion.

Key words: Energy transition, power system, policy, finance, market, LNG.

1. Introduction

The commercial electricity demand of Vietnam grew by 9.6% per year during 2011 - 2020 [1]. The Ministry of Industry and Trade (MOIT) expects this growth rate to decline gradually in the coming years, to 9.09% per year in 2021 - 2025 and 7.95% per year in 2026 - 2030 in the central case. In absolute numbers, the national electricity consumption will increase from 215 TWh in 2020 to around 500 TWh in 2030 [1].

On June 21st, 2022, the national power load set a new record at 45,582 MW. On July 4th, 2022, the supply was interrupted to several substations during the noon peak in the North. Regarding the North's power consumption, on July 18th, it set a new peak record of 22,800 MW - about 4,200 MW higher than the same period last year in 2021 [2]. The Vietnam electric system is under stress and needs urgent solutions to ensure its development.

Date of receipt: 20/6/2022. Date of review and editing: 20/6 - 12/7/2022.
Date of approval: 5/10/2022.

MOIT estimated the average investment cost for the power system over 2021 - 2030 to be around USD 9.0 billion to USD 12.6 billion per year for generation sources and USD 1.5 billion to USD 1.6 billion for the grid [1]. For example, the Bac Ai pumped storage project, with the capacity to release 1,200 MW of flexible hydroelectricity, costs about USD 1 billion [3]. The investment for the Nhon Trach 3 and 4 LNG power plants, which provide 1,500 MW of dispatchable, LNG-based electricity, is about USD 1.4 billion. Renewable energy systems are even more upfront capital intensive than thermal power plants.

By thoroughly studying Vietnam's future energy scenarios, capital needs to expand the power system, the influences of the ongoing fossil fuels prices crisis and the zero-carbon goals, etc., this article discusses the financial mechanisms to mobilise capital as well as proposes some policy recommendations to develop the power system in Vietnam in the coming years.

2. Existing scenarios of power system expansion

Resolution No. 55-NQ/TW [4] effective from February 2020 marked a turning point of the energy sector away

from fossil fuels and towards renewable energy sources. In November 2021 at COP26, Vietnam announced it adopted the target to become carbon-neutral by 2050 [5]. This requires reforming the socio-economic development pathway and is more ambitious than Resolution No. 55-NQ/TW. Many official doctrine, strategy, roadmap and planning documents need to be revisited to that end.

The official adoption of the net-zero goal renewed the research interest in low-carbon development scenarios for Vietnam. Reviewing the literature provides a basis to understand the technical opportunities and policy options, which lead to different investment and financial needs for the power sector.

- The Power Development Plan 8 (PDP8) was not originally defined towards a net-zero goal [6]. Its first draft [7] was released prior to the COP26 announcement. The draft follows the 2015 Renewable Energy Development Strategy and Resolution No. 55-NQ/TW. It is constrained by the commitments already taken in the previous development plan, the revised PDP7. For example, authorisations given to thermal power projects are legally binding.

The current PDP8 draft [1] lists ongoing investment in new generation capacities during the 2021 - 2030 period as: LNG power plants (+20.4 GW), coal power plants (+11.0 GW, plus 1.3 GW with cogeneration), wind power plants onshore (+20.9 GW) and offshore (+7 GW), hydroelectricity (+8.1 GW). Investment in domestic gas power plants (+7.8 GW) assumes the development of the Lot B and Blue Whale offshore fields. Investment in utility-scale solar is limited (+3 GW), but rooftop solar is unlimited. There is also investment in electricity from biomass and other renewables (2.5 GW total capacity by 2030), in interconnectors to neighbouring countries (total capacity 5 GW by 2030), in electricity storage (2.7 GW by 2030, including two 1.2 GW pumped hydro projects and 300 MW of batteries), and in flexible thermal engines (0.3 GW).

- The Vietnam Climate Change Strategy [8] caps the energy sector emissions (including electricity production, fuel, industry) to 457 metric tons of CO_2 equivalent ($MtCO_2eq$) by 2030, down 32.6% compared to the business-as-usual scenario. In 2050, the energy sector should emit less than 101 $MtCO_2eq$. By that time, the land use and forestry sector should absorb at least 185 $MtCO_2eq$ per year. The supporting technical study shows that greenhouse gas emissions shall peak in 2035. It notes that a solar PV option is lower in cost than using carbon capture and storage in the long run but would require 500,000 ha for installing fixed solar panels[1]. Though the climate change strategy recommends considering nuclear energy and carbon capture and storage research, it does not call for large scale investment in these technologies before 2030.

- The draft Vietnam Energy Masterplan [9] proposes a scenario where the total primary energy supply reaches 154 million tons of oil equivalent (Mtoe) in 2030 and 335 Mtoe in 2050. Of which, wind and solar roughly provide 100 Mtoe each in 2050, and fossil fuels still participate: coal for 16.8 Mtoe, oil for 17.2 Mtoe and gas for 31.1 Mtoe. The total CO_2 emissions from energy reach 401 Mt in 2030, falling to 96 Mt in 2050. The scenario rests upon energy efficiency, electrification, renewable energy, hydrogen and hydrogen-based fuels, and carbon capture and storage.

- The Vietnam Energy Outlook [10] 2021 produced three scenarios: baseline (BSL), renewable energy (RE), and net-zero. Electricity generation and storage capacity in 2050 net-zero scenario are mainly composed of: storage: (47%), solar (43%), and wind (7%). The primary sources of RE-based power production are solar-dominated compared to wind (75% vs. 21%). The majority of solar is utility-scale (838 GW installed in 2050). Floating PV and rooftop are subsidiary. For wind power, onshore and offshore are balanced. Coal and gas power generation are fully phased out in this scenario.

In addition to the four official studies enumerated above, existing scenarios from other sources [11 - 16] explore various strategies to achieve deep decarbonisation. Different scenarios call for different investment trajectories in thermal power generation, solar PV, offshore and onshore wind, grid, and electricity storage.

Net-zero scenarios agree that Vietnam's emissions should peak in 2035. They also agree that a low-carbon society entails a high rate of electrification and mainly renewable electricity sources to reduce the use of fossil fuels in all sectors.

Existing studies also have limits. Most do not achieve full net-zero from the energy sector, they keep some fossil fuels and rely on carbon sequestration in forests. Methane emissions reduction receives little attention compared to

[1] *According to General Statistics Office, Vietnam area is 33,134 thousand ha, of which 3,931 thousand is non-agricultural land, 786 thousand is water surface land for fishing, and only 191 thousand is unused flat land.*

its urgency. They overlook the carbon market mechanism which is due to open in 2028 according to the Law on Environment, and underplay the opportunities offered by an ASEAN grid.

The reviewed literature on long-term scenarios uses technical and economic models. However, it has an overall low connection to the immediate problem of financing the sector in the next five years and providing electricity to the northern area next year. For example, the Energy Outlook notes that the optimal use of LNG is very price-sensitive but does not recommend policies to respond to the prices seen today.

3. Climate and energy crisis changed the power sector investment conditions

In the mid-2021, a strong economic recovery after the Covid-19 pandemic drove the international oil and gas prices up. By fall 2022, they remain way higher than they were during the 2015 - 2020 period, particularly for LNG prices (Figure 1).

Fossil fuels are like other commodities or stocks: analysts spend a lot of time trying to estimate their future pricing, but their efforts yield little more than the general expectation that "What goes up will eventually go down". Surprises and uncertainties are common. Within these predictability limits, we argue that three forces are pushing the market prices to remain relatively high in the forthcoming 3 years: project development inertia, geopolitical uncertainty, and climate policy.

- Project development inertia: The oil and gas industry uses large industrial facilities that take time to build. The high prices of LNG have motivated the construction of new liquefaction trains in 2021 and 2022, after investors observed a pause in 2020. Still, the IEA notes [17] that the industry record for constructing a large-scale greenfield LNG project was 29 months at the Calcasieu Pass project.

- Geopolitical uncertainty: Following the Covid-19 crisis, crude oil prices rebounded to more than USD 100 per barrel during the strong recovery year of 2021. Any hopes of a restoration to pre-crisis levels were crushed by the Russia - Ukraine war. Oil and gas exports of Iran and Russia face significant political restraints. The US shale oil industry exhibits capital restraint, slowing its rate of expansion. As a result, the crude oil market is still dominated by the OPEC+, which has an incentive to keep prices high.

- Climate policy: From a physical perspective, no new fossil fuel infrastructure is acceptable. The amount of carbon from fossil fuels being produced exceeds what is compatible with a 1.5°C global warming [18]. The economic perspective is more nuanced: as more severe climate policies bear on the use of fossil fuels, opening new fields and mines becomes less profitable, and capital moves towards other enterprises. As the IEA [17] summarises: High levels of uncertainty about the longer-term market evolution and the role of gas in the energy transition still cast a shadow over investment decisions. Less investment means less supply, translating into higher prices.

Asian spot LNG prices hit records in the third quarter of 2022, over USD 45 per MMBtu as shown in Figure 1. IEA notes that markets expect this situation to persist through 2023 [17]. China and India were able to switch back to coal for generating electricity. Japan and Korea implemented policies to restart nuclear and use more coal in the near future and were otherwise relatively protected by having robust long-term LNG contracts at around USD 15 per MMBtu. Pakistan and Bangladesh experience blackouts and macroeconomic shock due to high LNG prices. Compared to these two countries, Vietnam has done better. In the first 10 months of 2022, the general average consumer prices index was up only 2.89% in Vietnam compared to the same period in 2021 [19].

Exploiting the Block B offshore gas field would mitigate the impact of this kind of energy crisis on Vietnam's economy. Contrary to the spot market LNG prices, the domestic gas production costs will be stable. The project has stalled for years because technical and geological constraints make the cost of gas from Block B too high for baseload power. However, it may not be excessive to provide security, flexibility, and capacity services at scale.

According to MOIT [1], Vietnam plans to have 32.7 - 38.8 GW of gas-to-power generation capacity in 2030. At that scale, the domestic fuel extraction is certainly not enough to avoid importing fuels for electricity. The country will need to import gas as it is importing coal.

For an LNG power plant to sell electricity at the price of UScent 8 - 9 per kWh, the input LNG price must be around USD 12 per MMBtu. If the LNG price is up to USD 40 - 50/MMBtu, then the electricity selling price cannot be below UScent 20 per kWh [20]. While long-term supply contracts offer better conditions than the spot market, their prices

Figure 1. *Price of LNG in Asia since 2015. The JKM index spiked to over USD 50/MMBtu in March 2022 and remains well above its 2015 - 2020 levels. Source: Tradingviews.*

have risen in 2022, especially for contracts starting before 2026 [21].

The first LNG import facility in Vietnam will be in Thi Vai, to feed the new Nhon Trach 3 & 4 power plants.

It is not clear who will supply the LNG and at what commercial conditions. It is not clear how many private investors will take the final investment decision for the LNG-to-power projects currently under consideration in Vietnam. For example, in 2019 the Bac Lieu LNG power project was added to the Masterplan after its investors proposed to sell electricity at UScent 7/kWh, but is not moving forward. The electricity cost now appears too optimistic. And most floating storage and regasification units, which the project planned to use, have moved to Europe. The current context is not favourable for private companies to invest in new LNG-to-power projects starting before 2026.

This is not the first time that a generation of thermal power projects get delayed in Vietnam. This was already the case a few years ago [22]. The policy response to avoid power shortage was to install renewable energy sources. The case of the Vinh Tan power centre illustrates the story. It was initially planned with four thermal coal power plants projects. Only three were built. The Vinh Tan 3 project, a 1,980 MW plant scheduled to connect in 2018, saw its main investor One Energy (Hong Kong) withdraw. Now the site is surrounded by solar farms.

Private investors financed the rush of new renewable energy capacity installation. They were attracted by incentives. In 2017 the government started the renewable electricity boom started by giving a feed-in tariff of UScent 9.35/kWh to solar projects[2]. The tariff was reduced three years later to UScent 7.09/kWh, except for rooftop solar power projects[3] which still received UScent 8.38/kWh. In 2018, the wind industry received a tariff of UScent 8.5/kWh for onshore projects, and UScent 9.8/kWh for offshore[4].

Feed-in-tariff worked well to start the industry but will not be continued. This way to attract investment is not sustainable. In 2022, the average retail electricity price in Vietnam is equivalent to US cent 8.3 per kWh[5]. EVN cannot thrive if it sells retail for less than it buys wholesale.

Will the costs for the next wave of solar and wind farms in Vietnam be lower than the feed-in-tariff initially given? On one hand, most best locations are already developed, and the price of PV modules and wind turbines are not declining as fast as they used to, due to general inflation in materials and shipping costs. On the other hand, compared to the 2017 - 2018 period, the sector is mature in Vietnam and the industry has made five years of technical progress. According to IRENA [23], "the global weighted-average levelised cost of electricity of onshore wind fell 56% between 2010 and 2020, from USD 0.089/kWh in 2010 to USD 0.039/kWh in 2020" and "the global weighted-average levelised cost of electricity for utility-scale PV projects fell by 85% between 2010 and 2020".

Another factor to drive down the costs of renewable electricity in Vietnam will be using competitive mechanisms: auctions and direct power purchase agreement. The results of recent solar and wind auctions in most other countries are way lower than the feed-in-tariff given in Vietnam for 2017 - 2020. For example, bids from solar farm investors around US cent 1.3/kWh have been seen at auctions in Abu Dhabi, Portugal and Chile.

Thus, the evolution of the global economy since 2019 now makes it easier to attract investment for solar and wind farms than for thermal power plants. Mobilising private capital to install renewable power generation sources solves only half of the financing problem. Developing a reliable electricity system requires much more than building plenty of renewable-based generation capacities. It requires i) sufficient transmission and distribution networks, ii) backup capacities for the times when the renewable power sources are not available, and iii) flexibility solutions to compensate for the short-term variability of solar and wind.

[2] *Decision No.11/QĐ-TTg dated 11/4/2017.*
[3] *Decision No. 13/QĐ-TTg dated 6/4/2020.*
[4] *Decision No. 39/QĐ-TTg dated 10/9/2018.*
[5] *Decision No. 648/QĐ-BCT dated 20/3/2019.*

4. The private sector can finance demand reduction for its own benefit

Limiting the increase in electricity consumption reduces the need to find fund to finance the system's development. The main approaches to reducing power system growth are energy efficiency regulations, distributed generation such as incentives to build rooftop solar systems, and dynamic demand-side reduction:

- Improving energy efficiency typically entails purchasing newer equipment and implementing wiser energy management strategies. Energy reductions result in cost savings, which can compensate for the investment. It is up to energy consumers, whether they are private firms, individual families, or public organisations, to identify and invest in the energy-savings measures that will provide the greatest return on investment. When energy users do not take such steps, there is room for energy service firms to invest in energy efficiency improvements while receiving a portion of the realised energy savings as payment. This business strategy has shown to be successful in many nations, but is not yet widespread in Vietnam. Government intervention must be more decisive in order to expedite the adoption of energy efficiency measures.

- Rooftop solar is now the most popular distributed generation technology for reducing grid demand. The national PV rooftop capacity increased from 378 MWp in 2019 to 9.6 GWp in 2020, spreading among over 100,000 systems (see http://solar.evn.com.vn). Most were entirely funded by the private sector. Incentives to invest in the rooftop solar sector were reduced in 2021, but there is still a demand for carbon-neutral electricity from industrial, businesses and homeowners. There is also the possibility of equipping public sector organisations such as schools, hospitals, and governments: in a carbon-neutral society, all levels of government - central, provincial, and municipal - will provide green public services.

- Demand response management aims to lower the consumer electricity demand when the supply is tight. Demand side reduction programs are often operated by power companies. It may seem counter-intuitive to ask a company, even a state-owned one, to reduce its demand. However, there are times when power providers sell electricity at a loss, particularly when load peaks must be met by generating electricity from expensive gas turbines. In these circumstances, lowering peak demand is lucrative for the utility. It enables the avoidance of the installation of power generation capacities.

Smart appliances and the internet of things hold great potential for demand response management. Rooftop PV systems that include battery storage and a smart connected bidirectional meter can theoretically deliver more benefits to the grid than just reducing daytime demand. This will be economically significant over a 10-year time horizon.

Even if demand reduction initiatives are effective, they will not be enough to prevent the need for investment in extending Vietnam's power system. Figure 2 illustrates that a high-income country lifestyle necessitates four times the amount of electricity per capita than Vietnamese use today. Furthermore, high-income countries successfully transitioned to a falling electricity production trajectory around 2007, but as they take the lead in reducing greenhouse gas emissions, several are considering the necessity to boost their electricity output once more. Electricity will be used to replace fossil fuels wherever it is technically practicable, and it will also be used to help synthesise carbon-neutral fuels for applications where electrification is not practical.

To sum up, the bulk of investment for demand-side reduction will come from the private sector. The State can lead by example, but its essential function is to enable the markets.

5. Shaping markets to attract private sector's investments

Installing more production and transmission capacity, backup power sources, and flexibility solutions necessitates the mobilisation of billions of dollars each year. We're talking about new power lines and transformers, hydroelectric dams, interconnectors to neighbouring countries, pumped hydro storage, large batteries, internal combustion engine natural gas power plants, natural gas open or combined cycle power plants, and equipment to make coal power plants more flexible, in addition to new solar and wind farms. There is no single way to pay for all of this. A package of policies and regulations is required.

Historically, the electricity industry was managed by the State, with a vertically integrated national company providing everything from power generation to its distribution. State-owned enterprises still play a central role in Vietnam's power sector, and we will discuss how to finance them in the next section. However, as the current electricity sector policy is oriented to increase the role of the market, we start by discussing how to attract investment from the private companies.

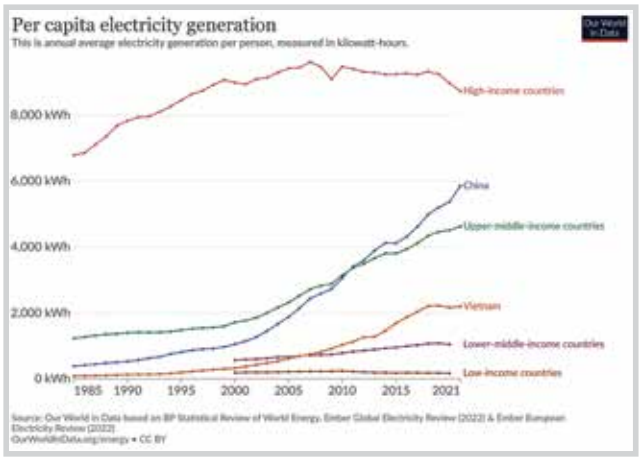

Figure 2. *Electricity generation per person. High-income countries produce four times as much electricity per capita as Vietnam does. Source: Our World in Data.*

The needs of an electric system operator are classified into three types: energy needs, capacity needs, and ancillary service needs. Deregulation tries to meet some of these demands through private firms motivated by market profits. The fundamental mechanism of markets is that prices realise an equilibrium between supply and demand. When there is a great demand for electricity, prices rise, attracting high-cost power producers such as those who use natural gas to generate electricity. When demand is low, only low-cost power producers compete in the market. This mechanism ensures an order-of-merit dispatch, which is economically efficient.

- In the energy market, producers are compensated in proportion to the number of kWh delivered. The load dispatch centre solicits bids from power producers and selects the most competitive ones to determine day-ahead electricity production plans.

- The ancillary services are those needed to ensure the reliable operation of the grid. Some power plants must be guaranteed to restart without external power, in case of a blackout. Some facilities must regulate the frequency of the grid, fine-tuning their production to match the demand in real time. Other ancillary services include voltage control and maintaining the operational readiness in case a component of the system suddenly goes offline.

- In a capacity market, the producers are pre-paid in advance proportionally to the maximum level of electric power they commit to supply at a certain point in time in the future. For example, if the system operator could determine a specific demand in a specific daily time in the summer of 2030 available, it could pay producers in advance to ensure that the supply will be available.

Energy markets are the most straightforward of these three. Vietnam had a competitive generation market. By mid 2022, the 108 participating power plants, half of them from the private sector, represented 30,940 MW of generation capacity [24]. Vietnam may use auxiliary services and capacity markets someday, but this is not a guarantee. In the medium term, such future prospect cannot be counted on to offer incentives to build natural gas power plants by 2030. And, while auxiliary markets are an incentive to invest in battery storage, their scale is limited - "ancillary" means "of secondary importance".

Free-market enthusiasts argue that an unrestricted energy market works as a capacity market: if the electricity prices are allowed to climb very high during super-peak hours, then peaker plants will be profitable to build even if they run few hours per year. This idea is dangerous. The February 2021 blackouts in Texas demonstrated that the theory does not work in practice. The Enron frauds in 2000 - 2001 leading to blackouts in California also demonstrated the vulnerability of a deregulated power market to manipulation.

In Vietnam as in other countries, the renewable electricity sector was started by giving feed-in-tariffs to producers. After that, the government works on two mechanisms to attract investors:

- Public procurement auctions where solar or wind projects will bid for a selling price to EVN, with the lowest bidders winning.

- Renewable electricity generators can participate in Vietnam's electricity market. Market dynamics may be difficult for them: the concurrent supply of solar energy during sunshine hours depresses the market. To work around this, renewable energy producers can enter a contract-for-difference directly with a third-party buyer interested in green electricity. Such direct power-purchase agreement will guarantee the solar or wind electricity company's income level regardless of the spot market price.

Considering the limits of markets to motivate investors in grid, capacity and ancillary services, another way to involve the private sector is to bundle some system costs into the contracts binding investors in power projects. Here are 2 examples:

- Adding a two-hour battery storage component to PV projects helps shape the load curve. Such a battery could cycle almost daily to store electricity during the

afternoon production peak and to dispatch it during the evening consumption peak. It could avoid costly grid upgrades. Policy discussions in 2018 - 2019 concluded that mandating storage for PV projects in Vietnam was premature. Nowadays most new projects in California, Australia, or China include a battery storage component. In September 2022 EVN proposed to aim for 1 GW of battery storage in 2025 and 3 GW in 2030.

- New power generation projects are normally only responsible to build a medium-voltage power line to connect their site directly to the substation. In the offshore wind industry, multiple projects could connect to a common offshore platform far from the coast, and then pool their resources to build the connection cable to the national high voltage grid shore. The artificial energy island concept is taking off in Europe. Vietnam could use Phu Quy Island to the same effect. Financing high-voltage transmission cable connecting multiple wind farms could arguably be a contribution of the offshore wind industry to the national transmission network.

Public-private partnerships also remedy the limits of markets. Many EVN or Petrovietnam projects use joint ventures to bring in outside equity and technical expertise. This allows them to leverage public capital in exchange for a share of profits and some control of the project's destiny. For example, the Son My LNG terminal is led by Petrovietnam with the US company AES. Partnership cannot make a project profitable if the technical and economic conditions are not favourable.

More recently, the electricity law has been modified to allow the private sector to finance new electricity transmission lines. This is a promising mechanism but delicate to implement. The build-own-operate-transfer model is of little interest since the electricity network operation has to remain centrally operated for technical reasons. The grid operator decides which sources get to produce electricity, so it must be an independent national load dispatch centre, to ensure all power producers are treated fairly in a competitive market. Moreover the power grid is a critical security infrastructure, so it has to be owned by national entities, at least for the high-voltage backbone lines. The pilot project built by the Trung Nam group in Ninh Thuan demonstrates the opportunities as well as the difficulties of private investment in power transmission infrastructure.

[6]*Decision No. 26/2019/QĐ-TTg dated 15/8/2019*

6. Financing the state-owned sector

Having exhausted the ways to mobilise private capital to finance the energy transition, the remaining needs must be met through public funding. State-owned enterprises operate the public investment to ensure the country's access to reliable and affordable energy. Companies finance growth through three methods: raising equity, emitting debt and reinvesting profits.

Each of these three funding sources have different limits and require different levels of remuneration. Equity and reinvested profits are the cheapest to access but the most limited. International loans are more expensive, and the private sector requires the highest rate of returns. The cost of debt depends on the credit rating of the borrower, which is a strong argument for avoiding the state-owned enterprises making losses.

- Equity means bringing new capital. In the early stages of economic development, the government could borrow to build infrastructure through its general state budget. Vietnam could receive official development assistance loans and grants at preferential rates from partner countries. This is no longer the case. The potential for Vietnam to borrow money from other states and from financial markets to finance the energy transition is limited, as the national debt level is at the maximum permissible level. The State is not looking to inject new capital in the public energy sector companies. On the contrary, the Commission for the Management of State Capital at Enterprises (CMSC) has a mandate to divest[6], that is to sell the shares owned by the State.

- Non-sovereign debt is created when a state-owned enterprise borrows without guarantee from the State. EVN did this for the first time in 2022, borrowing EUR 80 million from the French development agency AFD to finance the Southern power distribution grid improvement in the South. Countries have been talking about climate finance for decades. The increasing urgency of the climate chaos may at last motivate an effective mechanism to help finance the energy transition in countries like Vietnam. But that remains to be seen.

Enterprises conducting projects in the energy sector, like all others, also use commercial debt subscribed by financial institutions. For example capital for the Thi Vai LNG terminal comes from USD 85.5 million equity investment from PetroVietnam; USD 80 million loan from three foreign banks HSBC (UK), Mega Bank and Taipei

Fubon Bank (Taiwan); and USD 81.2 million loan from two Vietnamese banks, Southeast Asia Commercial Joint Stock Bank and Vietnam Export Import Bank. Text box 1 explains the financing limits of national banks.

Enterprises investing in large energy transition projects, for example energy storage or transmission network expansion to connect renewable energy sources, can raise funds directly from capital markets by emitting green bonds. Bonds allow a company to get money from numerous investors, unlike loans. Compared to a stockholder, the bond holder does not own a share of the company. It has a different risk: the issuer promises to pay dividends known in advance, and pay the capital back after a number of years. One of its advantages for the issuer is that global capital markets are very deep, so a company can borrow larger amounts with bonds than with loans. One of the disadvantages for the bond buyers is that it is difficult to assess the risk level of the investment. An individual investor cannot see if the company mobilising money really uses it for sound business.

A bond is "green" when the company promises to use the money raised to finance projects that have a positive environmental impact. Socially and environmentally responsible investors prefer to buy green bonds than bonds which finance greenhouse gases emitting industries. This form of financing has been developing exponentially on the international scene since 2007. Green bond issuance in the world reached USD 620 billion in 2021, more than doubling from the previous year [25]. They are a key instrument of international climate finance.

Yet Vietnam banks issued only USD 216 million in green bonds over the last 5 years (op. cit.). The bond market in Vietnam is young: the Government issued its first long-term bonds in 2015, and the corporate bonds sector only started growing after 2018. Structuring a robust green bonds market is a clear and present opportunity for Vietnamese banks and the government [26 - 27].

- Capitalisation. Enterprises can reinvest profits, instead of distributing dividends as contribution into the state budget. For example, Petrovietnam might have been assigned to build and operate power plants mainly because they had the financial capacities, even if it is not their core purpose.

The State regulates energy prices in Vietnam. Keeping them low benefits the consumers. However at some point EVN may start losing money if it does not pass its full costs to the consumers. As Fitch Ratings [28] writes: EVN's standalone credit profile, however, is constrained by the limited record of Vietnam's cost pass-through regulatory framework. In the years to come, increasing retail energy tariffs seem necessary to help state owned enterprises to invest in the infrastructure for the energy transition.

Regarding investment in the grid infrastructure, Nguyen et al. [29] argued that the current transmission fee, which is VND 86.25/kWh[7], was comparably low as it represented less than 5% of the electricity price, and would need to be gradually increased up to VND 168.79/kWh by 2025, in order to cover EVN investment needs in the national power transmission system.

Monetary creation and banks' lending limits

Nowadays the government does not mint coins or issue banknotes to pay its construction companies. But when a state-owned enterprise borrows money from the central national bank, the economic mechanism is identical: the central national bank creates money.

This monetary creation also happens when a domestic private bank issues a loan. The bank can credit the borrower's account without having to go find the same money elsewhere. Unlike normal economic agents, it can lend money it does not have.

To limit the risk, banks must have at least 8% of the amount they loan in their own capital. If a bank has USD 1.5 billion of capital (e.g., Techcombank, one of the largest in Vietnam), it cannot have more than USD 18.75 billion of outstanding loans. This is at any time, across all economic sectors, so the capacity to issue new loans to any specific sector will be a few hundred million USD per year at best. Thus, private domestic banks are limited in the capacity to finance the energy transition, which requires billions of new capitals every year.

Can't the State Bank of Vietnam just finance the energy sector by buying paper emitted by EVN and Petrovietnam, green bonds for example? After all, many central banks have been printing money generously during the Covid-19 crisis. While they accommodated governments' spending to avoid an economic crisis in 2020 and 2021, most central banks are refocusing now on their main objective: to keep inflation low. This means less monetary creation.

[7] *Decision No. 1769/QĐ-BCT dated 5/7/2020 updated by Decision No. 1052/QĐ-BCT*

Capital costs to invest in grid expansion, backup capacity and flexible sources are only one of the reasons pushing up the costs of electricity. Costs of operations are also increasing with the share of imported fossil fuels in the electricity mix, higher prices of fossil fuels on international markets since 2021 and a general increase in the costs of labour and all other inputs.

Only one factor may decrease the average cost of electricity: competitive auctions to procure electricity from renewable sources. This may not be enough to avoid increasing the electricity retail tariff in Vietnam.

Progressive electricity tariffs are in place to protect the low-income consumers: households consuming less than 50 kWh per month pay VND 1,675/kWh. Bigger consumers pay higher rates, up to VND 2,927 for each kWh above 400 kWh in the month. Even if the average tariff increases, it is possible to increase the redistribution towards the poor by keeping the low tariffs unchanged, or even decreasing them.

Since 2003 the electricity tariff has been used as a tool to fight against inflation and protect consumers. The last time the price rose in 2019, after a two-years freeze, they went up by 8.36% from VND 1,720/kWh (UScent 7.4/kWh) to VND 1,864/kWh (UScent 8/kWh) exclusive of VAT.

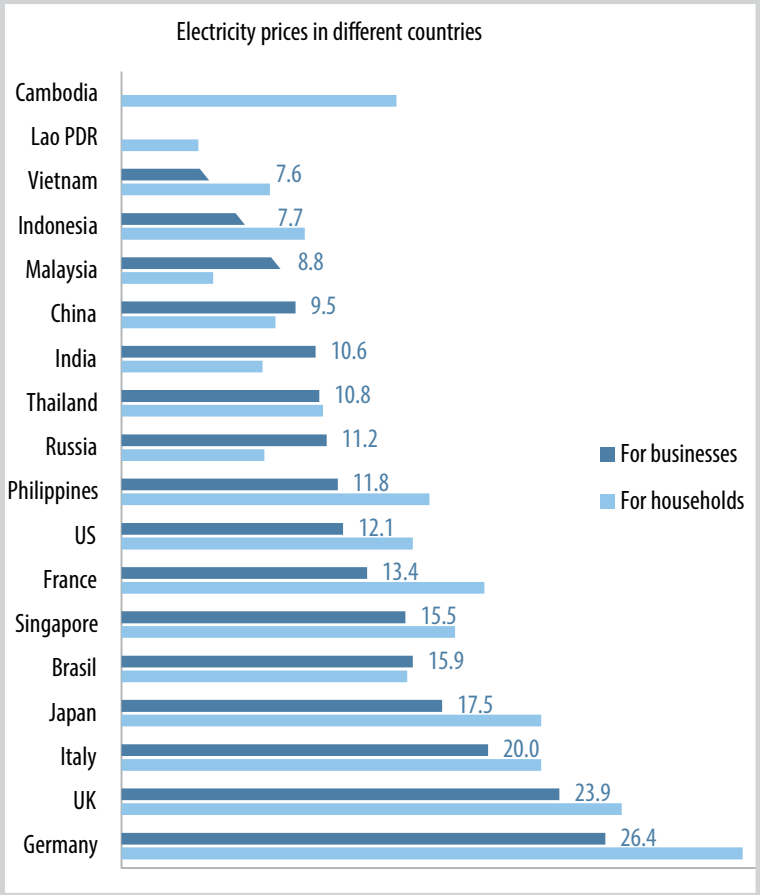

Figure 3. *Prices of electricity in ASEAN and G8 countries. Vietnam has room to increase the tariff and remains competitive. Source: Author with data from globalpetrolprices.com.*

Let us consider the implications of a one-cent rise in the average tariff. This represents a 12.5% increase, or VND 236/kWh. The increase is significantly more than a doubling of the previously discussed transmission fee. EVN sold 217 billion kWh in 2020, therefore the one-cent rise raises its revenue by 2.17 billion USD. This is not only enough to reinforce the grid; there is also money left over to invest in backup capacity and flexibility sources like battery storage, which the private sector in Vietnam finds difficult to fund under current market conditions.

According to MOIT, the average retail electricity price in Vietnam could rise to roughly 8.2 - 9.0 UScent/kWh by 2030 [1], and 10.2 - 10.5 UScent/kWh between 2021 and 2050 (in USD 2020). They would remain low compared to the competing countries [30], as Figure 3 shows. Furthermore, prices will increase in other countries as well. As a result, the proposed increase in Vietnam's electricity rates will not necessarily be detrimental to the country's macroeconomic competitiveness.

7. Conclusion

The power sector development since 2019 has shown that private investors are eager to finance new solar and wind projects. Market mechanisms like auctions, direct power purchase agreements, and self-consumption will set the conditions to maintain their engagement. But solar and wind resources aren't always there, so the power system needs to invest in backup capacity and flexibility solutions to ensure a steady supply. In addition to these capital needs, a growing power system needs investments in the transmission and distribution grid. We propose 5 suggestions to finance the development of the Vietnam power system in the coming years:

- Encourage the private sector to reduce electricity use by promoting energy efficiency (industry standards, appliance labelling), decentralised power generation (solar

rooftops with storage), and demand side management (smart meters, internet of things).

- When supporting private investment in renewable energy sources, prioritise projects in the region with the most unmet demand and available grid capacity to reduce system costs: the North.

- Promote the joint venture model for offshore wind: the offshore oil and gas industry must undergo a strategic reorientation to survive the energy transition. It has experience with leasing sea surface blocks and sharing earnings.

- Permit state-owned enterprises to acquire non-sovereign debt on financial markets to raise funds for long-term investments. Green bonds-based corporate finance is less expensive and more scalable than commercial debt-based project finance.

- Raise the retail price of electricity cautiously so that EVN can cover its generation costs and invest in the energy transition infrastructure. Take measures to lessen the burden on disadvantaged consumers and shift the energy bill to high-income households and the economic sector.

The 2022 global energy crisis is the fourth after 1973, 1979 and 2008. This time is different: electricity from solar and wind power generation capacities has become cheaper than electricity from equivalent coal- and gas-fired thermal capacity. Accounting for the social and environmental costs of greenhouse gas emissions further increases this differential. Energy storage is becoming affordable. Urgent decisions are needed to ensure investments in the power system sufficient and on track with the net-zero objective while preserving the nation's competitiveness and energy security.

References

[1] Bộ Công Thương, "*Tờ trình về việc phê duyệt Đề án Quy hoạch phát triển điện lực quốc gia thời kỳ 2021 - 2030, tầm nhìn đến năm 2050*", Tờ trình số 6328/TTr-BCT, 13/10/2022.

[2] EVN, "The intense heat makes power consumption in the North to a new peak at noon on 18 July 2022, EVN recommends economical power use", 18/7/2022.

[3] EREA and DEA, "Vietnam technology catalogue for power generation and storage". [Online]. Available: https://ens.dk/sites/ens.dk/files/Globalcooperation/technology_catalogue_e.pdf.

[4] Ban Chấp hành Trung ương, "*Nghị quyết của Bộ Chính trị về định hướng Chiến lược phát triển năng lượng quốc gia của Việt Nam đến năm 2030, tầm nhìn đến năm 2045*", Nghị quyết số 55-NQ/TW, 11/2/2020.

[5] Pham Minh Chinh, "Remarks by H.E. Mr Pham Minh Chinh, Prime Minister of the S.R. of Vietnam at the 26th United Nations Climate Change Conference of the Parties", COP26, Glasgow, UK, 1/11/2021. [Online]. Available: https://unfccc.int/sites/default/files/resource/VIET_NAM_cop26cmp16cma3_HLS_EN.pdf.

[6] Thủ tướng Chính phủ, "*Quyết định phê duyệt nhiệm vụ lập Quy hoạch phát triển điện lực quốc gia thời kỳ 2021 - 2030, tầm nhìn đến năm 2045*", Quyết định số 1264/QĐ-TTg, 1/10/2019.

[7] Bộ Công Thương, "*Tờ trình về việc phê duyệt Đề án Quy hoạch phát triển điện lực quốc gia thời kỳ 2021 - 2030, tầm nhìn tới năm 2045*", Tờ trình số 1682/TTr-BCT, 26/3/2021.

[8] Thủ tướng Chính phủ, "*Quyết định phê duyệt Chiến lược quốc gia biến đổi khí hậu đến 2050*", Quyết định số 896/QĐ-TTg, 26/7/2022.

[9] Nguyen Ngoc Hung, "Net zero pathways for energy sector in Vietnam", *AFD Macro/Energy modelization of a net zero strategy in Vietnam, Hanoi, 24/6/2022*.

[10] EREA and DEA, "Vietnam energy outlook report 2021", 5/2022. [Online]. Available: https://ens.dk/sites/ens.dk/files/Globalcooperation/vietnam_energy_outlook_report_2021_english.pdf.

[11] Vishal Agarwal, Jonathan Deffarges, Bruce Delteil, Matthieu François, and Kunal Tara, "Charting a path for Vietnam to achieve its net-zero goals". [Online]. Available: https://www.mckinsey.com/capabilities/sustainability/our-insights/charting-a-path-for-vietnam-to-achieve-its-net-zero-goals.

[12] Wärtsilä Energy, "Rethinking energy in Southeast Asia", 9/2022. [Online]. Available: https://wartsila.prod.sitefinity.fi/docs/default-source/downloads/rethinking_energy_in_southeast_asia.pdf?utm_source=press-release&utm_medium=CTA&utm_term=energy&utm_content=report-pdf&utm_campaign=rethinkingenergy.

[13] IRENA and ACE, "Renewable energy outlook for ASEAN: Towards a regional energy transition (2nd edition)", 9/2022. [Online]. Available: https://irena.org/publications/2022/Sep/Renewable-energy-outlook-for-ASEAN-2nd-edition.

[14] K. Handayani, P. Anugrah, F. Goembira, I. Overland, B. Suryadi, and A. Swandaru, "Moving beyond the NDCs: ASEAN pathways to a net-zero emissions power sector in 2050", *Applied Energy*, Vol. 311, 2022. DOI: 10.1016/j.apenergy.2022.118580.

[15] World Bank, "Vietnam country climate and development report", 1/7/2022. [Online]. Available: https://openknowledge.worldbank.org/handle/10986/37618.

[16] IEA, "Southeast Asia energy outlook 2022", 5/2022. [Online]. Available: https://www.iea.org/reports/southeast-asia-energy-outlook-2022.

[17] IEA, "Gas market report, Q4-2022 including global gas security review 2022", 10/2022. [Online]. Available: https://www.iea.org/reports/gas-market-report-q4-2022.

[18] Kjell Kühne, Nils Bartsch, Ryan Driskell Tate, Julia Higson, and André Habet, "Carbon bombs' - mapping key fossil fuel projects", *Energy Policy*, Vol. 166, 2022. DOI: 10.1016/j.enpol.2022.112950.

[19] Tổng cục Thống kê, "Chỉ số giá tiêu dùng, chỉ số giá vàng và chỉ số giá đô la Mỹ tháng 10 năm 2022", 29/10/2022.

[20] Nguyễn Huy Hoạch, "Giá LNG tăng cao và vấn đề phát triển nguồn điện khí ở Việt Nam", Năng lượng Việt Nam, 29/3/2022. [Online]. Available: https://nangluongvietnam.vn/gia-lng-tang-cao-va-van-de-phat-trien-nguon-dien-khi-o-viet-nam-28490.html.

[21] OGJ Editors, "WoodMac: 2022 LNG contracting off to quick start", Oil & Gas Journal, 16/5/2022. [Online]. Available: https://www.ogj.com/pipelines-transportation/lng/article/14276636/woodmac-2022-lng-contracting-off-to-quick-start.

[22] Bộ Công Thương, "*Báo cáo về tình hình thực hiện các dự án điện trong Quy hoạch điện VII điều chỉnh*", Báo cáo số 32/BC-BCT, 25/05/2020. [Online]. Available: https://moit.gov.vn/upload/2005517/20210705/bc-32-bct-quy-hoach-dieu-chinh-dien-77f94.pdf.PDF.

[23] IRENA, "Renewable technology innovation indicators: Mapping progress in costs, patents and standards", 3/2022. [Online]. Available: https://www.irena.org/publications/2022/Mar/renewable-technology-innovation-indicators.

[24] EVN, "10 years of operating a competitive electricity market", 6/7/2022. [Online]. Available: https://en.evn.com.vn/d6/news/10-years-of-operating-a-competitive-electricity-market-66-163-2965.aspx.

[25] Sarika Chandhok, Jonathan Deffarges, Bruce Delteil, and An T. Nguyen, "Can Vietnamese banks seize the green-bond opportunity?", 3/8/2022. [Online]. Available: https://www.mckinsey.com/industries/financial-services/our-insights/can-vietnamese-banks-seize-the-green-bond-opportunity.

[26] Sang Tang My, Nhi Tran, Nguyen Uyen, Van Nguyen Thi Hong, and Ngoc Do Hong, "Vietnam green bond market", *International Journal of Research and Review*, Vol. 7, No. 10, pp. 53 - 57, 2020. DOI: 10.4444/ijrr.1002/2293.

[27] Luu Quoc Thai, "Green bonds: world's experiences, current status and proposal for improving Vietnamese law", *American International Journal of Social Science Research*, Vol. 9, No. 1, pp. 56 - 69, 2021. DOI: 10.46281/aijssr.v9i1.1437.

[28] Fitch Ratings, "Vietnam electricity", 6/9/2022. [Online]. Available: https://www.fitchratings.com/entity/vietnam-electricity-96630179.

[29] Nguyen Dinh Cung, Le Duy Binh, Nguyen Hung Quang, Do Tien Minh, Nguyen Thi Mai Anh, Ngo To Nhien, and Duong Viet Duc, "*Policy recommendation on amending and supplementing the Electricity Law*". VIET, PN/11-VIET12.2021/EN, 12/2021. [Online]. Available: https://vietse.vn/en/publication/amending-and-supplementing-the-electricity-law/.

[30] EVN, "Where is the average electricity tariff of Vietnam compared to the world?", 27/10/2021. [Online]. Available: https://en.evn.com.vn/d6/news/Where-is-the-average-electricity-tariff-of-Vietnam-compared-to-the-world-66-163-2575.aspx.

PETROVIETNAM JOURNAL
Volume 10/2022, pp. 70 - 76
ISSN 2615-9902

INTEGRATION OF LOCAL KNOWLEDGE IN THE DEVELOPMENT OF ENVIRONMENTAL SENSITIVITY MAPS

Tu Vi Sa
Vietnam Oil and Gas Group (Petrovietnam)
Email: satv@pvn.vn
https://doi.org/10.47800/PVJ.2022.10-09

Summary

The environmental sensitivity maps would be envisaged as an elaborated scheme exchanging knowledge among numerous stakeholders at decision-making and execution levels. Local knowledge, scientific knowledge and public knowledge are required to associate toward the development of environmental sensitivity maps, particularly the identification of shoreline types and its sensitivity; compiling biology, human-use resource information; ranking, prioritising sensitive sites and resources at risk. Especially, the value of local knowledge has been recognised over time and the need for its effective integration into research and development has grown significantly. One of the options to enhance the role of this knowledge should be participatory tools emphasising researchers-facilitation to obtain indigenous perceptions as well as increase environmental sensitivity maps adoption in the planning, regulatory community in islands and coastal areas.

Key words: Environmental sensitivity maps (ES maps), local knowledge (LK), public knowledge (PK), scientific knowledge (SK).

1. Introduction

Environmental sensitivity maps for coastal provinces and islands, where there have been petroleum activities, are among the well-known research achievements of Petrovietnam in the period of 2010 - 2020. In order to produce such kinds of maps, internationally recognised methodology has been applied. With the growing recognition of knowledge systems in the last decade, this paper aims to examine the integration of three types of knowledge - local knowledge, public knowledge, scientific knowledge - in the methodology of mapping environmental sensitivity. The focus will be on local knowledge to find out (i) to what extent it has been used; (ii) whether it contributes to improving research results and (iii) what are the solutions to make it be fully and comprehensively used.

2. Theoretical framework

2.1. The concept of three types of knowledge and their role in collaborative research

Knowledge management is a formal approach to acquire, create, codify, store, share and use contextualised information, expertise, and other intellectual assets to fulfil objectives. Knowledge management is considered to promote policy-making through advancing informed debate and decision-making by accessing intelligence and insights from stakeholders [1]. Among different dimensions of knowledge and the dynamism of knowledge management, the basic concept of environmental research is incorporating local knowledge, scientific knowledge, and public knowledge to complement the consciousness of ecological functions and processes.

Local knowledge (LK) is a collection of facts related to the entire system of concepts and beliefs that people hold about the world around them. This includes the way people observe and measure their surroundings, how they solve problems and validate new information. Local knowledge is developed and adapted continuously to a gradually changing environment. It is passed down from generation to generation and closely interwoven with people's cultural values [2].

Scientific knowledge (SK) is produced through official methods by universities, researchers, or other institutions that satisfy demanding epistemic standards. Consequently, it is highly reliable, robust and well established [3].

Date of receipt: 28/4/2022. Date of review and editing: 28/4 - 26/7/2022.
Date of approval: 5/10/2022.

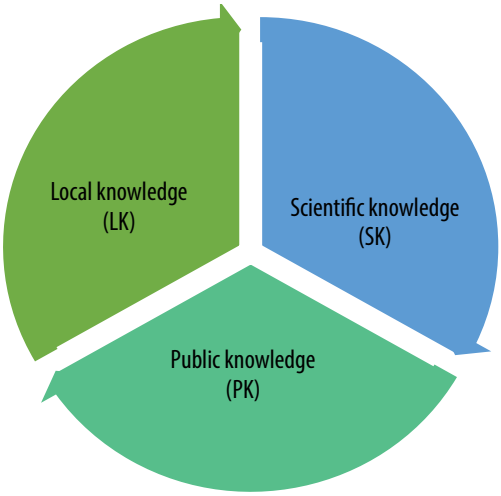

Figure 1. *Three types of knowledge.*

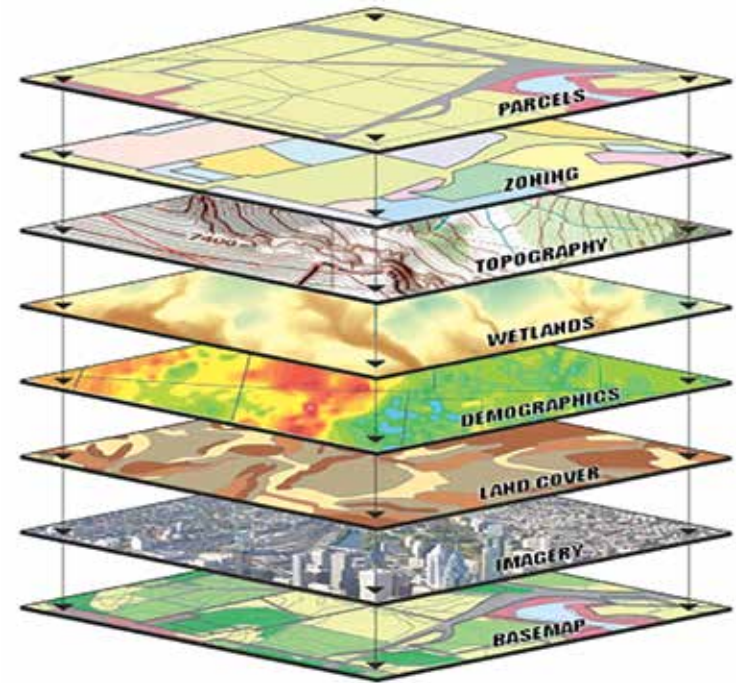

Figure 2. *Map layers.*

Public knowledge (PK) is generally captured from publications, newspapers, reports from national/local governments, laws, etc. [4]. Through the combination of various stakeholder's knowledge, we will be able to have a thorough understanding of the situation in each context.

2.2. The methodology for developing environmental sensitivity maps

Mapping the sensitivity of the environment to accidental oil pollution is developed by the oil and gas industry to deliver acceptable health, safety, and environmental performance. The environmental sensitivity maps are the maps of numerous categories of environment, resources potentially exposed to oil spills, enabling the identification of the most sensitive sites, thus providing a basis for the definition of priorities for protection and clean-up, and information to plan the best-suited response strategy [5].

Environmental sensitivity maps enclose baseline maps and tactical, strategic, operational sensitivity maps. Baseline maps comprise a set of information to locate the diversified features such as: coastline and bathymetric depth contours, rivers, lakes; towns, villages, administrative borders, roads, railways, and central infrastructure. Tactical, strategic and operational sensitivity maps contain the shoreline facet, its general environmental sensitivity to oil spill; the

Table 1. *Methodology for developing environmental sensitivity maps [6]*

Identification of shoreline types and its sensitivity	• Aerial surveys: using fixed, high-wing aircrafts, helicopters or existing topographic maps, nautical charts, aerial photos, satellite images, GIS data. • Ground verification: an example of each habitat should be visited and photographed on the ground.
Compiling biology and human-use resource information	• Scientists, resource managers,... provide expert knowledge and have responsibilities for data compilation and creating two final products: - Environmental sensitivity index (ESI) maps that are bound together in a hard-copy atlas. - Digital data on CDROM that can be viewed using ArcInfo, ArcView, ESI viewer, or in portable document format (PDFs).
Ranking, prioritising sensitive sites and resources at risk	• Establishing a team comprised of GIS specialists, marine geologists, coastal zone environmental professionals, coastal and environmental economists, etc. • Ranking the sensitivity information via mathematical modelling, using multiple indices; aggregating the sensitivity information into one index; and using a map-based approach to simplify and rank the sensitivity information.

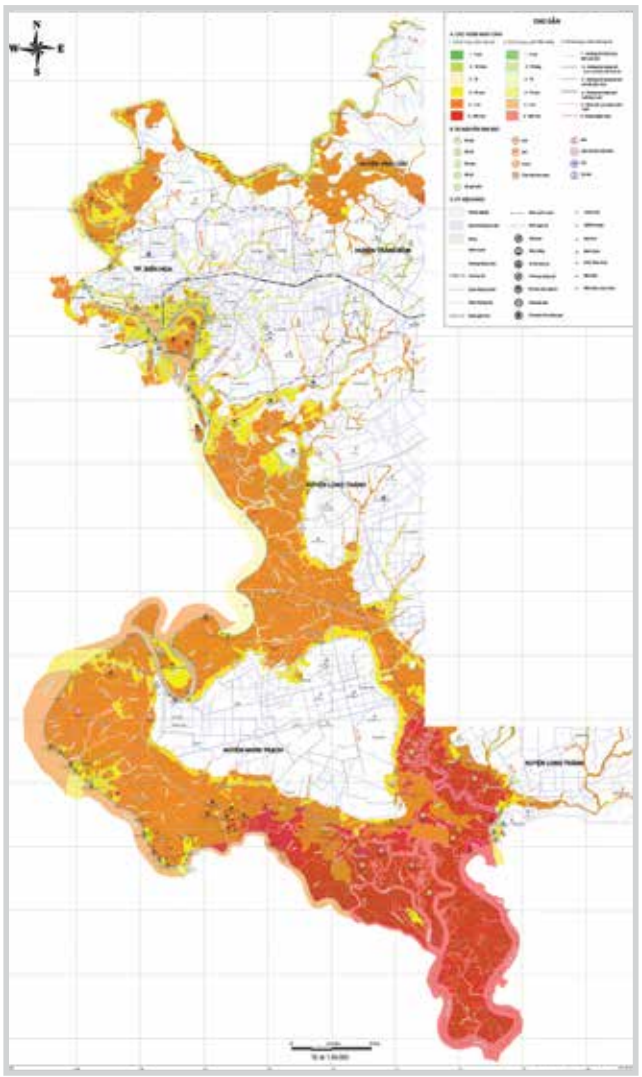

Figure 3. *Environmental sensitivity map for Dong Nai province in 2011 [7].*

sensitive ecosystems, habitats, species, natural resources; the sensitive socio-economic factors; and the logistical and operational oil spill response features.

The methodology for developing environmental sensitivity maps is described in Table 1.

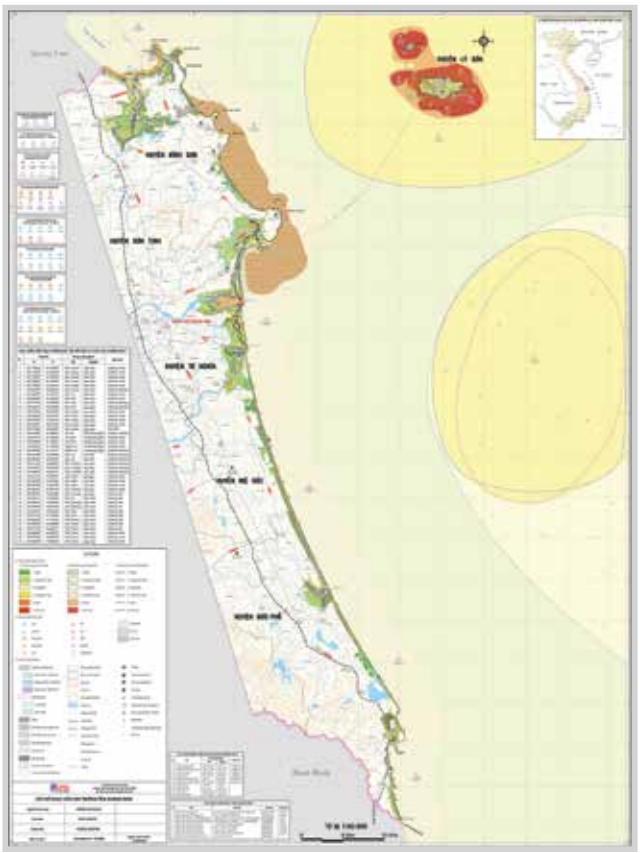

Figure 4. *Environmental sensitivity map for Quang Nam province in 2012 [8].*

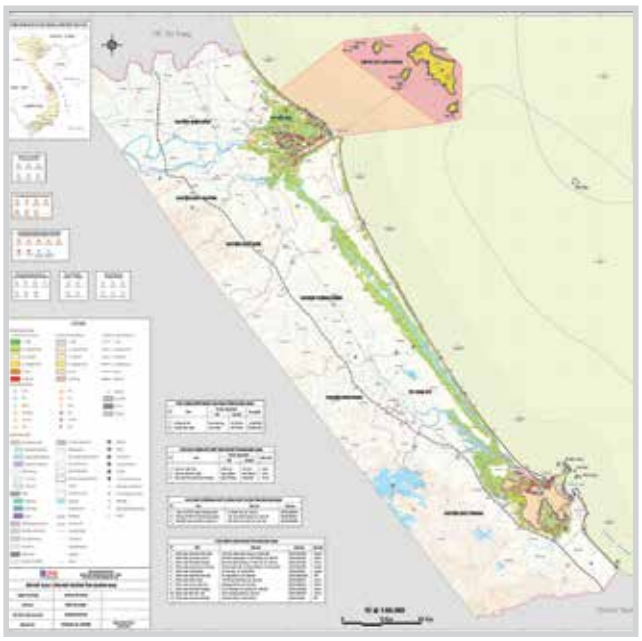

Figure 5. *Environmental sensitivity map for Quang Ngai province, 2013 [9].*

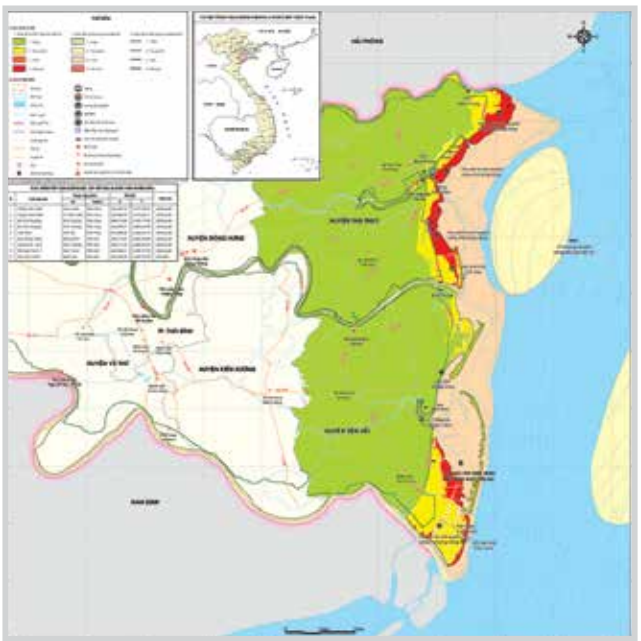

Figure 6. *Environmental sensitivity map for Thai Binh province in 2013 [10].*

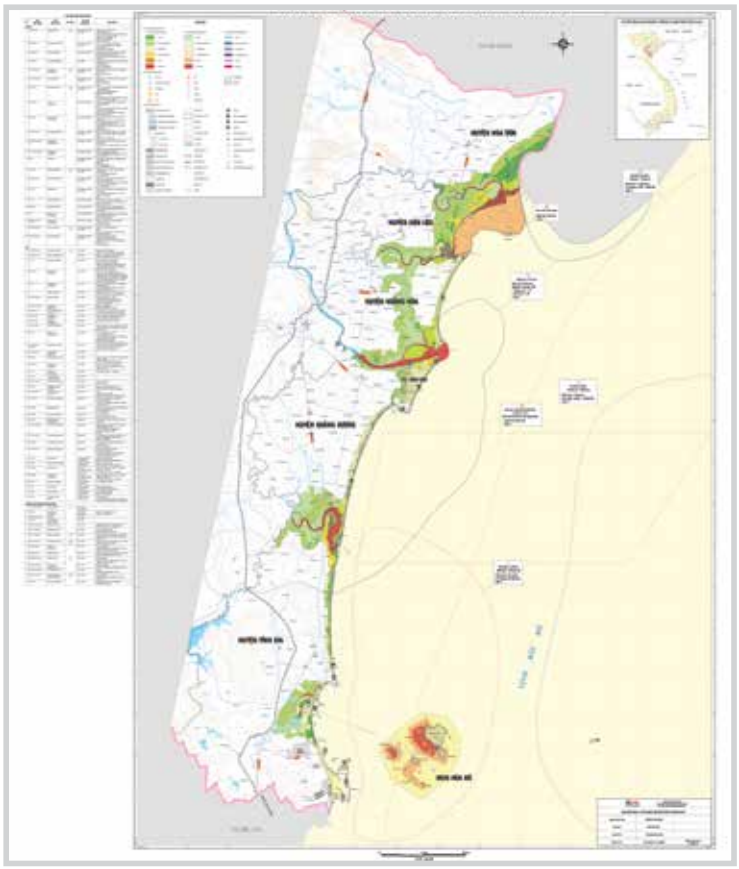

Figure 7. *Environmental sensitivity map for Thanh Hoa province in 2015 [11].*

Figure 8. *Environmental sensitivity map for central southern provinces in 2015 [12].*

3. Analysis

Since 2010, there have been many projects carried out by the Vietnam Petroleum Institute (VPI - a subsidiary of Petrovietnam) constructing environmental sensitivity maps for coastal provinces and islands which have occurred petroleum activities as shown in the following figures.

The research outputs are environmental sensitivity maps and oil spill response contingency plans transferred to local provincial agencies during this time.

The knowledge system symphonised in these cases

First of all, VPI researchers worked with local governmental agencies such as the Department of Natural Resources & Environment, Department of Agriculture & Rural Development, Management Board of National Forests, Protected Areas to collect data on natural resources (forests, coral reefs, wetlands, mangroves, biodiversity, national parks, etc.), agriculture, aquaculture, tourism together with land-use maps, residential maps, etc. and regional master plans, environmental impacts assessment reports, details on capacity of provinces to respond to oil spills.

Besides, Geological Mapping Division was cooperated to digitise the baseline maps and update the shoreline conditions whereas the Department of National Remote Sensing was consulted for advanced analysis of satellite imagery using python; Ground verifications were also conducted to confirm grain-size classifications for sedimentary substrates [5].

On the other hand, socio-economic surveys were conducted to gather the information on non-living resources that may be directly injured by oiling; managed areas that may suffer economic damages, e.g., through interruption of use if oiled; and areas that may be valuable in the event of a spill for access or staging activities [5]. Those include:

- Worked with People's Committee to identify tourism, recreation areas, port, infrastructures; industrial activities (relying on

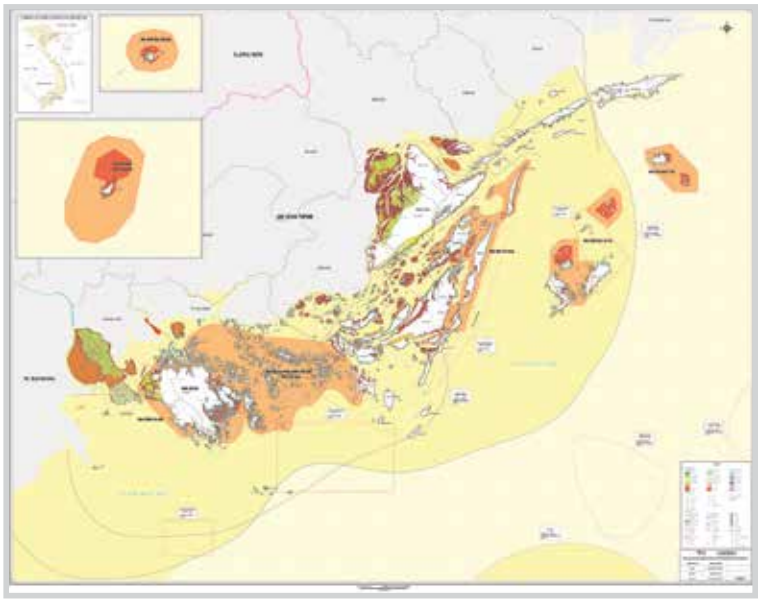

Figure 9. *Environmental sensitivity map for islands in Quang Ninh province, Hai Phong city, Quang Tri province in 2018 [13].*

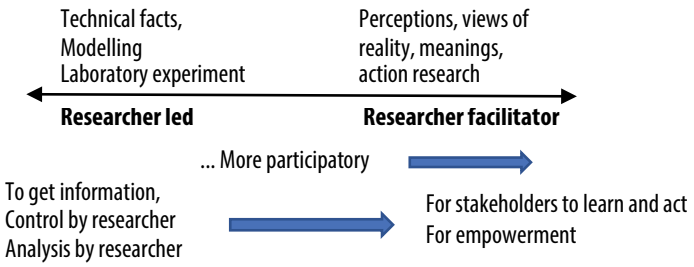

Figure 10. *Behaviour and attitude [17].*

maritime transport); infrastructures related to oil exploration, production, and transport activities; and cultural sites (archaeological, historical, religious, etc.).

- Interviews with local communities focusing on incomes, income sources; livelihoods, for example: aquaculture activities (farm species, methods/areas of cultivation, farming seasons, water intake location, annual production, number of household members involved), fishery activities (fishing areas/routes, distance from shore, fishing methods, fishing depth, fishing seasons, fishing species, number of fishermen, boat capacity); salt production activities, impacts of offshore oil and gas activities/oil spills, impacts of environmental incidents (typhoons, tsunami, etc.) (if any); In mapping socio-economic components, the concentration is to locate the activities and areas potentially suffering the most impacts.

The final step was employing the Raster Calculator of ArcGIS[1] to adjust the environmental sensitivity indexes. All layers were assigned class ranks that range from low to high, where the lowest represents

Table 2. *Comparison between practices and theory under the spectrum of knowledge system*

<table>
<tr><th></th><th colspan="3">The theory</th><th colspan="3">Practices</th></tr>
<tr><td rowspan="2">Stage 1: Identification of shoreline types and its sensitivity</td><td colspan="3">Classification through existing topographic or thematic maps and studies; remote sensing data, local knowledge, etc.
Ground trothing mission, socio-economic surveys to validate existing information and complete the information for the areas where no data is available.</td><td colspan="3">Utilise the available data;
Field surveys/Ground verification;
Socio-economic surveys.</td></tr>
<tr><td>Public knowledge</td><td>Local knowledge</td><td>Scientific knowledge</td><td>Public knowledge</td><td>Local knowledge</td><td>Scientific knowledge</td></tr>
<tr><td rowspan="2">Stage 2: Compiling biology, human-use resource information</td><td colspan="3">Biologists, resources managers compile biological and human-use (socio-economic) resources onto maps and data tables for data entry.</td><td colspan="3">Done by scientists.</td></tr>
<tr><td>Public knowledge</td><td>Local knowledge</td><td>Scientific knowledge</td><td>Public knowledge</td><td>Local knowledge</td><td>Scientific knowledge</td></tr>
<tr><td rowspan="2">Stage 3: Ranking, prioritising sensitive sites and resources at risk[2]</td><td colspan="3">The relative ranking of sensitive assets desires broad stakeholder engagement to understand the demands and concerns of those affected by decisions, specifying a set of agreed criteria. Therefore, a steering group consisting of the potential users of the maps may also be set up to ensure the involvement of the key stakeholders [5].
Methods to rank the sensitivity information as shown in Table 1.</td><td colspan="3">Consult more advice, opinions from the People's Committee, local governmental agencies for ranking/AHP
Raster Calculator of ArcGIS</td></tr>
<tr><td>Public knowledge</td><td>Local knowledge</td><td>Scientific knowledge</td><td>Public knowledge</td><td>Local knowledge</td><td>Scientific knowledge</td></tr>
</table>

[1] *ArcGIS is a family of client software, server software, and online geographic information system (GIS) services developed and maintained by Esri, an international supplier of GIS software, web GIS and geodatabase management applications. The company is headquartered in Redlands, California, the USA.*

[2] *Ranking the sensitive ecosystems and natural resources in the context of oil industry, sensitive natural resources may depend on their recovery time after a spill. Existing classifications or lists can also be used to rank them: IUCN red list (conservation status and distribution information on endangered species), lists of rare, endangered and threatened species and habitats, etc. The likelihood of impact must be considered. The sensitivity ranking may include managed areas, e.g. low to medium sensitivity for local protection status, medium for national status and high for international status [5].*

the least suitable condition (highest oil spill risk) and the highest - the most suitable condition (lowest oil spill risk) [14]. Analytic hierarchy process (AHP) was handled via quantifying criteria and alternative choices for relating those elements to the overall goal. AHP process represents an approach to quantifying criteria and options that traditionally are difficult to measure with numbers. Inputs can be obtained from actual measurements, such as price, weight etc., or from subjective opinions such as feelings of satisfaction and preference. The paired comparison matrix is established for the eigenvector as the priority. The AHP can be implemented in 3 consecutive steps: i) weight of the criteria vector, ii) matrix of option scores, iii) ranking of options. Having all stakeholders weigh in is important as various divisions will value criteria differently [15].

4. Discussion

To conceive the gap in terms of utilising local knowledge between practices and the theory, an in-depth comparison is made as follows.

From the perspective of knowledge management, Stage 1 is a synthesis of scientific knowledge, public knowledge and local knowledge. In Stage 2, there are basically scientific knowledge, public knowledge as the centre is biologists, resources managers who compile and edit environmental sensitivity index (ESI) data. In Stage 3, the sole use of automated computer-aided methods is not advisable since the environmental sensitivity prioritisation should be done through consensus building with the main stakeholders of the contingency planning process. The prominent players are resource managers and governmental agencies, the importance of local communities is implicitly mobilised in this phase. In theory, the knowledge system has been harmonised in building up environmental sensitivity maps along with the presence of local knowledge in almost three stages. In practice, due to certain circumstances, local knowledge has only been engaged at the beginning, public knowledge has been lacked in the middle stage; scientific knowledge seems to be dominant through the whole procedure.

Conventional approaches imply that development processes always drive for technology dissemination from places that are perceived to be more advanced. This practice has often led to overlooking the potential of local experiences and practices [16]. In the past, local knowledge was regarded as having little value for research method development. In fact, recognition of the existence and value of local knowledge, often collected over generations, in addition to the prerequisite for its adequate connection into research and development, have grown immensely in the last two decades. This rising interest can be attributed to: (i) the growing importance of local knowledge in defining research agenda; (ii) the realisation that local knowledge is a useful source which can be complementary to scientific knowledge and public knowledge [16].

Researchers lead refers to the fact that information is controlled, analysed by researchers (based on technical facts, modelling, laboratory experiments). Whereas Researchers facilitate implies for stakeholders to learn and act, for empowerment (owing to views of reality, meanings).

Despite the research agenda and various conditions, it is necessary to leverage local knowledge up to a basis with reference to researcher facilitation. Among the above cases, local knowledge is only the vital element of data input to structure environmental sensitivity maps, investigate shoreline types and its sensitivity. Participatory tools such as participatory landscape analysis (PaLA[3]) might be considered in scoping studies that can inform more detailed subsequent analysis of specific functions and issues. In relation to ranking, prioritising sensitive sites and resources at risk, AHP has played a primary part. However, a wider range of participants entailing the grassroots level is fundamental, not only the People's Committees but local governmental agencies also as they represent public knowledge in the knowledge system.

[3]Participatory Landscape Appraisal (PaLA) developed by World Agroforestry Center (ICRAF) is a diagnostic tool of the issues in a landscape, helps document a process of participatory appraisals of local concern - farmers as research partners. The technique is holding group discussions with unique tools to capture local knowledge at relevant temporal and spatial scales. At the district level, the participants are head of district people's committee, district cadastral officer, agriculture officer, meteorology and hydrology officers, head of communal people's committees, cadastral and agriculture officers of each commune. At communal level, the attendants are Head of communal people's committee, cadastral officers, agriculture officers, head of all villages. At the village level, people are selected based on criteria, for example: experiences in cultivation/fishery; being representatives for ages, genders, living standards of households. The village history, timeline for hotspots, seasonal calendar (specific months of cultivation, fishery) with major changes overtime related to the coastal lines, water resource and people's livelihoods are drawn by the inhabitants. Researchers then support them to outline the problem trees to find causes and describe their own management options. The village sketch is also depicted from the native angle. Thanks to that, researchers design transect-walk along hot spots using Global Positioning System - GPS, which assists to increase accuracy and facilitate imagination during spatial analysis [17].

5. Conclusion

Developing environmental sensitivity maps is the complex methodology assembling both digital data, socio-economic surveys, and mathematical models, etc. The knowledge conveyed and transmitted in these maps is a result of effective interactions with distinct social and ecological contexts, significantly contributing to the research outcomes. Among environmental sensitivity maps implemented by Petrovietnam, the involvement of local knowledge is remarked as one of the data sources at the starting point and indirectly portrayed throughout the rest of the course. In favour of attaining indigenous perceptions for objective assessment, evaluation for promoting efficient integration with other types of knowledge, participatory tools, analytic hierarchy process with broader stakeholder engagement accommodating local people might be the options. This mechanism at the same time increases environmental sensitivity maps adoption in the planning, regulatory community in islands and coastal areas.

References

[1] Deborah Ann Blackman, Katie Moon, Stephen Harris, and Stephen Sarre, "Knowledge management, context and public policy: Developing an analysis", *Handbook of Research on Knowledge Management Framework*, IGI Global, 2014, pp. 208 - 233. DOI: 10.4337/9781783470426.00022.

[2] FAO, "A training manual: Building on gender, agrobiodiversity and local knowledge", 2006. [Online]. Available: https://www.fao.org/publications/card/en/c/79c1ae5f-c15a-567f-9467-6beca7e90797/.

[3] Kevin McCain and Kostas Kampourakis, *What is scientific knowledge? An introduction to contemporary epistemology of science*. Routledge, Taylor & Francis Group, 2019.

[4] Law Insider, "Public knowledge definition". [Online]. Available: https://www.lawinsider.com/dictionary/public-knowledge.

[5] IPIECA, "Sensitivity mapping for oil spill response: Good practice guideline for incident management and emergency response personnel", 2012. [Online]. Available: https://www.ipieca.org/resources/good-practice/sensitivity-mapping-for-oil-spill-response/.

[6] Jill Petersen, "Environmental sensitivity index guidelines version 3.0", 2002. [Online]. Available: https://repository.library.noaa.gov/view/noaa/10263.

[7] Vietnam Petroleum Institute, *"Developing environmental sensitive maps for Dong Nai province"*, 2011.

[8] Vietnam Petroleum Institute, *"Developing environmental sensitive maps for Quang Nam province"*, 2012.

[9] Vietnam Petroleum Institute, *"Developing environmental sensitive maps for Quang Ngai province"*, 2013.

[10] Vietnam Petroleum Institute, *"Developing environmental sensitive maps for Thai Binh province"*, 2013.

[11] Vietnam Petroleum Institute, *"Developing environmental sensitive maps for Thanh Hoa province"*, 2015.

[12] Vietnam Petroleum Institute, *"Developing environmental sensitive maps for central southern provinces"*, 2015.

[13] Vietnam Petroleum Institute, *"Developing environmental sensitive maps for islands in Quang Ninh province, Hai Phong province, Quang Tri province"*, 2018.

[14] John Andrew Welhan and Carol Moore, *"An objective GIS screening tool for rating the suitability of land for septic-based development"*, University of Idaho, 2012.

[15] Ahmad Almodayan, "Analytical Hierarchy (AHP) Process Method for Environmental Hazard Mapping for Jeddah City, Saudi Arabia", *Journal of Geoscience and Environment Protection*, Vol. 6, No. 6, pp. 143 - 159, 2018. DOI: 10.4236/gep.2018.66011

[16] Laxman Joshi, S.W. Suyanto, Delia C. Catacutan, and Meine Van Noordwijk, "Recognizing local knowledge and giving farmers a voice in the policy development debate", *ASB Lecture Note 09*, Indonesia: International Centre for Research in Agroforestry, 2001.

[17] Hoang Minh Ha, "Participatory landscape analysis (PaLA) training", The World Agroforestry (ICRAF), 2008. [Online]. Available: http://apps.worldagroforestry.org/downloads/Publications/PDFS/LE08322.pdf.

PETROVIETNAM JOURNAL
Volume 10/2022, pp. 77 - 84
ISSN 2615-9902

KPI AS A TOOL TO CONSOLIDATE INTERNAL MANAGEMENT COMPETENCE - PRACTICE AT PVEP

Phung Mai Huong[1], Dang Quang Vinh[2]
[1]Petrovietnam Exploration Production Corporation
[2]VNU Vietnam Japan University
Email: huongpm@pvep.com.vn
https://doi.org/10.47800/PVJ.2022.10-10

Summary

The article introduces the key performance index (KPI) system on its way to application in the Petrovietnam Exploration Production Corporation (PVEP). The paper provides comprehensive information with regard to KPI measurement, the implication behind indices related to business administration, alongside procedural steps to be taken. Factors supposedly contributing to work and budget performance management are also considered and presented.

Key words: KPI, weight, standard point, target, index, business plan.

1. Introduction

Key performance index (KPI) has been widely used in business management for a long time with various modifications and adjustments to suit the actual needs of companies. At PVEP's head office, the KPI system is understood as the indices used to measure and assess the quality of implementation of the annual business plan assigned and delegated to PVEP's divisions, branches, and working teams (commonly understood as functional units). The indices also measure the efficiency of quality management, work progress, and budget control as well as efforts to improve the administrative competence of in-charge managers, which are indirectly a tool to improve PVEP's development.

PVEP's KPI system was first developed and implemented in 2012 but has not yet been formalised. The system basically creates a non-metric evaluation of the performance of the annual business plan delegated by Vietnam Oil and Gas Group - the holding company, or by PVEP's Board of Directors and Management Board. The system is not a comprehensive tool that addresses every corner of the Corporation's business performance, nor does it cover the time dimension, i.e. short-term and long-term targets for administrative efficiency. In addition, there are neither specific guidelines for measuring indices nor any constructed formula for index calculation. Simply, one can look at the annual assessment report to see whether the targets set and assigned since the beginning of the business year have been accomplished.

From the above facts, PVEP's Management realises that KPI assessment applied in PVEP needs to be standardised through detailed study, methodology build-up, data collection and calculation to enable appropriate rating among divisions, branches and working groups of different disciplines, under an overall umbrella of internal management competence. In turn, the rating will allow an accurate reflection of work/budget efficiency, business administration as well as internal management improvement.

Developed from a dataset collected through a company-wide survey covering responses from all divisions, branches and working teams of PVEP, the KPI questionnaire is conducted every quarter or every year depending on management purposes. In that manner, KPI is expected to fully reflect PVEP's image in every walk of its business, represented by the responsible subordinate units.

The KPI system is not intended for pure scientific research or to applaud/criticise divisions with high/low KPI. Instead, it is a tool for the Management to look into the root causes and to clarify internal and external reasons

Date of receipt: 23/6/2022. Date of review and editing: 23/6 - 24/7/2022.
Date of approval: 5/10/2022.

shaping the management practices, to present the work and budget performance in figures, to explain why at the end of the business year some units can accomplish tasks planned and assigned at the beginning of the year while others cannot.

With the evaluation results reported to PVEP Management periodically, KPIs are expected to be a useful information source to help find bottlenecks in internal business administration, and thereby to have appropriate solutions to improve management and execution efficiently.

2. Methodology

2.1. Focal point

The KPI system is used for PVEP's annually assigned business plan assessment and applied for PVEP headquarters' divisions, branches and working teams. The system (as well as the plan assignment and assessment) is constructed and conducted by PVEP's Planning and Investment Division as the focal point. Data controllers and data analysts from PVEP headquarters' divisions also collaborate to fulfil the planning and assessment process.

2.2. Approaches

The KPI system applied at PVEP includes 10 targets, equivalent to 10 groups of indices and sub-indices, which are selected using samples from interdisciplinary information covering key factors of the annual business plan and effectively reflecting the Corporation's administration improvement.

With the 10 targets (listed in the content of assessment in Table 1) , there are approximately 130 indices used for KPI construction. Details of indices and sub-indices are displayed in the past-year KPI assessment forms and additional indices supporting and interpreting the 10 groups.

2.3. Basis for selection and construction of indices

- A thorough review of the effective legal framework;

- A comprehensive study of the feasibility of indices applied in PVEP:

+ Measurable indices that have been in place and systematically applied, including the indices of production, finance, investment, and labour targets as assigned in the annual business plan;

+ Quantitative indices that have not been appropriately in place and systematically applied: to be collected through the survey (designed online quiz);

+ New qualitative indices: to be quantified for measuring purpose through the survey (online quiz) and using dummy variables.

- An out-and-out study on differences among concepts, calculation methods, application period, and application coverage of each index.

- Contribution from PVEP's Management and PVEP's divisions/branches/working teams.

2.4. Key rules

- Procedures for KPI construction used to assess the annual business plan performance of PVEP headquarters' divisions/branches/working teams need to reflect the Corporation's internal management targets.

- The index system measuring and assessing business execution and management quality is based on the assigned functions and responsibilities of PVEP's divisions/branches/working teams, the efficiency of quality control, work progress and budget supervision of each unit as well as efforts spent on management efficiency improvement of responsible managers.

- The KPI system includes 10 general targets and 130 indices to be approved by PVEP's Management.

- Indices measurement combines three dimensions to resolve conflicting viewpoint problems: PVEP Management's assessment, units' self-assessment, and units' cross assessment.

- Internally applied PVEP's KPI system needs to ensure:

+ Compliance with the Ministry of Planning and Investment's guidance on constructing statistical indices, and Petrovietnam's Regulation on annual business plan assignment and assessment of annually assigned business plan performance of subsidiaries;

+ Compatibility, comparability, and applicability of current systems of indices in Vietnam such as the provincial competitiveness index (PCI) conducted by the Vietnam Chamber of Commerce and Industry (VCCI) and the United States Agency for International Development (USAID); the Vietnam provincial governance and public administration performance index (PAPI) conducted by the Centre for Community Support and Development Studies (CECODES), the Centre for Research and Training

Table 1. *Assumption of weights identified for each index target/group of the KPI system*

Target/ group of indices	Content of assessment	Weight			
		Divisions: Exploration, Subsurface, Development, HSE- R&D, Planning & Investment, Petroleum Asset Management, Finance & Accounting, Human Resource Management, Administration	Legal & Compliance Division	PVEP ITC, PVEP Ho Chi Minh	Foreign branches
I	Annual business plan (work and budget) is efficiently constructed, executed, and supervised.	45%	-	-	-
II	Annual work plan is accomplished with proper progress (work progress is scheduled at the beginning of the business year and assigned by PVEP CEO's decision	15%	20%	20%	20%
III	Annual budget plan is accomplished with proper cost-saving (cost-saving target is projected at the beginning of the business year and assigned by PVEP CEO's decision)	5%	10%	10%	10%
IV	PVEP's Management gets stress-free and smooth access to information and data sources of their in-charge discipline(s).	5%	10%	10%	10%
V	Internal management within each divisions/branches/working teams is transparent; information is issued through the system of corporate-level procedures/regulations/guidance and instruction ; the regulatory compliance is assessed by ISO Department.	5%	10%	10%	10%
VI	Specific measures are executed to push authorities of various levels to pass/approve PVEP's submission	5%	10%	10%	10%
VII	Time allocated for administrative procedures is efficient and adaptive to deadlines assigned by PVEP's Management	5%	10%	10%	10%
VIII	Annual training and G&A cost-saving targets are accomplished in line with the division's annual work and budget assigned by the CEO	5%	10%	10%	10%
IX	Managers of divisions/branches/working teams are dynamic and creative in problem solving in co-operation with other PVEP divisions and relevant authorities	5%	10%	10%	10%
X	Managers of divisions/branches/working teams are able to have efficient management of internal human resources to contribute to PVEP's human resource development, presenting through internal training assessment and personal assessment form	5%	10%	10%	10%
Total		**100%**	**100%**	**100%**	**100%**

of the Vietnam Fatherland Front (VFF-CRT) and the United Nations Development Programme (UNDP);

+ Feasibility and synchronisation with PVEP's other systems of indices which are already in place and systematically applied including key tasks and KPI assigned to PVEP petroleum projects' chief representatives, PVEP's legal representatives and PVEP's Management Committee members.

2.5. Targeted users

PVEP's management and PVEP headquarters' divisions/branches/working teams within their functional competencies as assigned by PVEP's Board of Directors.

2.6. KPI content and indicators

- PVEP's list of KPIs includes index numbers, target codes, target contents/names, groups of index codes, index codes, sub-index codes, and assessment terms.

- Content of PVEP's KPIs includes the concept, calculation method, key classification, report time interval; sources of information; and divisions/branches/ working teams responsible for data collection.

2.7. Index construction

The KPIs are constructed in a three-step sequence: (1) collect data through different channels; (2) calculate

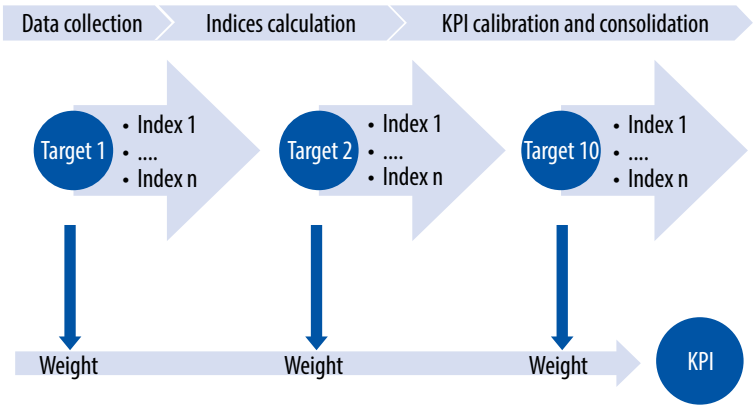

Figure 1. *The flowchart of KPI assessment.*

10 sets of indices; and (3) adjust the composite KPI as the weighted mean of 10 indices with a maximum score of 100 points. The flowchart is shown in Figure 1.

Step 1: Survey, data collection:

Data used for KPI construction consist of 2 groups:

(i) The first one is collected from survey and assessment of PVEP's Management and division managers' self-assessment and cross-assessment;

(ii) The second is collected from various sources such as periodic comprehensive/consolidated business reports, headquarters' periodic internal work and budget reports, ISO assessment reports, and actual data provided by relevant units.

The purpose of data collection through these two channels is to combine and develop a comprehensive dataset reflecting interdisciplinary viewpoints and make the final KPI set an image composed of different angles of management.

Step 2: Calculation of 10 index sets:

The KPIs are calculated as the weighted means of 10 groups of indices (equivalent to 10 targets) with a maximum score of 100 points. Therein, indices are composited based on the weighted mean of sub-indices using a standard 10-point scale. For targets with extremely high performance, the benchmark is set to 5 for balance effect.

Regarding proportional indices, the higher the calculated indices are, the more efficient the management quality is.

Regarding inversely proportional indices, the higher the calculated indices are, the less efficient the management quality is.

There are 2 types of indices: regular indices that are assigned in the decisions on annual comprehensive/consolidated business plan assignment and the decisions on annual internal work and budget plan assignment; irregular indices that are purposely adjusted depending on the business targets of the relevant business year.

Step 3: KPI calibration and consolidation

In this step, each group of indices is assigned a weight representing the contribution and importance of the indices.

2.8. Who is responsible for answering annual surveys and making assessments?

- Members of PVEP's Management Board are responsible for answering annual surveys and making assessments in compliance with their disciplinaries and responsibilities.

- Managers of divisions/branches/ working teams are responsible for self-assessment of their in-charge units and cross-assessment of other units.

2.9. KPI questionnaire

Within KPI assessment time intervals, questionnaire templates are attached to the relevant year KPI system. Annual questionnaires are continuously adjusted and complemented with necessary contents that are adaptable to annual business targets and mid/long-term management targets. The system of indices also needs to be closely linked with the decision on comprehensive/ consolidated business plan assignment and the decision on internal work and budget plan assignment of the relevant year.

Depending on substantial changes of the petroleum industry or PVEP's target adjustments, questionnaire templates will be sent for data collection. After consultancy, demonstration surveys and suitable adjustment, correction or elimination can be made depending on the actual conditions at the time of KPI assessment.

2.10. PVEP's management assessment questionnaires

The questionnaires used for PVEP's Management consist of questions relating to work execution and budget control in order to fulfil PVEP's annual business targets. Besides,

the questionnaires also aim at collecting assessments and best practices of PVEP's Management during their plan execution and interactions within the assigned authorities.

2.11. Self-assessment and cross-assessment

The questionnaires used for managers of PVEP divisions/branches/working teams are designed for:

(i) Self-assessment of the deployed activities via questions relating to actual working performance at the in-charge units;

(ii) Cross-assessment by the in-charge units with regard to their collaboration with other units.

2.12. Weight identification assumption

Based on the KPI construction and assessment, the indicators that have to be accomplished in the business year are assigned with bigger weights, especially ordinance indices, quantity indices, production indices, financial indices, and investment indices. Indicators representing management and execution quality of functional units, which are supposed to improve gradually on a long-term basis instead of instant efficiency, are assigned with smaller weights.

Assumption of weights identified for each index target/group of the KPI system is shown in Table 1.

Within each target/group of indices, the weight of an index is determined based on its importance and influence on the whole target/group.

The formula for calculating the weighted KPI is as follows:

Weighted KPI = (Target 1 × weight 1 + Target 2 × weight 2 + … + … Target 10 × weight 10)

2.13. Collecting KPI data

Online quiz:

- Questionnaires are digitalised on Microsoft Form (Figures 2 and 3);

- Questions are responded by PVEP's Management and managers of divisions/branches/working teams;

- Samples are collected by PVEP's Planning and Investment Division;

- Survey data are exported to Excel for calculation and analysis.

Online data collection:

- Annual KPI reports are posted on PVEP's intraweb.

- Internal users can log in and make use of the needed data.

3. Reporting procedures

KPI reports are made quarterly/annually, at the end of each quarter/year or subject to PVEP Management's demand. The flow chart presenting KPI construction and assessment is shown in Table 2.

4. Implication of the KPIs

As mentioned above, the KPI system includes 10 index groups (namely 10 targets in certain contexts) covering key sectors of internal business management. The use of these 10 index sets is to reflect the management quality of PVEP's divisions/branches/working teams known as functional units).

Implementation of each target is quantified, measured, and controlled by the system of indices and sub-indices, including:

4.1. Targets/groups of indices

4.1.1. Target 1. Annual business plan (work and budget) is efficiently constructed, executed and supervised

Target 1 comprises 40 quantitative indices and sub-indices. Target 1 is presented in the form of indices in the annual business plan assigned by Petrovietnam, or by PVEP's Board of Directors and Management Board, comprising:

- Production plan: 14 indices;

- Financial plan: 20 indices and 7 sub-indices;

- Investment and budget plan: 10 indices and 17 sub-indices;

- Labour plan: 5 indices.

Target 1 reflects PVEP's comprehensive/consolidated business management efficiency as well as indirectly mirrors the Corporation's foothold in the entire system of Petrovietnam's activities and the national economy.

4.1.2. Target 2. Annual work plan is accomplished with proper progress; work progress is set at the beginning of the business year as assigned in PVEP CEO's decision

Table 2. *KPI construction and assessment*

Division in-charge	Process	Description
Planning and Investment Division	KPI system construction	
PVEP's Management	Annual KPI approval	Approval of the annual KPI system based on the decisions of annual business plan/internal work and budget plan assignments.
Planning and Investment Division	Questionnaire design	
PVEP's Management	Consultancy	The Planning and Investment Division makes appropriate adjustment.
PVEP's Management and managers of functional units	Questionnaire feedback	Respondents answer Online Quiz sent out by the Planning and Investment Division.
Planning and Investment Division	KPI calculation and grading	The Planning and Investment Division calculates corresponding KPIs of each unit.
Planning and Investment Division	Result report to PVEP's Management	The Planning and Investment Division publicises the annual KPI report.

Target 2 comprises 13 quantitative indices and annually customised indices. The customised indices are constructed based on the internal work and budget plan assigned annually by PVEP's Board of Directors and Management Board.

Accomplishment of work items is calculated and measured based on the percentage of the achieved progress versus the planned progress. Cost estimation at the time of assessment compared to that at the beginning of the business year is also an applicable measure in contingent cases.

Target 2 reflects PVEP's business management efficiency through work progress accomplishment (and cost performance in certain contexts) assigned to every functional units. Comprehensively, Target 2 assessment corresponds to PVEP's internal business management efficiency based on the annual internal work and budget plan.

4.1.3. Target 3. Annual budget plan is accomplished with proper cost saving; cost saving target is projected at the beginning of the business year and assigned by PVEP CEO's decision

Target 3 is composed of 10 indices and 9 sub-indices, all are quantitative. Target 3 is used to redirect PVEP's internal cost control quality to accomplish the annual business plan.

Indices are calculated based on per capita basis, the purpose of which is to represent the cost effectiveness of the Corporation's human resources. Through the years, after excluding inflation and force majeure causes, the cost control trend will be reflected by annual statistics of this group of indices.

4.1.4. Target 4. PVEP's Management gets stress-free and smooth access to information and data sources of their in-charge discipline(s)

Target 4 consists of 10 indices. These indices describe the access of PVEP's Management to specific information of their relevant in-charge discipline(s). Equal access, up-to-date and predictable information in regulatory

compliance, and document publicity are also considered. Qualitatively, target 4 is quantified based on a 5-graded scale depending on data transparency and management adaptability.

Target 4 is the most important factor to reflect if a functional unit's information environment is convenient for PVEP's Management.

4.1.5. Target 5. Internal management within each division/ branch/working team is transparent. Information is issued through the system of corporate-level procedures/ regulations/guidance and instructions, of which regulatory compliance is assessed by ISO Department

Target 5 is composed of 8 qualitative indices indicating PVEP's and functional units' internal regulation control system.

Target 5 is quantified based on a 5-graded scale depending on their corresponding level to management purposes of a work item or a legal document. Those include regulatory impact assessment before issuance, regulation framework management in line with PVEP's divisions/ branches/working teams' functions, accountability, and internal apparatus. Apart from that, regulatory compliance assessment and supervision as well as updates necessary for actual business circumstances are also observed. Minor/major errors identified by independent ISO auditors are also accounted for.

Target 5 reflects business management excellence through the regulatory system manipulating specialty and administration relations as well as legal compliance in PVEP and among divisions/branches/working teams.

4.1.6. Target 6. Specific measures are executed to push authorities of various levels to pass/approve PVEP's submission

Target 6 consists of 11 indices measured by dummy variables (yes/no answer). The 5-graded scale is used to classify the superiority of electronic tools application. Target 6 also measures the percentage of the assigned task accomplishment/percentage of inbound and outbound documents/duties resolved by the functional units. The measurement helps display the effectiveness of work control and work capacity through multidimensional relations to authorities of various levels, Petrovietnam and PVEP's subsidiaries and petroleum project operators.

Target 6 also reflects the interaction and internal work promotion inside PVEP and among PVEP's functional units.

4.1.7. Target 7. Time allocated for administrative procedures is efficient and adaptive to deadlines assigned by PVEP's Management

Target 7 measures the ability to meet progress and deadlines required by various authorities or PVEP's Management. The group of indices is measured on a 5-graded scale reflecting the importance of the assigned duties/tasks.

Target 7 therefore relays solutions for work completion competence.

4.1.8. Target 8. Annual training and G&A cost-saving targets are accomplished in line with the division's annual work and budget assigned by the CEO

Target 8 is composed of 8 qualitative indices, representing the percentage of training cost and G&A cost-optimised over a business year compared to the planned target at the beginning of the year on a functional unit basis.

Target 8 represents the cost control efficiency of PVEP's divisions/branches/working teams in particular and the entire Corporation in general.

4.1.9. Target 9. Managers of divisions/branches/working teams are dynamic and creative in problem solving in co-operation with other PVEP divisions and authorities

Target 9 consists of 6 qualitative indices that replicate 6 key factors quantified by a 5-graded scale on adaptability to management demand. Target 9 implies the equal and co-operative interaction among PVEP's divisions/branches/working teams.

Target 9 is the only one that is measured multidimensionally through assessment channels of PVEP's Management, self-assessment of PVEP's divisions/ branches/working teams, and functional units' cross-assessment of their counterparts. Statistics from these three groups are used as input for calculation.

4.1.10. Target 10. Managers of divisions/branches/working teams are competent in managing their personnel, which in turn contributes to PVEP's human resource development, presenting through the internal training assessment and personal assessment form

Target 10 comprises 10 indices, mostly qualitative, which are quantified through grading scale. This group of indices mirrors the level and quality to which disciplinary training and specialty development are carried out by the functional units to support the Corporation's business. Being an annual assessment indicator, Target 10 is a long-term rather than an instant efficiency indicator of the assessed year.

4.2. Data and data sources

- PVEP's Investment and Planning Division continues to collect and filter indices with in-place data by designing surveys, report templates and documentary sources (assignment documents of various levels of authorities) for statistical purposes.

- PVEP's Investment and Planning Division studies, scrutinises and develops new indices based on new data sources for management purposes;

- IT applications need to be promoted in data collection and analysis (statistics collection through available tools such as database systems, Edoc, online quiz, etc.).

5. Conclusion

Performance management is the key factor for an enterprise to check whether they are going in the right direction and achieving their targets in terms of their pre-set objectives and goals. To manage the performance, managers are required to know about the performance indicators and continuously monitor them. This paper explores the key performance indicators (KPIs) applied in PVEP and predicts their impact on the overall business performance. The data used for KPI assessment is collected from the top-level management of PVEP and the functional units via a structured questionnaire. Applying the KPI system is an effort to measure the performance in terms of cost, finance, quality, time, flexibility, delivery reliability, safety, and top managers' satisfaction indicators and their impacts on PVEP's overall business. This paper puts together all important performance indicators used by PVEP in a single list and checks their impact on the overall performance of each division/branch/working team.

References

[1] Centre for Community Support and Development Studies (CECODES), Centre for Research and Training of the Vietnam Fatherland Front (VFF-CRT), and United Nations Development Programme (UNDP), *"The Vietnam provincial governance and public administration performance Index - PAPI annual reports"*.

[2] The Vietnam Chamber of Commerce and Industry (VCCI) and The United States Agency for International Development (USAID), *"The provincial competitiveness Index - PCI survey questionnaires and annual reports"*.

[3] General Statistics Office, *Results of the Vietnam household living standards survey 2018*. Statistical Publishing House.

[4] The Vietnam Chamber of Commerce and Industry (VCCI) and The United States Agency for International Development (USAID), *"PCI Handbooks 2016 & 2018"*.

[5] Ngô Thắng Lợi và Vũ Cương, "Phân biệt chỉ tiêu, mục tiêu, chỉ số trong lập kế hoạch phát triển", *Tạp chí Kinh tế và Dự báo*, Số 14, trang 40 - 42, 2008.

[6] General Statistics Office, "Overview of the set of sustainable development statistical indicators of Vietnam". [Online]. Available: https://www.gso.gov.vn/en/other-news/2019/11/overview-of-the-set-of-sustainable-development-statistical-indicators-of-vietnam/.

[7] Internal Submissions and Discussions PVEP, *"Publication of the guidance on PVEP's KPI system construction, assessment of annual business plan"*, 2021 - 2022.

[8] Vietnam Oil and Gas Group, *"Regulations on annual business plan assignment and assessment of annual assigned business plan performance of Petrovietnam's subsidiaries"*, Decision No. 5073/QD-DKVN, 2020.

[9] PVEP, *"PVEP's annual decisions on key tasks and KPI assignment to PVEP petroleum Projects' chief representatives, PVEP's legal representatives and PVEP's Management Committee Members"*.

[10] Resolutions and decisions of PVN/PVEP's Board of Directors and Management Board on annual business plan assignment to PVEP.

[11] PVEP, *"Annual KPI report"*.